Framework for Evaluation of Silent Installation Technologies

Evaluating Installation and Mitigation Strategies for Offshore Monopiles in an Early Project Phase: Balancing Noise Regulations with Technical, Operational, and Cost Considerations

Eva Wentink

Delft University of Technology and Norwegian University of Science and Technology

TUDelft

Van Oord
Marine ingenuity

NTNU

Framework for Evaluation of Silent Installation Technologies

Evaluating Installation and Mitigation Strategies for Offshore Monopiles in an Early Project Phase: Balancing Noise Regulations with Technical, Operational, and Cost Considerations

by

Eva Wentink

University	Degree
TU Delft	MSc Offshore & Dredging Engineering
NTNU	MSc Wind Energy Technology

Thesis Committee:	TU Delft Supervisor:	Dr. Ir. Jeroen Hoving
	TU Delft Chair:	Prof. Dr. Andrei Metrikine
	NTNU Supervisor:	Prof. Dr. Gudmund Eiskund
	NTNU Internal Censor:	Prof. Dr. Gustav Grimstad
	NTNU External Censor:	Dr. Ir. Jeroen Hoving
	Van Oord Daily Supervisor:	Ir. Apostolos Reppas
	Van Oord Chairman:	Ir. Ferdy Hengeveld

Cover Image: (DredgeWire, 2025)

Preface

This thesis marks the final step of my master's studies within the European Wind Energy Master (EWEM) programme, combining Offshore and Dredging Engineering at Delft University of Technology with Wind Energy Technology at the Norwegian University of Science and Technology (NTNU). It has been an enriching and challenging journey that brought together a wide range of disciplines, ranging from offshore structural design and installation logistics to wind turbine aerodynamics, while offering the opportunity to work closely with professionals in the offshore wind industry.

This research was conducted in collaboration with Van Oord, where I was warmly welcomed and supported throughout the project. I am particularly grateful for the valuable input, time, and expertise shared by experts across various departments, which helped shape the direction and content of this work. In particular, I would like to thank my Van Oord supervisors, Apostolos Reppas and Ferdy Hengeveld, for their continuous guidance and thoughtful feedback during all phases of the project.

Special thanks also go to my academic supervisors, Jeroen Hoving at TU Delft and Gudmund Eiksund at NTNU, for their support and critical input throughout the thesis process. I also wish to thank Andrei Metrikine, who was part of my thesis committee, for his helpful feedback during the progress meetings.

Lastly, I would like to thank my friends and family for their support and encouragement throughout this project. In particular, I'm grateful to my fellow students, who made my time in Denmark and Norway truly memorable and helped turn long days in the university library into genuinely enjoyable ones thanks to their great company.

I hope this thesis provides useful insights and offers a practical contribution to the ongoing development of silent offshore wind installation practices.

Eva Wentink
Delft, July 2025

Abstract

As offshore wind turbines grow in size, the installation of monopile foundations faces increasing technical, operational, and environmental challenges. A key concern is underwater noise pollution generated during pile driving, which poses risks to marine life and must comply with increasingly strict environmental regulations. While conventional impact piling is still the most commonly used technique, it often requires extensive mitigation measures to reduce noise levels. As turbine dimensions, and consequently the required driving energy, continue to increase, these mitigation measures may no longer be sufficient to ensure compliance with noise limits. This has led to growing interest in alternative installation techniques, such as vibropiling and vibrojetting, which are expected to operate more quietly but introduce technical uncertainties, particularly regarding drivability.

This thesis presents a comparative evaluation framework to support early-phase decision-making for low-noise monopile installation and related mitigation strategies. The framework quantifies trade-offs between underwater noise emissions, technical feasibility (drivability risk), operational duration, and total cost across a wide range of installation-mitigation combinations. It is implemented as a modular Python model with Excel-based inputs, in which the user can specify the relevant project parameters. This setup enables flexible and transparent comparison of fundamentally different technological strategies.

The framework was developed through an iterative process of four main steps. First, the current state of installation methods and mitigation technologies was assessed, including recent innovations. Second, internal Van Oord data was analysed to identify key parameters, complemented by expert interviews to validate assumptions and fill data gaps. Third, a dynamic model was implemented and verified through logic testing. Lastly, the framework was applied to case studies to evaluate performance trends, with sensitivity analyses to assess robustness under varying assumptions.

The results demonstrate how the framework enables systematic comparison of installation strategies and the trade-offs between noise, technical feasibility, and cost. This integrative approach is made possible by linking expertise from different specialisation fields within Van Oord. Information that was previously considered in isolation is now combined, creating a holistic overview. While still in its early stages, the framework shows strong potential to provide valuable insights for decision-making, particularly as it is further expanded and refined with additional data.

The case studies indicate that, under current conditions, impact piling remains the most cost-efficient option, primarily due to uncertainties in the drivability of alternative methods. For Van Oord, meeting noise regulations is essential, but achieving the required penetration depth is equally critical, and this is still most reliably achieved with impact piling. According to the model, compliance with noise limits can be reached using an impact hammer with full mitigation, although this relies on idealised assumptions and leaves very little margin, as the hammer operates close to the noise threshold. In practice, site-specific conditions may still lead to exceedances. Moreover, this framework is based on a 15 MW turbine, and as turbine sizes are expected to increase towards 20 MW or beyond, the likelihood that impact piling can meet noise regulations will further diminish. This underlines the importance of advancing alternative installation methods.

For vibropiling and vibrojetting, however, it cannot yet be guaranteed that the target penetration depth will consistently be achieved. A backup impact hammer is therefore still required to ensure installation can proceed if the primary method fails. This increases vessel requirements, raises costs, and, if the hammer is used, adds to the total noise emissions. Vibropiling appears attractive in theory, but its application is currently limited by uncertainty in drivability. Vibrojetting shows somewhat greater promise in terms of technical feasibility, but it requires additional equipment, making it more expensive than vibropiling. If either method can be demonstrated to reliably achieve full penetration, the interpretation

of the results would change significantly, shifting the balance in favour of vibratory techniques. Improving the technical feasibility of vibropiling therefore emerges as one of the most promising directions for future development. Beyond additional jetting, other methods of reducing drivability risk should also be explored.

The framework also evaluates combinations of mitigation strategies, showing how different near- and far-field systems interact in terms of noise reduction and cost. These comparisons highlight, for instance, that enhanced or double bubble curtain systems can provide substantial additional noise reduction at relatively modest extra cost. In this way, the framework not only quantifies trade-offs but also identifies leverage points where meaningful noise reductions can be achieved without disproportionate increases in cost.

Finally, the robustness of the framework has been tested through uncertainty analyses, demonstrating how key assumptions influence comparative outcomes. Recommendations have been formulated for future improvements, identifying which elements should be refined or expanded to increase accuracy, and which currently excluded aspects should be incorporated. A practical usage guide is provided in the appendix, enabling Van Oord staff to apply the framework directly to different projects. This ensures the framework serves its primary purpose: to support repeated, structured comparisons across a wide range of project scenarios and thereby inform well-balanced installation strategy decisions.

Contents

List of Figures

List of Tables

1

Introduction

1.1. Noise Challenges in Offshore Wind Foundation Installation

As climate change accelerates and global energy demand continues to rise, the transition to sustainable energy sources has become increasingly important. Wind energy plays a crucial role in this shift, offering a clean, renewable, and economically viable alternative to fossil fuels. Offshore wind, in particular, is gaining momentum due to its higher and more consistent wind speeds, larger potential scale, and fewer spatial and acoustic constraints compared to onshore installations.

However, the installation of offshore wind farms presents considerable challenges. One of the most pressing concerns is underwater noise pollution generated during foundation installation, particularly when using impact piling to drive monopiles into the seabed. Impact piling remains the most widely used method for installing monopile foundations. This technique involves the repeated use of a hydraulic hammer to drop a heavy ram onto the top of the pile, gradually driving it into the seabed. The process requires significant energy and generates high noise levels through repeated impact. These elevated sound levels pose serious risks to marine life, prompting governments to enforce strict underwater noise regulations. As turbine capacities scale up to 15-20 MW, accompanied by corresponding increases in monopile dimensions, increasingly more energy is required to install the foundations. As a result, it is becoming ever more difficult to comply with noise limits using conventional installation methods.

Although various noise mitigation techniques have been introduced, they offer only partial reduction. For this reason, there is growing interest in alternative installation methods that inherently produce less noise, such as vibratory hammers, jetting, vibro-jetting, EQ-piling, and vibrotwisting. While promising, these methods come with their own technical, operational, and cost-related uncertainties.

1.2. Relevance of Comparative Evaluation for Van Oord

Van Oord is a leading Dutch offshore installation contractor. For the company, it is essential to apply responsible engineering practices that minimise harm to marine life and the natural environment during installation. Another fundamental requirement is ensuring that the monopile can be successfully installed, meaning it can be driven to the required depth. Once these objectives are secured, the focus can shift toward optimising operations and costs. From a commercial perspective, Van Oord aims to evaluate alternative installation and mitigation technologies in terms of compliance with environmental regulations, technical feasibility, and cost efficiency. Particularly in early project or tender phases, the ability to assess these strategies in a structured manner enables more informed and balanced decision-making, ensuring that wind turbines are installed as effectively as possible while reducing overall project costs.

Each installation method comes with specific operational characteristics and corresponding mitigation needs. A comparative framework is therefore essential to understand their combined implications. Such a tool would allow Van Oord to make project-specific choices that meet regulatory noise limits while simultaneously minimising total installation costs.

1.3. Objective of This Project: Building a Comparative Evaluation Framework

The objective of this project is to develop a comparative evaluation framework that supports early-phase decision-making for offshore monopile installation and noise mitigation strategies. The framework is designed not to prescribe a single optimal solution, but to serve as a flexible and transparent tool that allows project developers to compare alternative strategies based on project-specific constraints and priorities.

By integrating cost, operational duration, underwater noise levels, and regulatory compliance, the framework enables users to assess the trade-offs between environmental performance and installation efficiency. It aims to provide Van Oord with a structured basis for evaluating the feasibility and impact of different technology combinations in the planning phase of offshore wind projects.

To support this main objective, the following sub-objectives are formulated:

- Determine which parameters most significantly influence the performance and environmental impact of offshore monopile installation methods.
- Evaluate the potential of alternative installation and mitigation technologies in reducing underwater noise while maintaining installation feasibility and efficiency.
- Develop a modelling structure that captures the interactions between installation method, mitigation strategy, and project-specific conditions in a transparent and adaptable way, verify its correct functioning through internal consistency checks, and generate outputs that allow direct comparison of candidate installation strategies in terms of noise compliance, technical feasibility (drivability), installation duration, and total cost.
- Quantify and compare the trade-offs among noise compliance, technical feasibility (drivability risk), installation duration, and total cost across representative installation strategies using a consistent set of assumptions and normalised metrics.
- Assess how uncertainties in key input parameters, such as drivability assumptions and noise reduction effectiveness, influence the reliability and robustness of the framework's outcomes.
- Identify the main limitations of the current framework resulting from its underlying assumptions, and suggest priorities for future data collection and framework improvements.

1.4. Methodology for Developing and Applying the Comparative Framework

To meet the objective and sub-objectives outlined in the previous section, a structured and iterative approach has been followed. The methodology is divided into several stages, each contributing to the development, implementation, and evaluation of the comparative decision-making framework.

The report begins with a review of the current state of the art in offshore monopile installation, with a focus on silent installation techniques. This literature study also includes insights from the Specialisation Project previously carried out at NTNU (Wentink, 2024). Where relevant, the information from that earlier study is extended with additional findings and reflections, particularly where it proved incomplete for the current research scope. The chapter concludes with a summary of identified knowledge gaps and a clear definition of this project's scope.

Next, an internal analysis is performed using Van Oord's internal project data. By reviewing both completed and planned installation projects, a better understanding is gained of which parameters influence performance and how different components interact. Based on these insights, a list of assumptions is compiled and knowledge gaps are identified. To address these, experts from various Van Oord departments are consulted. Their input is used to validate assumptions, supplement missing data, and align the framework with operational reality. All assumptions are documented in the report, along with the reasoning or references on which they are based.In parallel, the collected knowledge is translated into a set of components that represent key aspects of the installation process.

Following this, the structured components are brought together in a dynamic model, implemented in both Python and Excel. Excel serves as the input interface and contains fixed project data, while Python is used to process inputs, apply logical relationships between components, and generate the final output. The way this model is structured and how specific calculations, such as the estimation of noise reduction or total cost, are performed, is explained in detail in Chapter 4. The model is also subjected to a series of verification tests to ensure it functions as intended and that the relationships between the components are correctly implemented.

Once verified, the model is applied to a range of case studies. These evaluate the performance of different combinations of installation and mitigation techniques, providing insight into their relative strengths and weaknesses. In addition, sensitivity analyses are performed to assess how the assumptions made earlier in the project influence the model's outcomes, thereby identifying the robustness of the framework under varying input conditions.

The report concludes with a summary of the key findings in Chapter 6, including a reflection on the main objective and the value of the developed framework, followed by practical recommendations for its further development and future use in offshore wind installation projects.

To support future users, a user guide is included in Appendix B. This appendix provides a practical explanation of how to use the framework, how to input project data, and how to interpret the results. It is intended to facilitate further use of the framework within Van Oord, in line with the original goal of enabling structured early-phase decision-making in offshore monopile installation projects.

2

State of the Art in Offshore Monopile Installation

For this graduation project, a literature report was previously written as part of the course TBM4501 Specialization Project at NTNU. Although the scope of the project has since been slightly adjusted and made more specific, the report contains useful and relevant information for this thesis. This chapter briefly highlights the main topics covered in that literature report. The full version, including all referenced sources, can be found in (Wentink, 2024).

2.1. Impacts and Regulation of Underwater Noise on Marine Life

The second and third chapters of the literature report discuss the impact of underwater noise on various marine species, as well as the frequency ranges to which different animals are most sensitive. While this information is important for understanding the broader ecological effects of piling activities, it falls outside the scope of this thesis. Instead, the research presented in this report focuses primarily on harbour porpoises as a representative species, since current government-defined noise regulations are especially based on their hearing sensitivity. This makes them particularly relevant from Van Oord's perspective.

Nevertheless, it is essential to take the regulation of underwater noise into account when developing the model for this project. Since regulations vary significantly between countries, and even between individual projects, this aspect will be implemented as an adjustable parameter in the model, which must always be met.

In many countries, there are no general or harmonized underwater noise regulations. However, Germany is known for having the strictest guidelines. These include threshold values for sound levels: a Sound Exposure Level (SEL) of 160 dB and a zero-to-peak Sound Pressure Level ($L_{p,\text{pk}}$) of 190 dB, both measured at a distance of 750 meters from the source. These thresholds are intended to minimize the risk of Temporary Threshold Shift (TTS) and Permanent Threshold Shift (PTS) in marine mammals. The selection of these specific values is based on scientific studies assessing the hearing sensitivity of various marine species to underwater noise.

2.2. Underwater Sound Metrics and Their Relevance to Installation Techniques

To assess whether an installation technique meets the required underwater noise limits, it is important to understand how underwater sound is measured. The first chapter of the literature report explains how underwater sound is measured and introduces the two main metrics used for this purpose: Sound Pressure Level (SPL) and Sound Exposure Level (SEL).

2.2.1. Sound Pressure Level (SPL)

Sound Pressure Level (SPL) is a measure of the instantaneous intensity of a sound wave and is expressed in decibels (dB) relative to a reference pressure. In underwater acoustics, this reference pressure is typically $1\ \mu$Pa. SPL is useful for describing the average sound level over a given period, which helps in assessing general sound intensity.

The SPL is calculated using the following formula:

$$\text{SPL} = 10 \cdot \log_{10} \left(\frac{1}{T} \int_0^T \frac{p(t)^2}{p_0^2} \, dt \right) \quad [\text{dB re } 1\ \mu\text{Pa}^2] \tag{2.1}$$

where:

- $p(t)$ is the instantaneous sound pressure,
- p_0 is the reference pressure ($1\ \mu$Pa),
- T is the averaging time period.

For impulsive sounds like pile driving, the *zero-to-peak SPL* ($L_{p,\text{pk}}$) is used to capture the maximum instantaneous pressure during the event. This metric is particularly relevant for regulatory compliance and evaluating peak pressure impacts on marine life. It is calculated as:

$$L_{p,\text{pk}} = 20 \cdot \log_{10} \left(\frac{|p_{\text{peak}}|}{p_0} \right) \quad [\text{dB re } 1\ \mu\text{Pa}] \tag{2.2}$$

where p_{peak} is the peak sound pressure. High SPL values, whether averaged or peak, can result in Temporary Threshold Shift (TTS) or even Permanent Threshold Shift (PTS) in marine organisms.

2.2.2. Sound Exposure Level (SEL)

To quantify the total acoustic energy over time, the Sound Exposure Level (SEL) is used. It integrates the squared pressure over the duration of a sound event and normalizes it to a reference time period of 1 second. SEL is especially valuable when comparing different types of exposures, for example, a short loud impulse versus a longer low-intensity noise.

The SEL is calculated as:

$$\text{SEL} = 10 \cdot \log_{10} \left(\frac{1}{T_0} \int_{T_1}^{T_2} \frac{p(t)^2}{p_0^2} , dt \right) \quad [\text{dB re } 1\ \mu\text{Pa}^2\text{s}] \tag{2.3}$$

where:

- $p(t)$ is the sound pressure over time,
- p_0 is the reference pressure ($1\ \mu$Pa),
- T_0 is the reference time (usually 1 s),
- T_1 and T_2 define the sound event duration.

Measurements are typically made using hydrophones, and the pressure data is squared, integrated, normalized, and converted to decibels. This provides a consistent basis for evaluating total sound exposure.

It is also important to highlight that, according to the following report (Bellmann et al., 2020), all German offshore construction projects that met the commonly applied noise limit of 160dB SEL at a 750m distance, based on the 5% exceedance level (SEL_{05}), were also found to comply with the 190 dB zero-to-peak Sound Pressure Level ($L_{p,\text{pk}}$) at that same distance. This indicates a strong correlation between the two metrics and suggests that meeting the SEL threshold typically ensures compliance with peak pressure limits as well.

Although SEL is the official and scientifically accepted way to express total underwater sound exposure, in practice, Van Oord and its clients typically refer to SEL values simply in terms of decibels (dB), without explicitly mentioning SEL or the full reference notation (dB re $1\ \mu$Pa^{2}s). Since the data used in this report is presented in the same manner, this report will, for the sake of consistency and alignment with industry practice, adopt the same convention and express sound levels in dB throughout.

2.2.3. Equal Energy Hypothesis

The Equal Energy Hypothesis assumes that two sound exposures with the same total energy will have the same biological effect, regardless of how that energy is distributed over time. For instance, a 190 dB impulse lasting 1 second and a 160 dB continuous sound lasting 1000 seconds could result in the same SEL. However, studies show that impulsive sounds generally cause more damage than continuous ones at the same energy level. This highlights the importance of considering not just energy, but also the temporal characteristics of sound when assessing environmental impact.

This consideration is especially relevant when comparing offshore monopile installation techniques, such as impact piling and vibratory driving. Impact piling produces high-intensity impulsive sounds, while vibratory driving generates lower-intensity but continuous sound over longer durations. Although impulsive sound is generally more harmful per unit of energy, it is important not to underestimate the potential impact of continuous sound, particularly when it is sustained over extended periods. Lower sound levels do not automatically imply lower ecological risk. Therefore, both the type and duration of sound must be taken into account when evaluating and comparing installation methods.

2.3. Alternative Offshore Monopile Installation Techniques

One of the final chapters of the literature report contains highly relevant information for the remainder of this project. It begins by describing the current standard installation technique: impact piling. This method involves the use of a hydraulic impact hammer, positioned above the pile, which drops a heavy mass to generate a powerful impact that drives the pile into the ground. The technique generates substantial impulsive noise, which can be harmful to the hearing of marine animals. As turbine sizes continue to increase, conventional mitigation techniques alone are no longer sufficient to meet regulatory noise limits. Therefore, the issue must be addressed at the source by developing new types of installation methods. These alternative techniques are introduced in the first part of this section.

Before evaluating these alternatives, it is important to understand the key factors that influence underwater noise generation. While discussed in more detail in the literature report, a brief summary is provided below for context.

2.3.1. Factors Affecting Noise in Pile-Driving

Underwater noise levels depend on both environmental and structural factors. Environmentally, soil type plays a key role through soil coupling, which affects how sound is transmitted or dampened. For example, sandy soils can reduce noise levels by up to 20 dB compared to direct water transmission. Water depth is another important factor, as it determines the cut-off frequency below which sound cannot effectively propagate. Shallow waters tend to dampen low frequencies more strongly. Transmission loss, due to geometric spreading, absorption, and reflection, also reduces sound levels with distance.

Structurally, noise levels are influenced by pile diameter, required driving depth, hammer type and settings, and the duration of installation. Larger piles and greater driving depths require more impact energy, resulting in higher noise emissions. Additionally, the noise characteristics vary with hammer type and operational parameters; for instance, larger hammers used at lower energy produce less intense but broader-frequency sound than smaller hammers at full capacity.

These dependencies highlight the importance of considering site- and design-specific parameters when modelling underwater noise in installation activities. They also influence several key variables within the framework developed in this project and will be further addressed in later sections of this report.

2.3.2. Alternative Low Noise Offshore Monopile Installation Techniques

In the final part of the chapter, five alternative offshore monopile installation techniques, currently still under development, are introduced. These installion techniques include: vibro piling, jetting, combined vibro-jetting, environmental quiet piling (EQ-piling), and vibrotwisting (Gentle Driving of Piles - GDP). For each method, the operating principle, test results (if available), and the corresponding Technology Readiness Level (TRL) are briefly outlined. The TRL scale, ranging from 1 (fundamental research) to 9 (market-ready technology), is used to assess how far each technique has progressed in its development and practical applicability.

Vibro Piling
Vibro piling uses a vibratory hammer to install piles through high-frequency vibrations, reducing friction between the pile and the surrounding soil. It produces significantly less noise than impact piling and is suitable for soft soils. During the KASKASI II project, underwater measurements revealed that the vibratory process consistently produced noise levels of at least 20dB above the background level, with sound remaining detectable up to 15kilometers from the source. While such levels naturally result in some degree of disturbance to marine life compared to non-operational conditions, they are clearly lower than the peak noise levels typically produced by impact piling.

Moreover, the noise spectrum was observed to evolve during the installation process. It initially featured low-frequency components at relatively low amplitudes, transitioning to higher-frequency sounds with increased amplitudes as the pile driving progressed. These shifts were associated with temporary interruptions in the vibratory process due to increasing soil resistance. Rather than indicating a disadvantage, this behavior demonstrates the adaptive interaction between the vibratory system and varying soil conditions.

Vibro piling has now reached Technology Readiness Level (TRL) 9 and is already being applied in commercial offshore projects, including by Van Oord at the Ecowende wind farm.

Jetting
Jetting involves injecting high-pressure water at the pile base to reduce soil resistance and facilitate installation. It is often combined with mechanical methods for improved efficiency. During the Gode Wind 3 project, jetting demonstrated a remarkable reduction in underwater noise levels; up to 34 dB lower than conventional installation methods. Even without the use of additional mitigation measures, noise levels were reduced to just above the ambient noise typical of the German Bight. These results highlight the significant environmental benefit of jetting as a low-noise installation technique.

In addition to its acoustic advantages, jetting also shows promise for increasing installation efficiency. This was demonstrated through the successful installation of next-generation wind turbines of up to 11 MW on the foundations at Gode Wind 3. The technique performed particularly well in sandy seabeds, confirming its suitability for such soil conditions. However, it should be noted that the effectiveness of jetting decreases significantly in cohesive soils such as clay, where water injection alone may be insufficient to overcome soil resistance.

Jetting is currently at Technology Readiness Level (TRL) 7, pending further validation in a wider range of soil types and project environments.

Combined Vibro-Jetting
This method integrates vibro piling and jetting, combining vibration and water injection to improve drivability and reduce noise. Developed by GBM Works under the SIMPLE program, it has shown promising results in dense sandy soils, achieving up to three times greater installation depth and four times faster progress compared to vibro piling alone. Strain measurements have also indicated substantial noise reduction during installation. A water flow control system has been developed to minimise potential impacts on lateral bearing capacity.

At the time of writing the Specialization Project, SIMPLE III was still planned to validate the technology offshore using 4-meter diameter, 62-meter long piles. Since then, the offshore trials have been successfully completed: the pile was driven to target depth, and the results were promising. Vibrojet is currently at TRL 7, with commercial deployment expected in 2026.

Environmental Quiet Piling (EQ-Piling)
EQ-Piling, developed by IQIP, uses a heavy water tank to deliver a cushioned impact to the pile, extending the impact duration and thereby reducing peak noise levels. Simulations show significant reductions in both sound exposure and pressure levels, often eliminating the need for additional mitigation

measures such as bubble curtains. This lowers project costs and simplifies logistics. The method is environmentally friendly, requiring fewer vessels and less energy, and aligns with long-term climate goals. Additionally, the smooth force application reduces pile fatigue by up to 90%, extending foundation lifespan. EQ-Piling is currently at TRL 6 and remains in an advanced testing phase, aiming to support the installation of larger monopiles in more challenging soil conditions.

Vibrotwisting: Gentle Driving of Piles (GDP)
GDP combines low-frequency axial and high-frequency torsional vibrations to reduce soil resistance and noise during pile installation. A specially designed shaker mobilizes soil shear resistance in a circumferential direction, lowering friction along the pile and reducing the energy required for installation. Medium-scale field tests at the Maasvlakte II site in Rotterdam demonstrated efficient installation and high penetration rates in dense soils, with no refusal and comparable energy consumption to conventional methods. The technique achieved faster installation while maintaining control and stability, highlighting its potential as a sustainable and innovative alternative for offshore applications. GDP is currently at TRL 5 and requires further development and offshore validation.

2.4. Noise Mitigation Techniques

The chapter following the installation techniques in the literature report is also highly relevant to this project. It addresses a range of noise mitigation techniques that can be applied in conjunction with both conventional and alternative installation methods. In the later sections of this report, the mitigation techniques most frequently applied by Van Oord will be discussed in more detail, as these are considered particularly relevant for inclusion in the model. These techniques can be broadly classified into three categories: at-source hammer dampers, near-field mitigation, and far-field mitigation.

Each of these mitigation categories represents a different approach to reducing the propagation of underwater noise, based on their position relative to the noise source. At-source mitigation methods, such as internal dampers, aim to reduce noise generation at the origin, typically the pile-driving equipment itself. Near-field mitigation involves techniques applied in the immediate surroundings of the monopile, for instance AdBm or isolation casings placed close to the structure. These serve to attenuate the sound before it propagates into the wider marine environment. Finally, far-field mitigation strategies operate at a greater distance from the pile, often by creating secondary barriers, for example, outer bubble curtains, that intercept and scatter sound waves further away from the source. In Figure 2.1, these three types of mitigation are illustrated in the context of offshore installation operations.

As part of the literature study, an overview was compiled of the most established and commonly applied mitigation systems. In several cases, their effectiveness was supported by results from experimental testing. Based on consultation with environmental specialists at Van Oord, a selection was made of the techniques most commonly used in practice, and therefore most relevant for incorporation into the modelling framework.

This selection also includes several systems that were not yet extensively discussed in the literature report, or that deviate somewhat from the standard classifications. For that reason, all mitigation systems considered in the framework will be described in more detail in the following subsections.

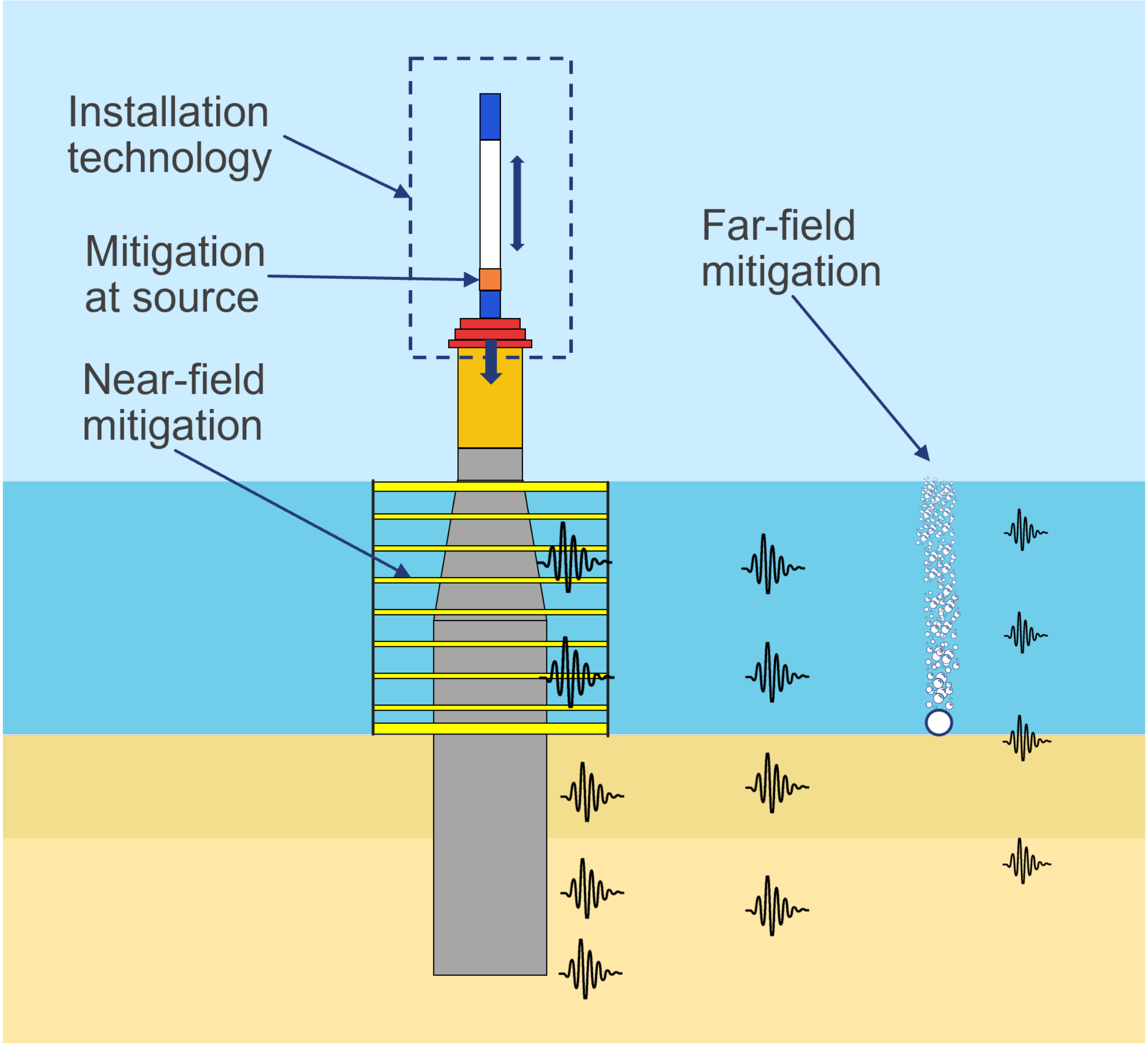

Figure 2.1: Overview of underwater noise mitigation strategies during monopile installation. Mitigation at the source addresses noise generation directly. Near-field mitigation surrounds the pile to block or absorb sound close to the structure. Far-field mitigation is positioned at a distance to further reduce noise propagation (Oord, 2025).

2.4.1. IQIP Pulse

PULSE is an at-source noise mitigation technology developed by IQIP to reduce underwater noise during pile driving. It consists of two plungers with a fluid layer in between, placed directly between the hammer and sleeve. This setup allows for adjustable stiffness during installation, enabling real-time optimization of noise reduction without compromising drivability or installation speed (IQIP, 2020).

Tests have shown that PULSE alone can reduce the Sound Exposure Level (SEL) by 6 to 9 dB and the peak Sound Pressure Level (SPL$_{z\text{-}p}$) by 9 to 12 dB, with greater reductions for larger hammers. When combined with IQIP's Integrated Monopile Installer (IMI), PULSE can eliminate the need for external bubble curtains.

In addition to noise reduction, PULSE significantly decreases fatigue damage in the pile (up to 60%) and avoids the use of additional vessels or compressors, making it a cost- and energy-efficient solution for offshore wind projects.

Figure 2.2: Integration of IQIP PULSE system in offshore monopile installation (IQIP, 2020).

2.4.2. MENCK Noise Reduction Unit (MNRU)

The MENCK Noise Reduction Unit (MNRU) is an at-source noise mitigation system integrated into MENCK's hydraulic hammers (MHU). It actively reduces underwater noise during pile driving by modifying the force-generation characteristics of each hammer strike. This reduces the peak noise levels by 9 to 12 dB, equivalent to a reduction of more than 80% in acoustic energy (Acteon, 2024).

By softening the impact without compromising drivability, the MNRU also reduces fatigue damage to the pile. This benefit may enable more efficient pile design and lead to material and cost savings. As an integrated solution, the MNRU requires no external equipment or vessels, making it a compact and efficient tool for reducing environmental impact during offshore construction.

Figure 2.3: MENCK Noise Reduction Unit (MNRU) deployed around a monopile offshore (Acteon, 2024).

2.4.3. Hydro Sound Damper (HSD)

The Hydro Sound Damper (HSD) is a near-field noise mitigation system designed to reduce underwater sound during offshore piling. It consists of gas-filled elastic balloons and polyethylene foam elements mounted on a ballasted net, which is deployed around the pile frame on the seabed (Koschinski and Lüdemann, 2020).

As a passive system, the HSD does not rely on external energy sources such as compressors. Instead, noise is reduced through physical mechanisms including absorption, scattering, material damping, and sound reflection at the water-to-air interface.

The system can be tuned to target specific frequency ranges by adjusting the size and composition of the damping elements. Larger components are suited for lower frequencies, while different balloon sizes are used to compensate for increased hydrostatic pressure in deeper waters. Its flexible net basket design allows for adaptation to various pile sizes and site conditions (Elmer, 2018).

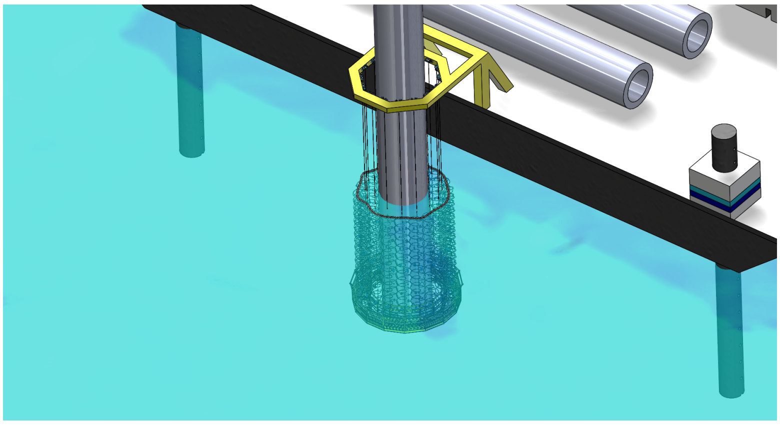

Figure 2.4: Visualisation of an installed HSD-System. (OffNoise-Solutions, n.d.)

Figure 2.5: Layered HSD-Net with sound-absorbing elements to reduce underwater noise. (OffNoise-Solutions, n.d.)

2.4.4. AdBm Noise Abatement System

The AdBm Noise Abatement System is a near-field noise mitigation technology that reduces underwater sound through arrays of tuned Helmholtz resonators. These resonators are optimized to absorb acoustic energy at specific frequencies, making the system particularly effective at targeting dominant noise components during offshore piling and other marine operations (AdBm Technologies, 2024).

The system is passive by default and does not require compressors or active power input. Its modular design is lightweight, flexible, and suitable for deployment under pile grippers, seabed frames, or templates. AdBm's approach is customizable in terms of resonator configuration, target frequency range, and structural integration, with optional bubble curtain support for enhanced high-frequency attenuation.

The technology has been proven to operate at water depths up to 40m, with capability beyond 100m. It meets European regulatory standards, offers rapid deployment times, and is supported by in-house modeling and acoustic expertise. Designed with logistical and environmental efficiency in mind, the system can be produced locally and leased to fit individual project needs.

Figure 2.6: AdBm system with Helmholtz resonators for underwater noise mitigation (AdBm Technologies, 2024).

2.4.5. IQIP NMS DG-12000

The IQIP Noise Mitigation System (NMS) DG-12000 is a near-field mitigation solution designed for XXL monopiles, building on the proven NMS architecture (NMS-8000/8800/T-10000) (IQIP, 2023, 2024). It consists of a double-walled steel screen with an air-filled annulus and multi-level bubble curtains, which attenuate underwater noise by creating strong acoustic impedance differences and reflecting sound.

The DG-12000 variant is engineered to accommodate monopiles up to 12m in diameter. Due to its substantial size, the system alone weighs approximately 2,000t, with the supporting frame adding another 600t, bringing the total to around 2,600t. The enormous deck footprint also typically reduces monopile carrying capacity by one per voyage, impacting logistics compared to more compact systems.

This system is typically deployed from floating vessels and includes integrated features to maintain pile alignment (inclination, rotation, leveling). Despite its heavy weight and space demands, the DG-12000 remains a crucial tool for offshore wind projects facing strict noise regulations, offering robust near-field attenuation (IQIP, 2023).

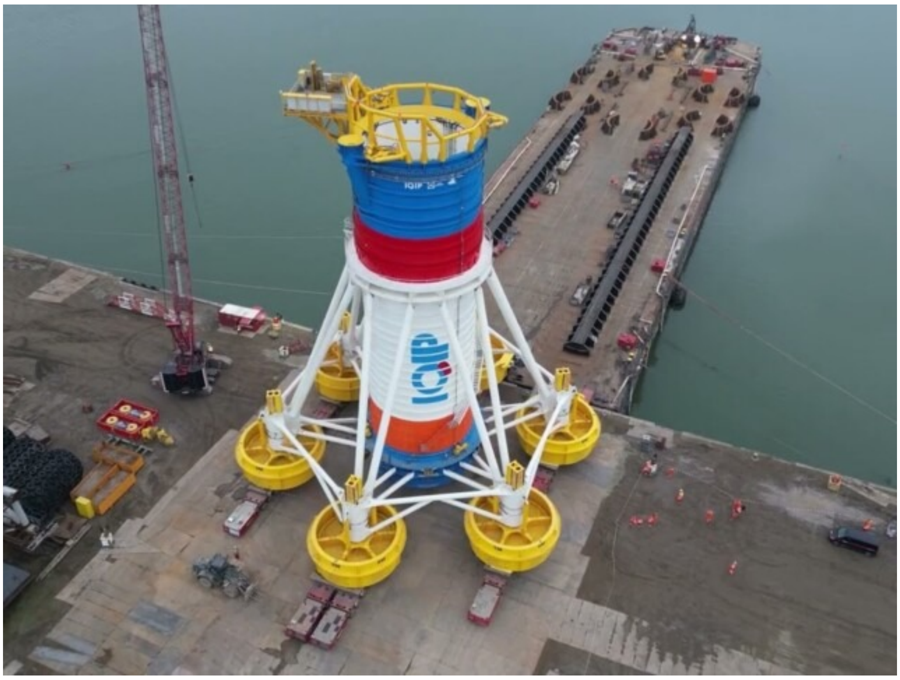

Figure 2.7: IQIP NMS-T-10000 during onshore assembly at Heerema yard (IQIP, 2024)

2.4.6. Bubble Curtains

Bubble curtains are classified as far-field noise mitigation systems. Rather than acting directly at the source or in the immediate vicinity of the pile, they mitigate underwater sound further outward by disrupting its propagation through a vertical curtain of air bubbles rising from the seabed. These systems are typically applied around the pile or installation frame and are especially effective in reducing sound transmission over larger areas during offshore piling activities.

Four common configurations can be distinguished: the single bubble curtain, double bubble curtain, and their enhanced variants. While all share the same fundamental working principle, they vary in complexity, installation effort, and effectiveness.

Single Bubble Curtain

The single bubble curtain is the most basic form, consisting of a single perforated hose placed on the seabed around the pile. Air is continuously pumped through the hose, producing a rising wall of bubbles that scatter and reflect underwater sound at the water–air interface. The system is quick to deploy, relatively inexpensive, and widely used (Atlas Copco Specialty Rental, 2025). However, its effectiveness may be reduced in strong currents or under high acoustic loads, as gaps in the bubble wall can allow sound to pass through.

Double Bubble Curtain

The double bubble curtain builds upon the single configuration by incorporating a second concentric hose, forming two layers of bubbles. This layered structure enhances acoustic shielding by increasing the path length and density of the bubble barrier. According to (Atlas Copco Specialty Rental, 2025), under ideal and controlled conditions, such systems can theoretically achieve up to 95% sound mitigation. However, in practical offshore environments, this level of performance is rarely achieved due to variability in current, depth, and pile geometry. The double curtain setup requires more deck space and installation time, and is generally regarded as the most logistically intensive bubble curtain variant. Nevertheless, it is widely applied and considered a best practice in modern offshore piling (Secretariat, 2019).

Enhanced Bubble Curtain

Enhanced bubble curtains refer to any bubble curtain system-single or double-that incorporates performance-improving features such as variable bubble sizes, multi-depth nozzle arrangements, or containment structures to stabilize the bubble plume in dynamic water conditions (Atlas Copco Specialty Rental, 2025). These enhancements extend the effective frequency range of the system and improve noise mitigation under strong currents or complex seabed geometries. While the use of such features increases the engineering effort and deployment complexity, they can significantly improve performance, particularly when targeting specific frequency bands or working in challenging conditions.

The choice between configurations depends on site-specific factors such as current velocity, water depth, environmental thresholds, and logistical constraints. More advanced systems offer better acoustic shielding but require a careful balance between performance gains and operational feasibility.

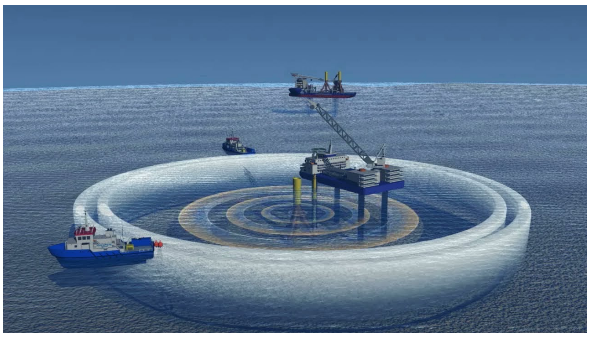

Figure 2.8: Double Bubble Curtain (Lewis, 2023)

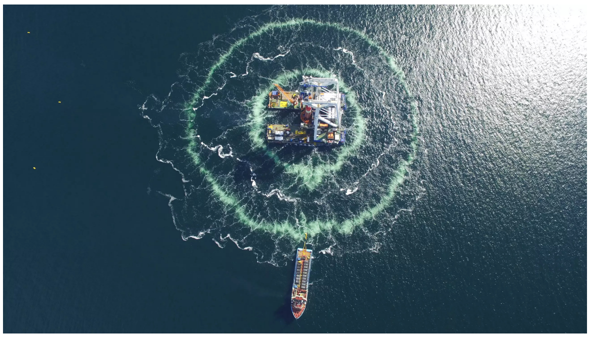

Figure 2.9: Bubble Curtain in Use (Hydrotechnik Lübeck GmbH, 2024)

An overview of all mitigation techniques is also presented in a table in Section 3.6, including the assumed noise reduction values based on practical experience within Van Oord. These assumptions are explained in more detail in the corresponding chapter.

2.5. Identified Gaps and Scope of the Project

As outlined in the preceding sections, both the development of low-noise installation techniques and the application of underwater noise mitigation systems have advanced significantly in recent years. However, there is currently no structured approach to evaluate their combined impact on installation duration, underwater noise levels, and overall project costs.

This lack of integration poses a challenge for contractors such as Van Oord, who are required to make critical early-phase decisions based on limited or fragmented information. There is a clear need for a practical, project-specific method that brings together technical performance, regulatory compliance, and financial feasibility. Such an approach would enable more informed decision-making that balances environmental responsibility with commercial considerations.

Given the broad range of technologies under development and the limited scope of this graduation project, the focus was placed on comparing vibro piling and combined vibro-jetting. These methods were selected due to their relatively high Technology Readiness Levels, anticipated application in upcoming Van Oord projects, and the availability of relevant internal expertise and data. Conventional impact piling is included in the framework as a benchmark to provide a clear reference point.

In total, the comparative framework includes four installation techniques: conventional impact piling using the IQ6 and MHU6000W hammers, vibro piling, and combined vibro-jetting. As two distinct variants of impact piling, both the IQ6 and MHU 6000W hammers are separately assessed within the framework to capture their respective technical and operational characteristics.

The IQ6 hammer, developed by IQIP, is currently the largest hydraulic impact hammer in the world and part of IQIP's IQ-series. It is specifically designed for the installation of the next generation of offshore wind foundations, suitable for turbines of up to 16MW and even 20MW in the near future. With a maximum energy of 6600kJ, the IQ6 is capable of installing the largest monopiles. The hammer dynamically adjusts its energy output to match driving conditions, enabling more efficient and stable installation. Furthermore, the system can be combined with PULSE technology to reduce underwater noise, pile fatigue, and operational costs (WindpowerNL, 2023).

The MHU 6000W from MENCK, part of Acteon, is the most powerful hydraulic impact hammer developed by the company, with a maximum energy output of 6250kJ. Although slightly smaller than the IQ6, it remains one of the largest hammers available on the market and is suitable for monopiles with diameters of 9 metres or more. The system features a double-acting hydraulic drive, closed-loop control system, and shock absorber cartridges. It is connected to a digital platform that provides offshore operators with real-time data and uses environmentally friendly lubricants to reduce environmental impact (Group, 2025).

While both hammers are designed for the installation of extremely large monopiles, they differ in several relevant technical and operational aspects. The MHU 6000W is more compact, lighter, and less expensive than the IQ6. Due to its lower mass and smaller dimensions, the MHU 6000W requires a higher blow frequency to achieve equivalent pile-driving performance. This difference in blow rate may affect underwater noise emissions, pile fatigue, and overall installation duration. For these reasons, both hammers are included in the comparative framework, allowing an investigation into how these design characteristics influence total performance, cost, and environmental footprint.

The next chapters describe the development, structure, and implementation of the comparative framework, followed by case-specific results that demonstrate its value in supporting early-stage selection of offshore monopile installation strategies.

3

Data Analysis and Assumptions for Offshore Monopile Installation

The previous chapter outlined the current state of offshore monopile installation technologies and methodologies based on existing literature. While this provides valuable context, practical implementation often involves additional complexities that are only visible in real project data.

This chapter analyses internal project data from Van Oord to better understand how monopile installations are performed in practice. These insights help identify key dependencies, constraints, and influencing factors, providing a solid foundation for modelling installation strategies within the comparative framework developed in this study.

3.1. Assessment of Existing Knowledge

A preliminary assessment of internal Van Oord data was performed to evaluate conventional impact piling alongside emerging techniques such as vibro piling and combined vibro-jetting, in combination with various near-field and far-field noise mitigation measures.

3.1.1. Insights from Internal Projects and Studies on Developing Installation Techniques

As a starting point, data on impact piling was particularly relevant, since this method has been applied in multiple executed projects within Van Oord. This made it the most reliable and complete dataset, offering a clear picture of the typical activities, durations, and cost drivers involved in offshore monopile installation. Based on this, an initial structure was developed to define which components and relationships should be included in the comparative framework. The framework was divided into the following seven components, each representing a key aspect of the installation process:

- **General Input:** project-specific parameters such as soil type, water depth, and selected installation technique.
- **Weight:** weights of monopiles and equipment, affecting logistics and vessel capacity.
- **Operation Times:** durations of individual activities throughout the installation cycle.
- **Drivability:** Indicates the risk that the chosen installation method may not achieve the required penetration depth.
- **Noise - Installation Techniques:** noise levels generated by different installation methods.
- **Noise - Mitigation Techniques:** noise reduction achieved by various mitigation systems.
- **Costs:** cost estimates for equipment, vessels, operations, and mitigation.

These components are discussed in more detail in Section 3.1.3.

To gain insight into developing installation methods, the most relevant input was obtained from internal Van Oord studies, in which several techniques were assessed using shared reference cases. The findings provided valuable input on which parameters influence installation performance, how operational sequences and durations vary, and how vessel layout and capacity affect both time and cost under different project conditions.

In particular, these internal studies offered fixed durations for specific operations associated with alternative techniques, which could be directly incorporated into the framework. They also clarified how these durations are influenced by parameters such as soil type, monopile diameter, penetration depth, vessel type, and the number of foundations carried per trip. As such, they contributed both structural insight for the framework's logic and a practical basis of input values for its implementation.

3.1.2. Development of a Preliminary Model Structure

In addition, data from these internal sources was used to develop initial ideas for a suitable structure of the framework. A Python model was created based on this data, with the idea that the user can enter input parameters such as the installation method and project characteristics, and receive output in the form of operational time and corresponding costs.

Through this process, it was quickly found that a combination of Excel and Python provides the most effective approach. Excel is considered well suited for storing all fixed values related to monopile installation, such as standard equipment weights, typical durations for specific operations, and fixed costs for certain activities or equipment. It is also more user-friendly for managing and updating such values.

Python, on the other hand, is used to link these components together into a single dynamic model. Based on the user-defined input, which is entered in Excel, Python generates the appropriate output by importing the necessary fixed values. This allows for the evaluation of different cases using project-specific input parameters.

3.1.3. Input From Internal Experts to Address Knowledge Gaps

The previous subsection outlined the starting point of this study and described how initial insights were gained into the key parameters relevant for the comparative framework, as well as how the model could best be structured. By breaking the framework down into separate components, it also became clear which information was still missing and needed to be gathered in order to enable a meaningful comparison across different installation approaches.

To obtain this missing information, specialists from a wide range of departments and teams within Van Oord were consulted. These interviews quickly revealed the broad scope of the project. The strength of the framework lies in integrating many technical and logistical aspects into one coherent evaluation method. At the same time, it became evident that going too far into detail would not serve the purpose of the project. The goal is not to build a detailed engineering model but to support early-stage evaluations and comparisons between strategies.

As a result, many elements in the framework were simplified or represented through clearly defined assumptions. The next sections provide an overview of the departments involved in the interviews, the insights they contributed, and the assumptions that were made. It also explains why these assumptions are appropriate within the context of this study.

3.2. Assumptions for General Input Parameters

As part of developing the framework, it was necessary to determine which general input parameters would be included. This immediately raised the challenge of managing the broad scope of offshore monopile installation while maintaining a focused and workable model. Given the complexity of the subject and the limited time available for this study, a number of assumptions were made to keep the framework both practical and consistent.

The subsections below describe and justify the key assumptions applied to the general input parameters, including choices related to the installation techniques, soil conditions, monopile dimensions, vessel selection, and other representative project characteristics.

3.2.1. Installation Techniques

As introduced in Section 2.5, the framework includes four primary installation techniques: the IQ6 hammer, the MHU6000W hammer, vibro piling, and combined vibro-jetting. For impact piling, full penetration of the monopile is generally achievable. However, for vibro piling and vibro-jetting, there is currently no guarantee that the monopile can reach full depth using these methods alone, especially in challenging soil conditions.

To reflect this uncertainty, the framework also includes combined installation cases in which an impact hammer and its associated equipment are available onboard alongside the vibro system. In such cases, the vibro technique is applied during the initial phase of the installation, and if resistance becomes too high, the impact hammer is used to complete the final part of the driving process.

This results in eight installation cases evaluated in the framework:

Table 3.1: Overview of Installation Techniques and Combinations Considered in the Framework

Installation Technique	Configuration
impactIQ6	Individual
impactMHU	Individual
vibro	Individual
vibrojet	Individual
impactIQ6 + vibro	Combined
impactIQ6 + vibrojet	Combined
impactMHU + vibro	Combined
impactMHU + vibrojet	Combined

However, to enable a consistent comparison between these techniques, the framework assumes in all cases that the monopile can be installed to full depth without refusal or the need for prolonged interruptions. This also includes the theoretical cases where only vibro piling or vibro-jetting is applied. While this assumption facilitates a direct comparison of technical, cost, and noise performance, it does not necessarily reflect operational feasibility and should therefore be interpreted with caution.

To account for this limitation, a drivability factor is included in the framework for these techniques. This factor serves to reflect the increased uncertainty regarding full-depth installation when using vibro-based methods. Further details on the definition and application of this factor are provided in Section 3.5.

3.2.2. Soil

Following discussions with several specialists at Van Oord, a standard sandy soil profile was selected as the basis for the framework. This decision was primarily driven by the limited availability of reliable drivability data for vibro piling and vibro-jetting in non-sandy soil types, particularly at commercial scale. In contrast, for sandy soils, reasonable estimates could be made in consultation with a geotechnical engineering expert. These assumptions are further explained in Section 3.4.

Vibro-jetting is currently not suitable for use in cohesive soils such as clay. The method relies on high-pressure water jets to reduce soil resistance during installation, which is effective in non-cohesive soils like sand but fails in dense, water-resistant clay layers. Although research is ongoing to develop variants of vibro-jetting that can be applied in clay, the current technology remains limited to sand-dominated conditions. This supports the decision to assume a sandy seabed, ensuring consistency and realism in the evaluation of installation techniques.

Additionally, a statistical analysis of offshore construction projects in the German EEZs of the North Sea and Baltic Sea, as reported in (Bellmann et al., 2020), found that underwater noise levels in the Baltic Sea were up to approximately 2dB higher than those in the North Sea, despite comparable pile designs and blow energies. This difference is likely due to the more heterogeneous seabed composition in the Baltic Sea, which often includes alternating layers of sand, till, and chalk. In contrast, the North Sea typically features more homogeneous sandy soils. These findings highlight that seabed composition can significantly influence both drivability and noise emissions during installation, reinforcing the value of expanding the framework to cover a broader range of soil conditions in the future.

3.2.3. Turbine Size

Many of the assumptions used in the framework are based on what is currently most commonly applied within Van Oord. This approach was chosen not only because it provides the most reliable and complete dataset to build the framework on, but also because it ensures that the output remains realistic and aligned with present-day project conditions.

For this reason, the framework assumes a turbine size of 15MW. This capacity reflects the average turbine size currently being installed in offshore wind projects such as Hollandse Kust West (HKW) and the Nordseecluster (NSC). Fixing the turbine size is essential, as it directly determines the required monopile dimensions. In current industry practice, a 15MW turbine typically requires a monopile weighing approximately 1,600 to 2,000tonnes. This, in turn, defines critical aspects of the installation campaign, such as deck layout, vessel selection, and lifting capacity. The framework is therefore based on a representative monopile configuration capable of supporting a 15MW turbine, ensuring internal consistency across all related assumptions.

3.2.4. Installation Vessel & Crane Capacity

For similar reasons as those applied to the turbine size, the offshore installation vessel Boreas was selected as the fixed installation vessel within the framework. The new generation of heavy monopiles exceeds the operational capabilities of vessels such as the offshore installation vessel Aeolus, particularly regarding lifting capacity and deck space. Consequently, the current framework is fully based on the Boreas, both in terms of deck layout and cost assumptions.

This decision was made because internal feedback at Van Oord indicated that the Aeolus is currently facing operational challenges, and most upcoming projects are planned using the Boreas. Therefore, it made the most sense to use this vessel as the basis for the initial version of the framework.

In line with this, the Boreas is equipped with a main crane with a maximum lifting capacity assumed at 3250 tonnes at a 39-metre radius. This value has been adopted as the default crane capacity throughout the framework. It represents the maximum allowable hook load under specific offshore operational conditions, as defined by the crane manufacturer.

This capacity includes a Dynamic Amplification Factor (DAF), which in this case is assumed to be 1.1. The DAF accounts for additional dynamic forces caused by vessel motion, wave action, and load swinging. The specified lifting capacity also applies only under a defined maximum wind speed; if wind conditions exceed this limit, lifting operations must be postponed or modified to ensure safety.

Furthermore, the actual weight lifted includes not only the load itself (e.g., the monopile) but also the rigging and lifting gear between the crane hook and the load. In more demanding sea states, a higher DAF may be applicable, which further reduces the effective lifting capacity. These aspects should be considered in detailed project-specific assessments or when adapting the framework for alternative vessel configurations.

3.2.5. Water Depth to LAT

Water depth plays a critical role in multiple aspects of the offshore installation process. When installing in deeper waters, the crane must reach further and higher to lower the monopile from the vessel deck to the seabed. This increased reach affects the crane loading and vessel stability, and typically results in longer lifting durations.

For jack-up vessels such as the Boreas, water depth also significantly affects the jacking operation. As depth increases, longer leg extension is required before the vessel reaches its elevated working position, which directly increases jacking time.

A constant water depth of 40 metres is assumed in this model. This value was determined in consultation with a specialist from Van Oord, based on its representativeness for ongoing offshore wind farm developments in the North Sea. As the primary objective of the framework is to compare different installation methods for a specific wind farm site, it is necessary to fix the water depth in order to ensure consistency and comparability across all scenarios. The monopile dimensions used in the framework, comprising length, diameter, weight, and penetration depth, are defined in accordance with this reference condition.

If water depth were to increase, the required monopile length would also increase, resulting in heavier foundations. This would reduce the number of foundations that can be transported in a single trip, extend the required penetration depth, and may necessitate changes in the installation strategy. In addition to logistical and structural implications, water depth also affects the performance and feasibility of underwater noise mitigation systems.

Big Bubble Curtains (BBC), for example, are considered effective up to approximately 45 metres. However, above 40 metres, the required air volume increases substantially due to higher hydrostatic pressure, which complicates deployment and may reduce effectiveness. Hydro Sound Dampers (HSD) are typically suitable up to similar depths and provide consistent attenuation, particularly at lower frequencies, independent of current or depth. IHC Noise Mitigation Systems (IHC-NMS) have been successfully used at depths up to around 40 metres and offer omnidirectional attenuation unaffected by current or depth. Nonetheless, the system length is fixed, which limits adaptability in areas with significant depth variation. In general, most mitigation techniques are most effective up to about 40 to 45 metres. Beyond that, technical and operational challenges arise that often require system modifications or combined solutions (Cefas Noise and Bioacoustics Team, 2020).

By selecting a realistic and representative fixed water depth, the model ensures consistency across monopile design, vessel operations, and installation planning. It also guarantees that the noise mitigation systems assumed in the framework remain practically feasible. This allows the framework to produce technically coherent results that align with the depth ranges typical of current offshore wind projects in the North Sea.

3.2.6. Currents

In this framework, offshore currents are assumed to be negligible, meaning that the current is set to zero. This simplification was made to reduce model complexity and maintain focus on the comparative assessment of installation and mitigation techniques. Accounting for current would require vessel-specific responses and case-dependent parameters, such as dynamic positioning capabilities and soil interaction during pile lowering, which fall outside the scope of this generalised model.

Nevertheless, it is important to acknowledge that in real offshore conditions, currents can significantly influence various aspects of the installation process. Lateral forces caused by current can induce movement of the monopile during free-hanging lowering, reducing placement accuracy and increasing operational risks. Jack-up vessels may also be affected, as hydrodynamic loading on the jacking legs, especially when extended, can impact positioning precision.

The sensitivity to current can vary between installation methods. For example, vibratory piling in non-cohesive soils such as sand often results in limited lateral support during the early stages of installation, making the pile more susceptible to hydrodynamic loading (Achmus et al., 2020). Jetting-based techniques may also be affected, as horizontal currents can disturb the targeted distribution of the jetting fluid, reducing the efficiency and accuracy of the process. In general, installation methods with longer durations are more prone to current-induced deviations or delays.

In addition to affecting the installation process, currents also influence the performance of noise mitigation systems. Bubble curtains, for instance, depend on a stable vertical column of rising air bubbles, which can be disrupted or carried away by horizontal flow, reducing their effectiveness. Similarly, hanging screens and encapsulated net systems may deform or shift under lateral loads, compromising both their positioning and sound attenuation capabilities. Studies indicate that sound reduction performance typically declines at current velocities exceeding approximately 0.75 m/s, especially in the direction of the current, due to the drifting of bubbles and other mitigation elements (Cefas Noise and Bioacoustics Team, 2020).

Although current effects are not included in the present version of the framework, this omission is consistent with the high-level and comparative nature of the analysis. The framework is intended as a first-step evaluation tool to compare installation methods under uniform conditions. Prior to the final selection of an installation strategy for a specific project, more detailed and site-specific studies, including the influence of tidal and oceanic currents, are essential.

3.2.7. Pile Diameter

Several aspects of the installation process depend on the diameter of the monopile. The pile diameter directly influences the total weight on deck, which in turn affects the number of foundations that can be transported per trip and thus impacts the total operational time.

Additionally, pile diameter plays a role in drivability. Larger piles experience greater soil resistance, requiring more energy to install. This not only affects the driving speed and overall installation time but also influences the amount of noise generated during pile driving.

It is also important to note that the choice of pile diameter can be influenced by the installation technique due to differences in bearing capacity observed between impact driving and vibratory installation methods. Studies on large-diameter open-end steel pipe piles, have shown that vibratory installed pipe piles may exhibit up to approximately 50% reduction in bearing capacity compared with sister piles installed by impact driving (Lamiman and B. Robinson, 2022). This capacity loss is believed to result from the disturbance of soil around the pile shaft and tip during vibratory installation, affecting shaft resistance and tip bearing. While the magnitudes and exact behavior may differ for monopiles specifically designed for offshore wind turbines, these findings provide a useful indication of the potential impact vibratory installation can have on bearing capacity. Consequently, in practice, piles installed with vibratory methods might require larger diameters or alternative design approaches to meet capacity requirements. However, the detailed implications of pile diameter variation based on installation method and corresponding capacity effects are beyond the scope of this project.

To keep the scope of the model manageable and the development process feasible within the available timeframe, a standard monopile diameter of 9m was selected. This choice is based on the availability of relevant internal data within Van Oord regarding deck layouts, drivability, and noise production or reduction for this pile size. Furthermore, 9m is a commonly used diameter in current offshore wind projects, which ensures that the framework generates realistic and practically relevant output.

3.2.8. Weather Workability

The actual operational time is significantly affected by weather workability and must therefore be accounted for within the framework. While detailed analyses based on historical metocean data and probabilistic modelling are possible, weather-related delays are incorporated in this framework in a simplified yet realistic manner.

In consultation with specialists at Van Oord, it was established that a base weather workability of 80% is a reasonable average for general offshore operations. This value is adjusted depending on the type of vessel used. For large offshore installation vessels such as the Boreas, a conservative reduction of 5% is applied, resulting in an effective availability of 75%. For smaller vessels such as the Aeolus, the reduction may be up to 10%, yielding an availability of 70%. However, only the Boreas is considered in the current version of the framework.

To reflect seasonal variability, the model applies monthly weather workability factors based on the project's start month, which can be specified in the *General Input* sheet in the Excel file. The project timeline is divided into 30-day periods that correspond to calendar months. Each period is then classified as either a summer or winter month, based on typical North Sea conditions:

- **Summer:** May to September
- **Winter:** October to April

For each period, a weather workability percentage is applied:

- **Summer months:** 80%
- **Winter months:** 65%

These values can be manually adjusted in the *General Input* sheet to reflect project-specific weather conditions. To account for weather-related delays, the actual number of calendar days required to complete the calculated work duration is obtained by dividing the number of effective working days by the applicable workability factor. If the remaining duration in the final period is less than 30 days, it is proportionally adjusted using the same logic.

By summing all weather-adjusted periods, the framework derives the total adjusted installation duration. This approach enables the model to incorporate seasonal effects more realistically than applying a single uniform correction factor across the entire schedule.

3.3. Assumptions for On-Deck Weight

To gain insight into the typical weight distribution of offshore monopile installation equipment, the deck layouts from three Van Oord projects were analysed:

- **Nordseecluster (NSC):** In this project, all monopiles are installed using an IQ6 impact hammer. The monopiles have an average diameter of 9 metres.

- **Hollandse Kust West (HKW):** This is Van Oord's first commercial project in which vibro piling is applied as the primary installation method. However, earlier tests showed that vibro piling alone was not always sufficient to reach full penetration depth. As a result, an MHU impact hammer is also included on deck, making this project a representative example of a combined installation case. The monopiles in this project also have an average diameter of 9 metres.

- **SIMPLE III:** This R&D project was conducted in collaboration with GBM Works, CAPE, and several other partners, and involved the offshore installation of a 4-metre diameter monopile using a vibro-jetting system. As this was a pilot-scale project carried out using a smaller vessel, its deck layout must be scaled up to reflect the operational context of a full-scale offshore wind installation.

From these three projects, the equipment located on deck was identified and categorised into shared and method-specific items. For instance, certain components such as cranes, lifting tools, and safety equipment are present in all configurations, regardless of installation technique. In contrast, installation-specific components such as impact hammers, vibro units, or jetting skids vary depending on the applied method.

The data analysis incorporates several assumptions to ensure consistency and relevance within the comparative framework. One key consideration is the number of monopiles that can be transported per vessel trip, as this directly influences the total number of trips and the corresponding installation time. This number is primarily determined by the vessel's weight capacity and available deck space.

Jack-up vessels have a maximum elevated weight capacity that includes not only installation equipment and foundations, but also fuel, ballast water, personnel, and other operational loads. For example, the Boreas has an elevated weight capacity of XXXXX metric tonnes. Since this framework focuses exclusively on comparing different installation strategies, many of these broader operational elements are deliberately excluded. Only the weight of the deck equipment is taken into account.

To reflect this simplified scope, a reduced maximum weight threshold of 15,000 mT was assumed for the deck-related equipment. This assumption was discussed and agreed upon in consultation with a specialist from Van Oord's Operations Department, and is considered a realistic operational upper limit within the context of this study.

3.4. Assumptions for Operation Times During Installation

An overview was compiled of all individual activities involved in offshore monopile foundation installation, including lifting, positioning, pile driving, noise mitigation, and vessel transit. As outlined in Section 3.1, representative operation times were derived from internal Van Oord sources such as project schedules, post-execution reports, and previous internal studies.

The duration of certain activities depends on the selected installation technique and, in some cases, on specific project conditions. For example, the operation *Drive Pile* is defined separately for each technique, as drivability differs significantly between methods. Test data show that vibro piling generally proceeds faster than impact piling, while vibro-jetting is expected to be even quicker due to lower soil resistance. Based on recent experience and consultation with a geotechnical specialist, drivability speeds were estimated assuming 9-metre diameter monopiles with a penetration depth of 30 metres in sandy soil. Under these conditions, impact piling takes approximately 2 hours, vibro piling 1 hour, and vibro-jetting 30 minutes. These estimates exclude preparation time for the jetting system, which would need to be included in a more detailed model.

In projects where two techniques are combined, such as in the HKW project where vibro piling is followed by impact piling, pile driving operations are executed twice. It is assumed that the first 10 metres are driven using vibro piling or vibro-jetting, and the remaining 20 metres with impact piling. Accordingly, the total drive time is calculated using a weighted average:

$$\text{Total Drive Time} = \frac{1}{3} \times \text{Drive Time Vibro(jet)} + \frac{2}{3} \times \text{Drive Time Impact} \tag{3.1}$$

In addition to pile driving, other activities within the installation process are influenced by project-specific parameters. For example, the vessel's transit time to the offshore site depends on the selected transit speed, while lifting durations may vary depending on pile dimensions and the vessel's deck layout. These dependencies are further illustrated in the Dependency Diagram shown in Figure 4.1, which is included in Section 4.8. In some cases, operations may be carried out in parallel, depending on the chosen working strategy. When applicable, the durations of such parallel activities are not added to the total installation time.

An example of such a parallel operation is the installation of near-field mitigation systems. Based on input from a Van Oord expert specialised in project cycle times, this activity is typically carried out in parallel with other tasks in practice. The same assumption is therefore applied in this framework.

To calculate the total time for one installation trip, all applicable activity durations are summed. For operations performed per monopile, the base duration is multiplied by the number of foundations carried per trip. The total installation time for the entire wind farm is then determined by multiplying the number of required trips, calculated as the total number of monopiles divided by the foundations per trip, by the duration of one round trip.

For vibro piling, preparation and handling procedures are assumed to be similar to those for conventional impact piling. In contrast, vibro-jetting involves additional steps: deploying the jetting pump, assumed to be handled with the main crane, and connecting the umbilicals between the monopile and the manifold. Because no reliable duration data for these activities are currently available within Van Oord, the model includes an additional allowance of 2.5 hours per monopile covering both tasks. This provisional value was set in consultation with a Van Oord specialist and is highly sensitive to whether the main crane is used, as this would put the work on the critical path. As more information becomes available, the allowance can be updated in the *Operation Times* sheet.

3.5. Assumptions for Drivability Performance

Due to the limited available data on the drivability of vibropiling and vibrojetting, particularly regarding installation speed compared to impact piling and the likelihood of reaching the target depth depending on soil type, it is currently challenging to incorporate drivability in the framework with high accuracy.

Nonetheless, various test results have indicated that achieving full penetration depth with vibropiling can be challenging, and even with vibrojetting, full installation depth is not always assured. This highlights the inherent uncertainty surrounding the drivability of these alternative methods. To account for this in the comparative assessment, drivability has been included as a critical factor. In consultation with a Van Oord specialist, indicative refusal risks were defined: 30% for vibropiling and 20% for vibrojetting. The lower value for vibrojetting reflects the expectation that jetting facilitates soil loosening, thereby generally improving penetration performance. Notably, in recent projects such as SIMPLEIII, full target depth was successfully achieved using vibrojetting, demonstrating that this technique can be viable under favourable conditions.

This assumption is reflected in some of the generated results, such as those presented in Figures Figure 5.10 & Figure 5.11, to make the user of the framework aware of the potential risks and limitations associated with these alternative installation methods.

3.6. Assumptions for Produced and Mitigated Underwater Noise

After selecting an installation technique, it is essential to assess whether the associated underwater noise limits comply with the applicable regulatory threshold. If predicted levels exceed this threshold, mitigation measures must be considered.

3.6.1. Installation Techniques

For the framework, each installation method is associated with a representative unmitigated reference sound level, based on internal Van Oord project experience, literature values, and expert consultation. In the framework, these levels are expressed as Sound Exposure Level (SEL) rather than Sound Pressure Level (SPL), as SEL incorporates both sound magnitude and duration, providing a more accurate measure of total acoustic energy. This aligns with the format in which most governmental noise limits for offshore piling are specified, enabling direct compliance assessment.

The calculation of SEL differs between impact piling and vibro piling. Noise levels can be expressed in terms of SEL_{ss} and SPL. Here, SEL_{ss} refers to the single-strike sound exposure level, which applies to impulsive sound sources such as impact piling and represents the sound exposure from a single hammer blow. Its unit is dB re 1 $\mu\text{Pa}^2\cdot\text{s}$.

For techniques such as vibro piling and vibro-jetting, where the sound is more continuous or vibration-like without discrete strikes, the SEL_{ss} metric is not applicable. Instead, the relevant quantity is the Sound Pressure Level (SPL), expressed in dB re 1 μPa. SPL represents an instantaneous or equivalent continuous sound level (L_{eq}) over a specified time period and is suitable for characterizing continuous noise.

The difference in approach arises from the nature of the sound source-impulsive versus continuous. For impulsive sources, such as impact piling, the cumulative sound exposure level (SEL) can then be estimated from the single-strike value using:

$$\text{SEL} = \text{SEL}_{\text{ss}} + 10\,\text{log}_{10}(N) \tag{3.2}$$

where N is the number of strikes, which can be calculated as $r \cdot T$, where r is the blow frequency and T is the pile driving time.

For continuous sources, such as vibro piling, SEL can be derived from the measured SPL over the total operating duration by integrating the acoustic energy over time:

$$\text{SEL} = \text{SPL} + 10\,\text{log}_{10}(T) \tag{3.3}$$

where T is in seconds (Ainslie, 2011).

However, although this would provide a more accurate approach for determining the SEL levels of the various installation techniques, the limited availability of data, particularly on the SPL levels produced by vibro piling and vibro jetting, led to a different approach. In consultation with experts at Van Oord, SEL values were directly assumed based on existing data and logical reasoning. These values represent the average unmitigated sound exposure level generated during the installation of a 9 m diameter monopile in sandy soil, measured at a distance of 750 m from the source. The following sections outline the basis for these assumed values.

For impact piling with a large hammer such as the IQ6, the baseline unmitigated source level was estimated at approximately 185 dB re 1 μPa at 1 m. This estimate draws on multiple sources, including Bellmann et al. (2020), which reports an average source level of 179 dB for a 7.5 m monopile installed using a noise-optimised pile-driving procedure with blow energies exceeding 3000 kJ. Additional input came from internal consultation with a Van Oord specialist and project-specific predictions. For instance, a forecast for the NSC project predicted a source level of XXXXX dB for an 8.9 m monopile installed with XXXXX kJ blow energy. Taking into account these references and the assumption of a 9 m pile in the framework, the baseline source level was conservatively rounded to 185 dB.

For the smaller MHU hammer, a baseline unmitigated source level of 187 dB re 1 μPa at 1 m was adopted. This reflects the fact that smaller impact hammers generally require higher blow energy at full capacity to achieve comparable drivability, which typically results in higher underwater noise emissions. Analyses and practical experience from the NavES project (Bellmann et al., 2020) demonstrate that large impact hammers with a heavy falling mass, operated under noise-optimized procedures at reduced capacity (typically 50-60%), produce significantly lower peak noise levels compared to smaller hammers running at full capacity. This difference is attributable to the longer contact duration between hammer and pile head with large hammers, which reduces peak force and thus noise amplitude. The adoption of the higher source level for the MHU hammer is further supported by Van Oord's internal environmental engineering expertise.

Vibro piling and vibro-jetting are expected to generate significantly lower noise levels than impact piling. This is primarily because vibro piling produces a continuous, low-frequency vibration (typically between 0 and 35 Hz), rather than the short, high-intensity acoustic peaks associated with impact piling. As a result, vibro piling is generally considered less disturbing to the marine environment, provided that proper coupling between the pile and the hammer is ensured (Bellmann et al., 2020).

Based on internal test results and expert consultation, both vibro piling and vibro-jetting are currently assumed to provide a conservative noise reduction of approximately 20 dB compared to impact piling under sandy soil conditions and in the absence of additional mitigation measures. Vibro piling is therefore estimated to result in an average noise level of around 165 dB. Vibro-jetting, due to the further reduction of soil resistance by water jets and the expectation of shorter installation durations (as SEL is time-dependent), is assumed to emit even lower noise levels, estimated at approximately 160 dB. These assumptions are summarised in Table 3.2.

Table 3.2: Assumed unmitigated sound levels (expressed in SEL) produced by different installation techniques, measured at a distance of 750 m from the source (Bellmann et al., 2020).

Installation Technique	Assumed Noise Level [$\mathrm{dB\ re\ 1\ \mu Pa^2 \cdot s}$]
impactIQ6	185
impactMHU	187
vibro	165
vibrojet	160

It should be noted that the source levels presented here are indicative and subject to validation. Ongoing and future field measurements, such as those conducted in the SIMPLE III project and at the HKW site, are expected to provide additional data to support or refine these assumptions.

Furthermore, subsequent discussions with an environmental noise specialist at Van Oord indicated that the assumption of vibrojetting producing, on average, 5 dB less noise than vibropiling may not be correct. The rationale behind this assumption was that the vibro hammer would operate at a lower power output due to the reduced resistance, resulting in a lower noise level. However, it was also suggested that the water jetting process could reduce the soil confinement around the embedded pile section, potentially increasing vibration levels. This was likewise hypothesised by researchers at Delft Cymatics, as communicated in recent exchanges.

Based on these insights, it could be assumed that the produced noise levels for vibro piling and vibro jetting are similar, with the main effect of jetting being an extension of the applicability range of vibro piling rather than a reduction in noise. Nevertheless, in this report the originally assumed values have been retained due to the limited time available for revising the framework calculations. It should be noted, and this is also included in the recommendations, that if more data on the noise levels of vibro piling and vibro jetting become available and differ from the assumptions made here, the framework should be updated accordingly.

In the case of a combined installation strategy, the overall SEL cannot be obtained by taking the arithmetic mean of the SEL values from the two individual installation methods. As described in Section 3.4, when an impact hammer and vibro(jetting) are applied together, it is assumed that one-third of the pile length is installed using vibro(jetting) and the remaining two-thirds using impact piling. This shortens the driving duration for both techniques and, since SEL is time-dependent, reduces their SEL compared to the full-duration individual cases.

The time-adjusted SEL for each method is computed by scaling the original SEL with the ratio of the new driving duration to the original duration:

$$\Delta\text{SEL} \;=\; 10\,\text{log}_{10}\!\left(\frac{T_\text{new}}{T_\text{orig}}\right). \tag{3.4}$$

Example: combination of *impactIQ6* and *vibro*.

- **ImpactIQ6:** original SEL $= 185$ dB for $T_\text{orig} = 2$ h. In the combined case, $T_\text{new} = \frac{2}{3}\cdot 2 = \frac{4}{3}$ h, hence

$$\Delta\text{SEL} = 10\,\text{log}_{10}\!\left(\frac{4/3}{2}\right) \approx -1.76 \text{ dB}, \qquad \text{SEL}_\text{new} \approx 185 - 1.76 = 183.24 \text{ dB}.$$

- **Vibro:** original SEL $= 165$ dB for $T_\text{orig} = 1$ h. In the combined case, $T_\text{new} = \frac{1}{3}\cdot 1 = 0.33$ h, hence

$$\Delta\text{SEL} = 10\,\text{log}_{10}\!\left(\frac{1/3}{1}\right) \approx -4.77 \text{ dB}, \qquad \text{SEL}_\text{new} \approx 165 - 4.77 = 160.23 \text{ dB}.$$

The total combined SEL is then obtained by summing energies and converting back to dB:

$$\text{SEL}_\text{total} = 10\,\text{log}_{10}\!\Big(10^{\,\text{SEL}_\text{impact,new}/10} + 10^{\,\text{SEL}_\text{vibro,new}/10}\Big) \approx 10\,\text{log}_{10}\!\big(10^{183.24/10} + 10^{160.23/10}\big) \approx 183.26 \text{ dB}. \tag{3.5}$$

This procedure ensures that the time dependence of SEL is correctly accounted for when combining sequential installation methods. It should be noted that this is a simplified approach for combining the contributions of sequential installation methods, which assumes constant source levels within each phase, identical propagation conditions, and sequential (non-overlapping) phases. As such, it is most appropriate for comparative scenario analyses and conceptual design studies, rather than for detailed compliance assessments. For higher accuracy it would be preferable to model impact piling based on single-strike SEL (SEL_ss) combined with the number of blows N, and vibro(jetting) based on its sound pressure level (SPL) and effective drive time, applying the scaling and mitigation band-by-band in the frequency domain and using measured spectra where available. However, as such detailed input data were not available for this study, the simplified time-scaling method described above was adopted.

3.6.2. Mitigation Techniques

If the estimated noise levels exceed the applicable regulatory threshold, mitigation systems can be applied at different stages along the sound propagation path: at the source, in the near field, or in the far field. As described in Chapter 2, based on consultation with environmental specialists at Van Oord, the techniques most commonly applied in practice were selected for inclusion in the framework. These systems can also be combined to strengthen overall noise reduction, allowing the framework to explore which combinations yield the most effective results.

The actual noise-reducing performance of a mitigation system depends on various factors and cannot be described by a single fixed value. Therefore, a frequency-based modelling approach was adopted to simulate the noise reduction achieved by different mitigation techniques. This approach is described in more detail in Section 4.6.

To apply this frequency-based model, specific input data are required for each mitigation technique. First, indicative overall noise reduction values are needed. These values were established in collaboration with Van Oord's environmental engineering department, based on experience from previous projects and available test data. An overview of the assumed reductions is provided in Table 3.3.

Table 3.3: Assumed average noise reduction per mitigation technique

Mitigation Technique	Type of Mitigation	Assumed Noise Reduction [dB]
Pulse from IQIP	At source	3 - 6
MENCK Noise Reduction Unit (MNRU)	At source	3 - 6
HSD	Near field	10 - 13
AdBm	Near field	10 - 17
IQIP NMS	Near field	13 - 16
Single Bubble Curtain	Far field	10 - 12
Double Bubble Curtain	Far field	15 - 16
Enhanced Single Bubble Curtain	Far field	12 - 14
Enhanced Double Bubble Curtain	Far field	17 - 18

In addition, it is important to consider the frequency ranges in which each mitigation technique is most effective. Based on a review of literature and industry reports, frequency-dependent attenuation characteristics have been identified and incorporated into the model. This enables a more realistic spectral representation of each technique's performance. Moreover, it allows for the assessment of combined mitigation strategies, where multiple techniques targeting different frequency bands are applied simultaneously to achieve broader and more effective noise reduction.

Figure 3.1 illustrates the noise reduction performance of several mitigation techniques as a function of frequency. The figure shows that certain systems perform better in specific frequency ranges, and that these patterns vary between mitigation methods.

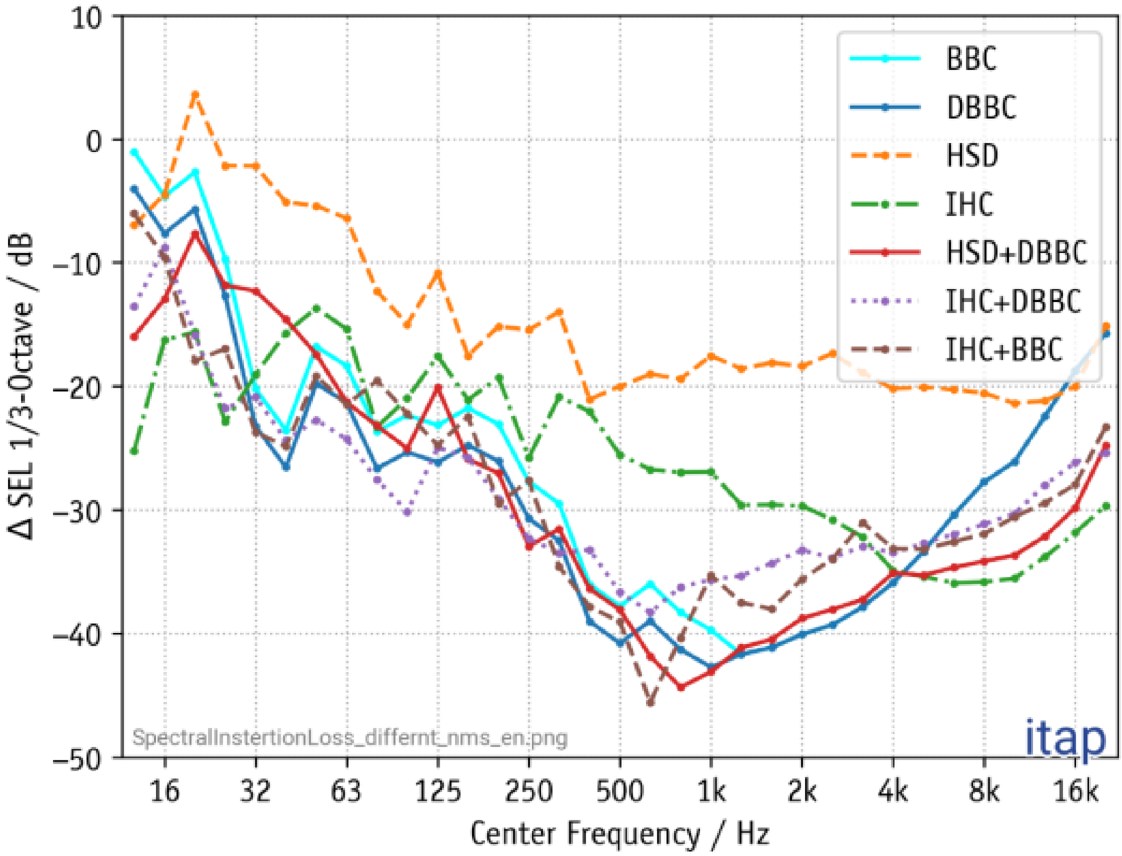

Figure 3.1: Average noise reduction (insertion loss) of NMS8000, HSD, and BBC/DBBC systems based on applications in the German North Sea EEZ (Bellmann et al., 2020)

According to (Maquil, Müller, and Wildemann, 2024), the PULSE at source mitigation system is most effective in the low to mid-frequency range, approximately between 40 and 250 Hz. The system optimizes the impact process to reduce sound energy within this critical band. This aligns with both the spectral characteristics of the optimized impact hammer and the typical underwater noise emission profiles observed in practice.

For the MNRU system, no specific optimal frequency range was identified. However, since it is also an at source mitigation technology, its effectiveness is assumed to fall within the same frequency range of 40 to 250 Hz.

Furthermore, (Jongbloed et al., 2021) point out a clear mismatch between the frequency range where piling noise typically peaks (around 80 to 400 Hz) and the range where conventional bubble curtain systems achieve their maximum noise reduction, which is generally above 500 Hz. Shifting the effective mitigation range of these systems toward lower frequencies could enhance their ability to reduce broadband underwater noise. This may be achieved, for instance, by generating larger bubbles with lower resonance frequencies.

This principle has been applied in alternative systems such as HSD (which uses encapsulated bubbles) and AdBm (which relies on Helmholtz resonators). These technologies are designed to perform best in the 80 to 400 Hz range but tend to be less effective at higher frequencies.

In contrast, traditional bubble curtain variants such as SBBC, DBBC, ESBBC, and EDBBC are reported in (Jongbloed et al., 2021) to achieve their peak reduction in the 250 to 1000 Hz range, with a noticeable decrease in performance above 1 kHz. As such, this frequency band is considered their primary zone of effectiveness within this framework.

The table below also briefly summarizes the assumed effective frequency range for the different mitigation systems.

Table 3.4: Assumed effective frequency range per mitigation technique

Type of Mitigation	Assumed Effective Frequency Range [Hz]
At Source Mitigation	40 - 250
Near Field Mitigation	80 - 400
Far Field Mitigation	250 - 1000

Finally, a few general assumptions have been made regarding noise. For impact piling, source mitigation is considered standard procedure and is always included by default. The associated cost is typically part of the hammer rental agreement. For the IQ6 hammer, this involves the use of the Pulse from IQIP, while for the MHU hammer the MENCK Noise Reduction Unit (MNRU) is used.

This does not apply to vibro piling or vibro-jetting, where this type of source mitigation is not relevant due to differences in the installation mechanism. However, the framework assumes that when additional near-field or far-field mitigation systems are selected, they are applied to both installation techniques if used in combination. For instance, in cases where both impact and vibro piling are employed, it is assumed that if mitigation is applied during the impact phase, the same systems remain active during the vibro phase. Since the equipment is already present on board, mobilisation and demobilisation costs are already covered, and extending the use of the systems incurs only marginal additional cost while supporting consistent environmental performance.

3.7. Assumptions for Calculating Monopile Installation Costs

In consultation with a cost specialist from Van Oord, the key elements contributing most significantly to the total installation expenses were identified. These include vessel rental (encompassing all associated costs such as personnel and onboard systems), fuel consumption, the costs of the selected installation and noise mitigation techniques, and the use of noise monitoring equipment. The related costs were grouped into three main categories: mobilisation, demobilisation, and operational costs. This classification reflects the primary cost drivers in offshore monopile installation projects.

The cost inputs were compiled from completed project evaluations, tender documentation, and expert estimates provided by the Cost Engineering department at Van Oord. The goal was to ensure that the comparative framework incorporates all components that have a significant impact on overall project costs.

3.7.1. Cost Structure and Assumptions

The framework distinguishes between different cost components to allow a structured and consistent comparison of installation strategies. Operational costs depend on time-based factors such as vessel usage, fuel consumption, the selected installation method, and the application of additional systems, such as noise mitigation or monitoring. These costs vary with project configuration and duration.

In contrast, mobilisation and demobilisation costs are treated as fixed values, as they generally represent standardised procedures for preparing and dismantling equipment and are not expected to vary significantly with project-specific parameters. Together, these cost categories provide a robust basis for evaluating the trade-offs between environmental impact and financial performance.

By varying the combination of installation and mitigation techniques, the framework enables assessment of the balance between underwater noise emissions and total project costs. This functionality is particularly relevant in early project phases, such as tendering, where decisions must often weigh environmental compliance against economic feasibility.

To ensure consistency across different project scenarios, several assumptions have been applied. The remainder of this section outlines how the main cost categories were defined and on what basis the underlying assumptions were made. First, the approach used to estimate mobilisation and demobilisation costs for each component is explained. This is followed by a description of how operational costs are calculated.

Mobilisation and Demobilisation Costs
The following assumptions apply to the configuration using the Boreas installation vessel and its associated equipment:

- **Vessel:** A mobilisation duration of 22 days is assumed (21 days for rigging and 1 day for transit), while demobilisation is estimated at 8 days (1 day for transit and 7 days for de-rigging). The daily vessel rate includes all associated costs, such as personnel, fuel, and onboard systems.

- **Fuel:** Boreas is currently assumed to run on Marine Gas Oil (MGO). Methanol (MeOH) could also be considered as an alternative, but its higher consumption and cost are not expected to significantly impact the relative comparison between scenarios. Therefore, it has been excluded from this analysis.

- **Installation Hammers:** The mobilisation and demobilisation durations for all hammer systems (including IQ6, MHU, vibro, and vibro-jetting) are defined as follows. Mobilisation includes 2 days for transport, 4 days for rigging, and 1 day of vessel transit, adding up to a total of 7 days. Demobilisation consists of 1 day of vessel transit, 2 days for de-rigging, and 2 days for transport, adding up to 5 days.

- **At Source Noise Mitigation:** The IQ6 hammer is always assumed to include the Pulse system, and the MHU hammer includes the MNRU system. These are considered part of the hammer system package and are not listed as separate mitigation items.

- **Near-Field Noise Mitigation:**
  - **AdBm system:** For the AdBm system, a base lump-sum mobilisation cost is applied, with an additional fixed rate charged per monopile. This means that the total cost of the AdBm noise mitigation system increases proportionally with the number of monopiles in the wind farm.
  - **HSD (Hydro Sound Damper):** It is assumed that one HSD net is required for every 40 monopiles. Based on this assumption, the framework applies a base cost for one HSD system covering up to 40 monopiles. If the wind farm contains between 41 and 80 monopiles, the cost is doubled, and for more than 80 monopiles, it is tripled accordingly. Since the HSD system is purchased rather than rented, no demobilisation costs are incurred.
  - **IQIP NMS:** Mobilisation includes 7 additional days of Boreas time to allow for rigging and the required sea-fastening of the system. Similarly, demobilisation includes 7 extra days for de-rigging. During operations, it is assumed that two dedicated operators are present on board Boreas to manage the system. The associated personnel costs are included in the operational cost estimates. It is further assumed that the IQIP NMS has a total weight of 2,600 mT, consisting of 2,000 mT for the system itself and an additional 600 mT for the supporting frame (Buitendijk, 2023).

- **Far-Field Noise Mitigation:** For the deployment of the far-field bubble curtain system, a two-vessel setup is assumed using Platform Supply Vessels (PSVs). These offshore support vessels, typically used to transport supplies to and from offshore platforms, are in this context repurposed to carry and operate the bubble curtain infrastructure. PSV #1 is fitted with an enhanced inner curtain system comprising 22 compressors and 4 spare units, while PSV #2 manages the outer curtain with 15 compressors and 3 spares. Additionally, PSV #2 is assumed to carry the noise monitoring equipment (Faunaguard), thereby eliminating the need for a separate monitoring vessel. The daily charter rates for both PSVs include the vessels themselves, the compressor systems, and all additional required equipment. Hose procurement is treated as a one-time additional cost.

- **Transportation:** Mobilisation and demobilisation costs also include equipment transport costs, in addition to vessel and equipment day rates.

- **Noise Monitoring:** The cost of noise monitoring equipment (Faunaguard) is always included, regardless of installation method, as continuous noise monitoring is typically required by authorities.

Operational Costs
Operational costs are calculated as the product of operational duration and the daily rates of all active components involved in the installation process. These include the main installation vessel, the selected hammer system, noise mitigation systems, and monitoring equipment.

Because these costs are directly linked to the total time required for offshore operations, they are sensitive to the chosen installation strategy and the number of activities performed. For example, applying multiple mitigation systems or using slower techniques increases operational duration, whereas efficient methods can reduce it. This makes operational costs a critical parameter in assessing trade-offs between environmental impact and total project expenditure.

To ensure the cost estimates remain realistic and applicable, all underlying assumptions were derived from supplier quotations, expert input, and recent project data from Van Oord. Since certain rates, particularly those for vessel rental or hammer systems, may vary between projects or over time, it is recommended to update these values when more accurate or case-specific information becomes available.

3.8. Additional Assumptions and Limitations

While the cost model aims to capture the most significant components of offshore monopile installation, several relevant factors have been excluded from the current framework due to limited data availability or scope restrictions. These elements are outlined below to ensure transparency and provide context for interpretation.

- **Uncertainty in Achieving Required Bearing Capacity with Jetting:** When applying jetting techniques, it remains uncertain whether the installed monopile will achieve the required bearing capacity, particularly in soils where loosening effects may occur. Similar to the reduction in horizontal bearing capacity observed for monopiles installed using jack-up platforms due to seabed disturbance from support leg penetration and extraction (Fabo et al., 2021), jetting can alter soil structure around the pile, potentially reducing lateral resistance. Assessing this effect would require detailed geotechnical analysis and site-specific testing, which is outside the scope of this study. Nevertheless, this represents an important technical consideration when evaluating jetting as an installation method.

- **Fatigue Effects on Equipment:** Fatigue-related effects, such as increased crane wear due to vibrations during impact piling, have not been included. It is known that such vibrations can significantly reduce the operational lifetime of crane systems, potentially affecting long-term equipment costs. However, incorporating these effects would require a lifecycle cost analysis or depreciation model, which falls outside the scope of this study.

- **Monopile-Related Costs Beyond T&I Scope:** In some cases, specific installation techniques may require design adaptations to the monopile. For example, vibrojetting typically involves the integration of internal jetting nozzles, which introduces additional fabrication costs. Similarly, certain techniques may necessitate deeper pile penetration to ensure sufficient geotechnical stability, resulting in longer and heavier monopiles with higher material and manufacturing costs. These implications are not included in the current analysis, as the framework focuses exclusively on Transport and Installation (T&I) activities. Monopile design and production costs are typically the responsibility of the client and therefore fall outside the contractor's scope in a Transport and Installation (T&I) setting.

Although these aspects are excluded from the cost calculations, their potential impact should not be overlooked. They represent relevant considerations that could influence the overall cost-effectiveness of different installation strategies. While not included in the current framework, these factors should be kept in mind when interpreting the results or applying this model to future project evaluations, as they may affect the overall costs of the wind farm, particularly in the context of an EPCI contract, where such elements may fall within the contractor's scope.

4

Implementation of a Model for Comparing Alternative Installation Technologies

4.1. The Position of the Model Within the Framework

As outlined in the previous chapter (Chapter 3), collecting and structuring the necessary data proved to be one of the most time-consuming aspects of developing the framework. A major part of this effort involved identifying which departments within Van Oord held the relevant information and coordinating across multiple teams to retrieve it. Since each department focuses on its own area of expertise, it was challenging to strike the right balance between digestibility and the technical detail needed to ensure reliability.

A key added value of this study is the integration of diverse data sources into a single framework. By combining operational, technical, environmental, and economic inputs from across the organisation, the framework enables meaningful data connections and supports practical, cross-disciplinary analysis. While individual aspects within the framework are simplified, this level of abstraction is considered acceptable given its intended use as a comparative decision-support tool in early tender phases.

Embedded within this framework is a model that processes inputs, establishes relationships between key variables, and compares different installation strategies. This allows users to explore a range of options and assess the effects of design and planning choices in a consistent and transparent manner.

To maintain clarity and structure, the collected information was categorised into key components that together form the model. This chapter explains how these components are integrated and how the model was made interactive. Users can adjust input parameters to simulate different project configurations, compare combinations of installation and mitigation techniques, and assess their impact on project performance.

The chapter first outlines the model's basic structure, including the required input parameters and the type of output generated. It then describes how the components are interconnected and the logic used to link them. As introduced in Section 3.1.2, the framework was developed using a combination of Excel and Python. Seven worksheets in the Excel file provide the data input for Python, where the calculations are performed.The noise model used to calculate the reduced underwater noise levels is also discussed in more detail.

Finally, Section 4.9 describes how the model was verified. This was done by conducting intermediate tests and breaking down the model into separate components, each of which was independently tested. Based on this verification process, it can be assumed with confidence that the model performs as intended.

4.2. General Input Parameters and User Interface

As shown in Table 4.1, the first worksheet in the Excel file contains the general input parameters. This is the most important sheet for the user, as it requires entering project-specific values that are used throughout the framework to calculate the output. In the figure, some cells are green while others are red. The red cells contain fixed values based on the assumptions described in Section 3.2 and cannot be changed by the user. Although these values could potentially be made adjustable in future versions of the model, this is not within the scope of the current project.

The green cells are open for user input. Some of them include dropdown menus, as illustrated in Table 4.2, offering a predefined list of options to choose from. Other fields require the user to manually enter a value. To guide the input process, the column to the left of each field indicates the expected data type, such as an integer or a float. The values entered in this sheet form the basis for the entire framework, as they are linked to all five other worksheets.

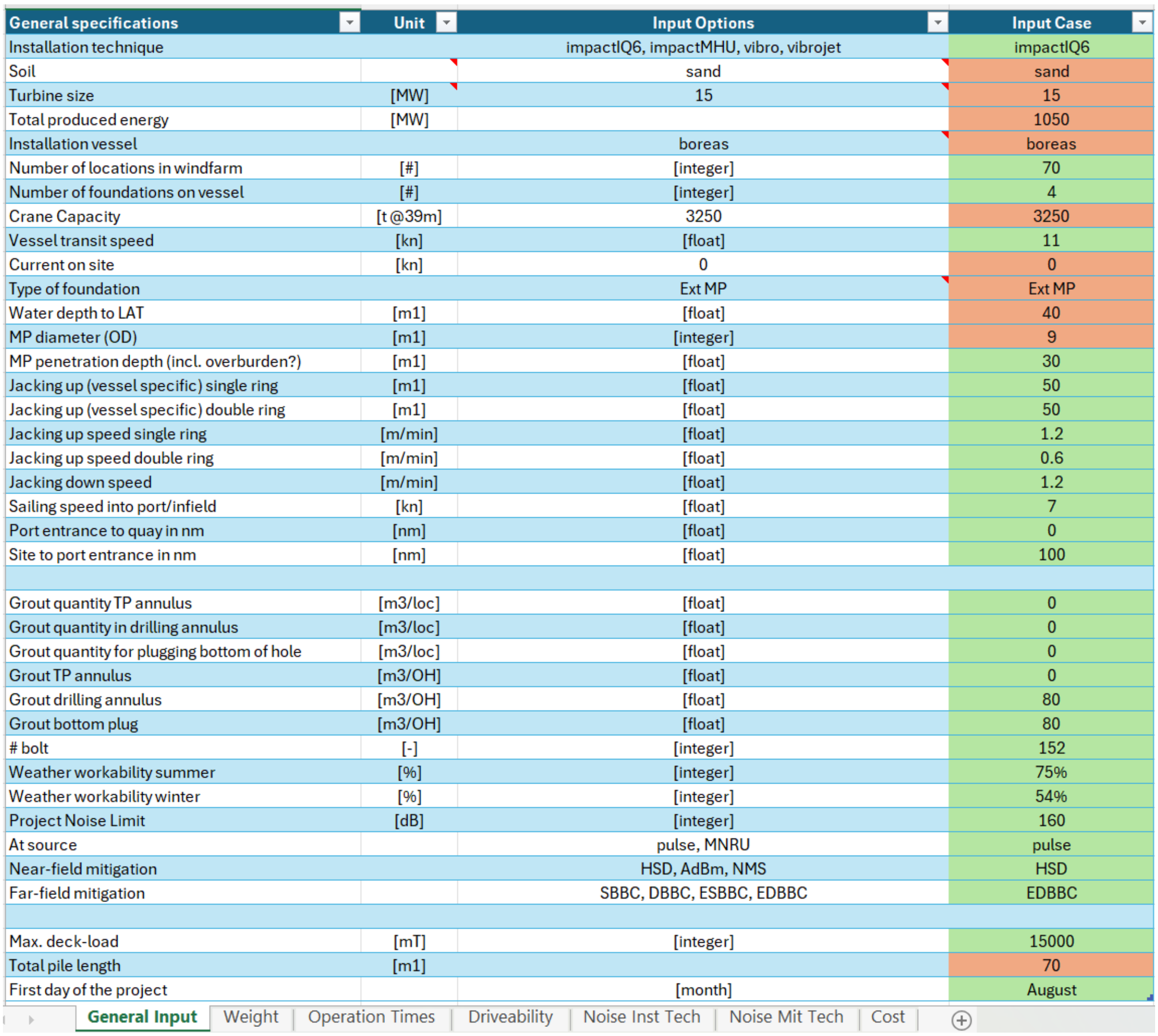

General specifications	Unit	Input Options	Input Case
Installation technique		impactIQ6, impactMHU, vibro, vibrojet	impactIQ6
Soil		sand	sand
Turbine size	[MW]	15	15
Total produced energy	[MW]		1050
Installation vessel		boreas	boreas
Number of locations in windfarm	[#]	[integer]	70
Number of foundations on vessel	[#]	[integer]	4
Crane Capacity	[t @39m]	3250	3250
Vessel transit speed	[kn]	[float]	11
Current on site	[kn]	0	0
Type of foundation		Ext MP	Ext MP
Water depth to LAT	[m1]	[float]	40
MP diameter (OD)	[m1]	[integer]	9
MP penetration depth (incl. overburden?)	[m1]	[float]	30
Jacking up (vessel specific) single ring	[m1]	[float]	50
Jacking up (vessel specific) double ring	[m1]	[float]	50
Jacking up speed single ring	[m/min]	[float]	1.2
Jacking up speed double ring	[m/min]	[float]	0.6
Jacking down speed	[m/min]	[float]	1.2
Sailing speed into port/infield	[kn]	[float]	7
Port entrance to quay in nm	[nm]	[float]	0
Site to port entrance in nm	[nm]	[float]	100
Grout quantity TP annulus	[m3/loc]	[float]	0
Grout quantity in drilling annulus	[m3/loc]	[float]	0
Grout quantity for plugging bottom of hole	[m3/loc]	[float]	0
Grout TP annulus	[m3/OH]	[float]	0
Grout drilling annulus	[m3/OH]	[float]	80
Grout bottom plug	[m3/OH]	[float]	80
# bolt	[-]	[integer]	152
Weather workability summer	[%]	[integer]	75%
Weather workability winter	[%]	[integer]	54%
Project Noise Limit	[dB]	[integer]	160
At source		pulse, MNRU	pulse
Near-field mitigation		HSD, AdBm, NMS	HSD
Far-field mitigation		SBBC, DBBC, ESBBC, EDBBC	EDBBC
Max. deck-load	[mT]	[integer]	15000
Total pile length	[m1]		70
First day of the project		[month]	August

Table 4.1: Overview General Input Parameters Framework

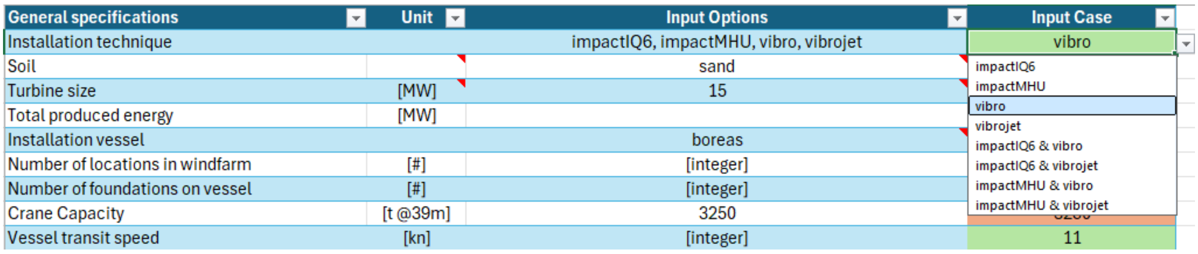

General specifications	Unit	Input Options	Input Case
Installation technique		impactIQ6, impactMHU, vibro, vibrojet	vibro
Soil		sand	
Turbine size	[MW]	15	
Total produced energy	[MW]		
Installation vessel		boreas	
Number of locations in windfarm	[#]	[integer]	
Number of foundations on vessel	[#]	[integer]	
Crane Capacity	[t @39m]	3250	
Vessel transit speed	[kn]	[integer]	11

Table 4.2: Example of Dropdown Menu for General Input Parameters

As shown in the dropdown menu in Table 4.2, it is also possible to select a combination of one of the impact hammers and a vibro-driven installation method. As previously discussed in this report, choosing such a combination implies that the activities related to pile driving must be carried out for both installation techniques, and that the required equipment for each method needs to be brought onboard. This leads to the next subsection.

4.3. Deck Load and Weight Calculation

The second worksheet in the Excel file provides an overview of all equipment included in the vessel's deck layout, together with the corresponding weights. A simplified version of this layout is shown in Table 4.3. Due to confidentiality, specific equipment names and weights are not displayed, but the figure still illustrates the structure and logic used in the model. The equipment is divided into separate sections, each representing a specific function. These include standard onboard equipment, as well as components related to different installation and mitigation techniques.

This worksheet is directly connected to the *General Input* sheet. Based on the selected installation and mitigation techniques, the relevant equipment sections are either included in or excluded from the total weight calculation.

Two other important input parameters that influence the total deck load are the *Number of foundations on vessel* and the *Max. deck-load*. The user can specify how many monopiles are transported per trip, and this number is used to compute the total weight. If the calculated weight exceeds the vessel's maximum capacity, the number of monopiles per trip is reduced by one. This means that more transport cycles are required, which increases both the total installation time and the overall project cost.

Additionally, when the IQIP NMS system is used, one less monopile can be transported per trip due to space limitations. Moreover, the use of the IQIP NMS eliminates the need for a gripper, which is therefore excluded from the total weight calculation. Instead, the weight of the IQIP NMS frame itself is included. All of this is accurately accounted for in the model.

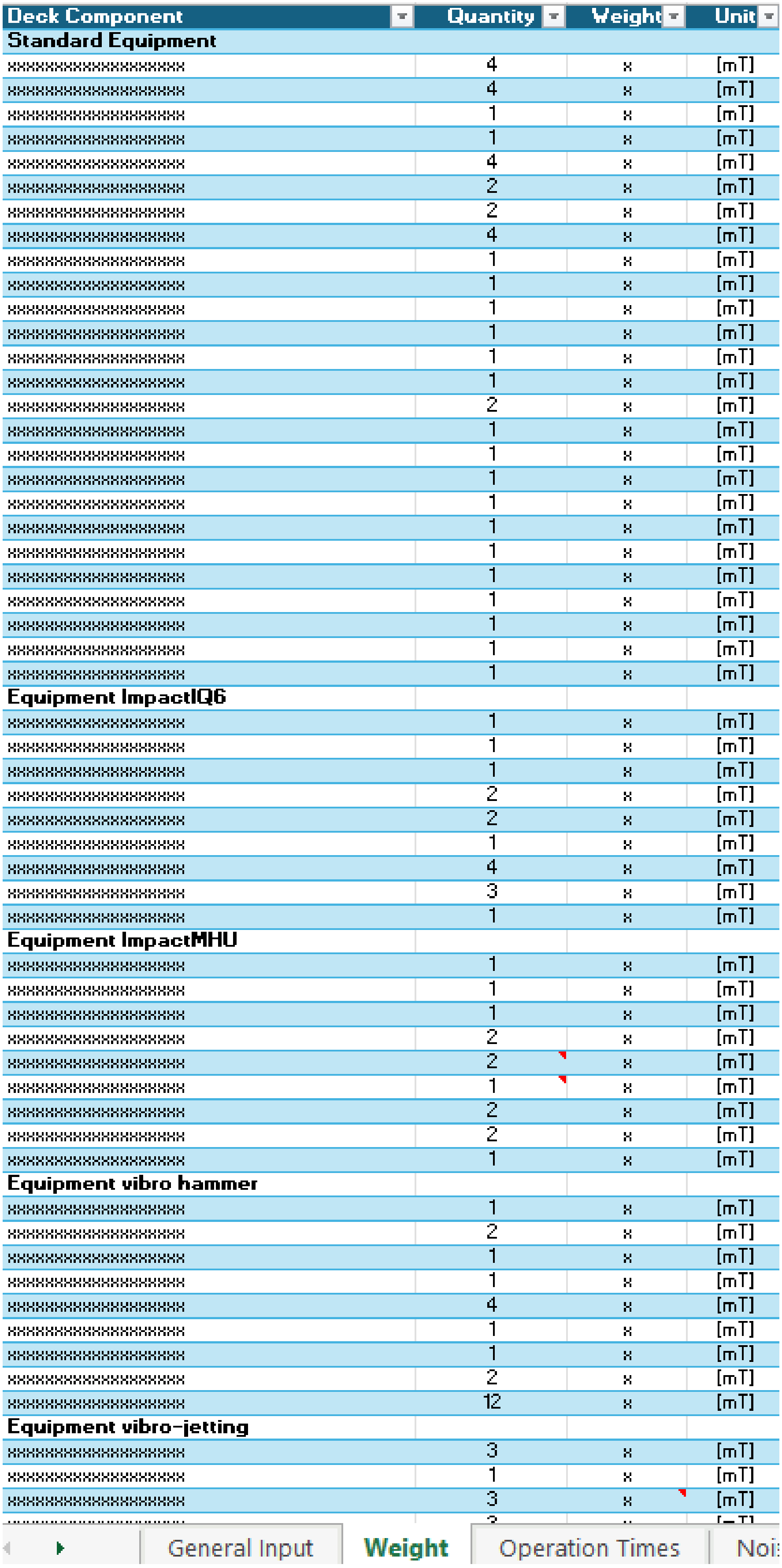

Deck Component	Quantity	Weight	Unit
Standard Equipment			
xxxxxxxxxxxxxxxxxx	4	x	[mT]
xxxxxxxxxxxxxxxxxx	4	x	[mT]
xxxxxxxxxxxxxxxxxx	1	x	[mT]
xxxxxxxxxxxxxxxxxx	1	x	[mT]
xxxxxxxxxxxxxxxxxx	4	x	[mT]
xxxxxxxxxxxxxxxxxx	2	x	[mT]
xxxxxxxxxxxxxxxxxx	2	x	[mT]
xxxxxxxxxxxxxxxxxx	4	x	[mT]
xxxxxxxxxxxxxxxxxx	1	x	[mT]
xxxxxxxxxxxxxxxxxx	1	x	[mT]
xxxxxxxxxxxxxxxxxx	1	x	[mT]
xxxxxxxxxxxxxxxxxx	1	x	[mT]
xxxxxxxxxxxxxxxxxx	1	x	[mT]
xxxxxxxxxxxxxxxxxx	1	x	[mT]
xxxxxxxxxxxxxxxxxx	2	x	[mT]
xxxxxxxxxxxxxxxxxx	1	x	[mT]
xxxxxxxxxxxxxxxxxx	1	x	[mT]
xxxxxxxxxxxxxxxxxx	1	x	[mT]
xxxxxxxxxxxxxxxxxx	1	x	[mT]
xxxxxxxxxxxxxxxxxx	1	x	[mT]
xxxxxxxxxxxxxxxxxx	1	x	[mT]
xxxxxxxxxxxxxxxxxx	1	x	[mT]
xxxxxxxxxxxxxxxxxx	1	x	[mT]
xxxxxxxxxxxxxxxxxx	1	x	[mT]
xxxxxxxxxxxxxxxxxx	1	x	[mT]
xxxxxxxxxxxxxxxxxx	1	x	[mT]
Equipment ImpactIQ6			
xxxxxxxxxxxxxxxxxx	1	x	[mT]
xxxxxxxxxxxxxxxxxx	1	x	[mT]
xxxxxxxxxxxxxxxxxx	1	x	[mT]
xxxxxxxxxxxxxxxxxx	2	x	[mT]
xxxxxxxxxxxxxxxxxx	2	x	[mT]
xxxxxxxxxxxxxxxxxx	1	x	[mT]
xxxxxxxxxxxxxxxxxx	4	x	[mT]
xxxxxxxxxxxxxxxxxx	3	x	[mT]
xxxxxxxxxxxxxxxxxx	1	x	[mT]
Equipment ImpactMHU			
xxxxxxxxxxxxxxxxxx	1	x	[mT]
xxxxxxxxxxxxxxxxxx	1	x	[mT]
xxxxxxxxxxxxxxxxxx	1	x	[mT]
xxxxxxxxxxxxxxxxxx	2	x	[mT]
xxxxxxxxxxxxxxxxxx	2	x	[mT]
xxxxxxxxxxxxxxxxxx	1	x	[mT]
xxxxxxxxxxxxxxxxxx	2	x	[mT]
xxxxxxxxxxxxxxxxxx	2	x	[mT]
xxxxxxxxxxxxxxxxxx	1	x	[mT]
Equipment vibro hammer			
xxxxxxxxxxxxxxxxxx	1	x	[mT]
xxxxxxxxxxxxxxxxxx	2	x	[mT]
xxxxxxxxxxxxxxxxxx	1	x	[mT]
xxxxxxxxxxxxxxxxxx	1	x	[mT]
xxxxxxxxxxxxxxxxxx	4	x	[mT]
xxxxxxxxxxxxxxxxxx	1	x	[mT]
xxxxxxxxxxxxxxxxxx	1	x	[mT]
xxxxxxxxxxxxxxxxxx	2	x	[mT]
xxxxxxxxxxxxxxxxxx	12	x	[mT]
Equipment vibro-jetting			
xxxxxxxxxxxxxxxxxx	3	x	[mT]
xxxxxxxxxxxxxxxxxx	1	x	[mT]
xxxxxxxxxxxxxxxxxx	3	x	[mT]

Table 4.3: Overview of Deck Layout Including Components, Quantities, and Weights (Confidential Values Not Displayed)

4.4. Operational Time Calculation

As explained in the previous subsection, the total operational time is partly influenced by the deck layout and the total weight carried on board. The overall installation duration of the wind farm is calculated using the third worksheet, titled *Operation Times*, which is visualised in Table 4.4. This sheet provides an overview of the various operational activities and the assumed duration of each activity, based on project experience within Van Oord. Due to confidentiality, specific activity names and values are not displayed in this report, but the figure still gives a clear impression of the number and variety of tasks involved in installing a single monopile.

The operational time depends on several factors. One of the most important is the number of monopiles that can be transported per trip. If fewer monopiles can be carried due to weight or space limitations, more trips are needed, which increases the overall installation time. The value for *Number of foundations on vessel* in the *General Input* sheet is directly linked to the operation times, as many activities are performed per monopile per trip and must therefore be multiplied by this number. This multiplication is applied after verifying compliance with the *Max. deck-load*. In addition to vessel capacity, other project-specific parameters from the *General Input* sheet also influence the operational sequence.

As described in Section 3.4, each installation technique has its own assumed pile drive speed. The selected technique in the *General Input* sheet determines which value is applied. If a combination of two techniques is selected, certain activities must be repeated, such as lifting and detaching the hammer or performing an intermediate flange inspection. Additionally, when vibrojetting is applied, the model incorporates an additional time allocation to account for the supplementary activities previously described in Section 3.4.

The operation time model also includes tasks related to installing a Transition Piece (TP), which are only relevant when a separate TP is used, such as an MPTP. Since the current version of the framework only considers the Extended Monopile concept, these activities are not triggered. However, the model is set up so that these can be included later when expanding the framework to other monopile types.

Finally, some activities can be performed at the same time and do not have to be added to the total installation time. This is indicated in the fourth column in Table 4.4.

4.5. Incorperating Drivability

To account for the risk that vibropiling and vibrojetting may not achieve the required penetration depth, the indicative refusal risks described in Section 3.5 are applied in the model. This is a simplified approach, and Section 6.2 suggests further refinement in future work. For the current framework, however, it provides a practical means of incorporating drivability into the comparison. This ensures that results do not present vibropiling as the most favourable option purely based on cost or noise, without considering the critical role of drivability in installation feasibility.

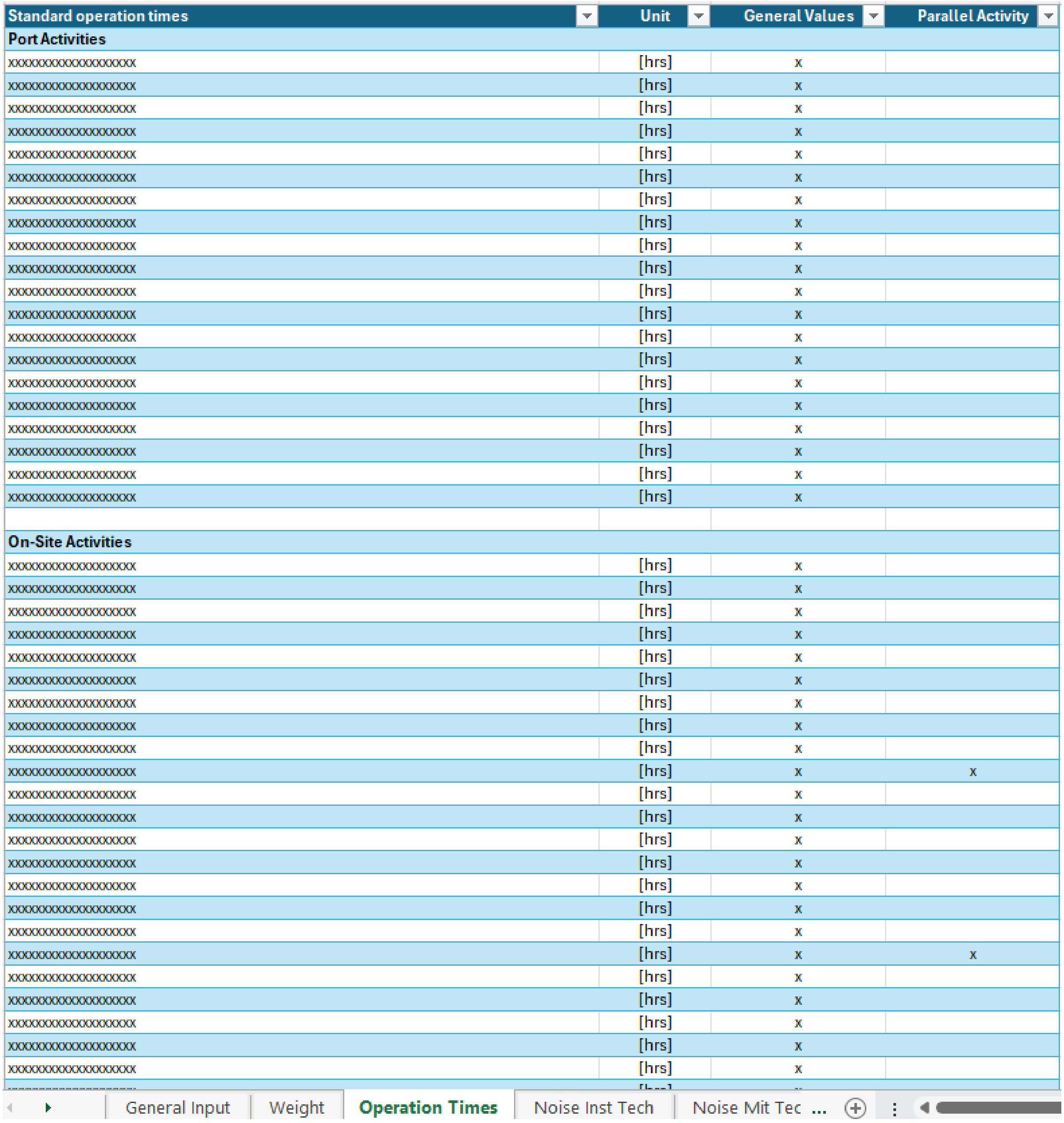

Standard operation times	Unit	General Values	Parallel Activity
Port Activities			
xxxxxxxxxxxxxxxxxxx	[hrs]	x	
xxxxxxxxxxxxxxxxxxx	[hrs]	x	
xxxxxxxxxxxxxxxxxxx	[hrs]	x	
xxxxxxxxxxxxxxxxxxx	[hrs]	x	
xxxxxxxxxxxxxxxxxxx	[hrs]	x	
xxxxxxxxxxxxxxxxxxx	[hrs]	x	
xxxxxxxxxxxxxxxxxxx	[hrs]	x	
xxxxxxxxxxxxxxxxxxx	[hrs]	x	
xxxxxxxxxxxxxxxxxxx	[hrs]	x	
xxxxxxxxxxxxxxxxxxx	[hrs]	x	
xxxxxxxxxxxxxxxxxxx	[hrs]	x	
xxxxxxxxxxxxxxxxxxx	[hrs]	x	
xxxxxxxxxxxxxxxxxxx	[hrs]	x	
xxxxxxxxxxxxxxxxxxx	[hrs]	x	
xxxxxxxxxxxxxxxxxxx	[hrs]	x	
xxxxxxxxxxxxxxxxxxx	[hrs]	x	
xxxxxxxxxxxxxxxxxxx	[hrs]	x	
xxxxxxxxxxxxxxxxxxx	[hrs]	x	
xxxxxxxxxxxxxxxxxxx	[hrs]	x	
xxxxxxxxxxxxxxxxxxx	[hrs]	x	
On-Site Activities			
xxxxxxxxxxxxxxxxxxx	[hrs]	x	
xxxxxxxxxxxxxxxxxxx	[hrs]	x	
xxxxxxxxxxxxxxxxxxx	[hrs]	x	
xxxxxxxxxxxxxxxxxxx	[hrs]	x	
xxxxxxxxxxxxxxxxxxx	[hrs]	x	
xxxxxxxxxxxxxxxxxxx	[hrs]	x	
xxxxxxxxxxxxxxxxxxx	[hrs]	x	
xxxxxxxxxxxxxxxxxxx	[hrs]	x	
xxxxxxxxxxxxxxxxxxx	[hrs]	x	
xxxxxxxxxxxxxxxxxxx	[hrs]	x	x
xxxxxxxxxxxxxxxxxxx	[hrs]	x	
xxxxxxxxxxxxxxxxxxx	[hrs]	x	
xxxxxxxxxxxxxxxxxxx	[hrs]	x	
xxxxxxxxxxxxxxxxxxx	[hrs]	x	
xxxxxxxxxxxxxxxxxxx	[hrs]	x	
xxxxxxxxxxxxxxxxxxx	[hrs]	x	
xxxxxxxxxxxxxxxxxxx	[hrs]	x	
xxxxxxxxxxxxxxxxxxx	[hrs]	x	x
xxxxxxxxxxxxxxxxxxx	[hrs]	x	
xxxxxxxxxxxxxxxxxxx	[hrs]	x	
xxxxxxxxxxxxxxxxxxx	[hrs]	x	
xxxxxxxxxxxxxxxxxxx	[hrs]	x	
xxxxxxxxxxxxxxxxxxx	[hrs]	x	

Table 4.4: Operation Times: Overview of Activities Performed On Site and In Port (Confidential Values Not Displayed)

4.6. Calculation of Noise Emission Levels with Mitigation

The fourth and fifth worksheets in the Excel file provide overviews of the different installation techniques and their associated noise levels, as well as the mitigation techniques and their corresponding noise reduction ranges, as shown in Table 4.5 and Table 4.6.

As illustrated in Table 4.5, the sheet includes both red and green cells. In the green cells, the user can indicate via dropdown menus whether a mitigation system is applied. For the *At Source* mitigation category, this choice is fixed: as previously explained in the report, source mitigation is always applied for both impact hammers, as it is included in the hammer rental price. For vibro piling and vibro-jetting, however, source mitigation of this type is not applicable and therefore not included.

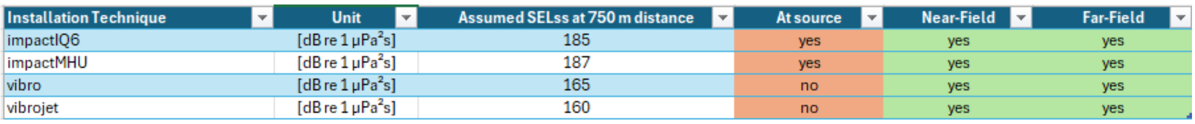

Installation Technique	Unit	Assumed SELss at 750 m distance	At source	Near-Field	Far-Field
impactIQ6	[dB re 1 $\mu Pa^2 s$]	185	yes	yes	yes
impactMHU	[dB re 1 $\mu Pa^2 s$]	187	yes	yes	yes
vibro	[dB re 1 $\mu Pa^2 s$]	165	no	yes	yes
vibrojet	[dB re 1 $\mu Pa^2 s$]	160	no	yes	yes

Table 4.5: Noise: Average noise levels per installation technique measured at a distance of 750 metres from the source

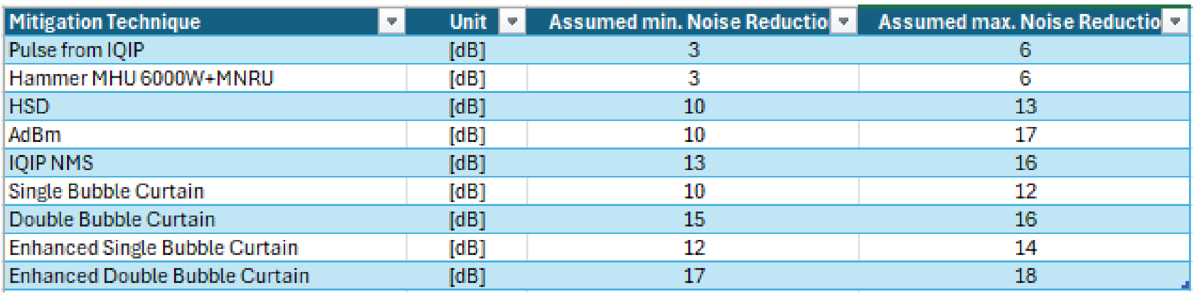

Mitigation Technique	Unit	Assumed min. Noise Reductio	Assumed max. Noise Reductio
Pulse from IQIP	[dB]	3	6
Hammer MHU 6000W+MNRU	[dB]	3	6
HSD	[dB]	10	13
AdBm	[dB]	10	17
IQIP NMS	[dB]	13	16
Single Bubble Curtain	[dB]	10	12
Double Bubble Curtain	[dB]	15	16
Enhanced Single Bubble Curtain	[dB]	12	14
Enhanced Double Bubble Curtain	[dB]	17	18

Table 4.6: Noise: Average noise reduction achieved per mitigation technique

4.6.1. Frequency-Based Modelling of Underwater Noise and Mitigation Effects

To estimate the expected sound level after the application of noise mitigation techniques during offshore monopile installation, a frequency-based modelling approach is applied. In this method, the total single-event sound exposure level (SEL), which represents the total acoustic energy released during a single pile-driving strike, is distributed across standard one-third octave bands. Frequency-specific attenuation values are then applied to each band to account for the effect of mitigation techniques.

One-third octave bands are standardized frequency intervals commonly used in acoustic analyses to divide the sound spectrum into manageable components. Each band spans approximately one third of an octave, meaning that the upper frequency limit is about 26% higher than the lower limit. For example, the band centered at 100 Hz typically covers the range from approximately 89 Hz to 112 Hz. This segmentation enables a structured representation of the spectral distribution of sound energy (Bellmann et al., 2020).

The standard center frequencies most commonly used in underwater acoustic modelling, and also applied in this framework, are as follows (in Hz):

```
[12.5, 16, 20, 25, 31.5, 40, 50, 63, 80, 100, 125, 160,
200, 250, 315, 400, 500, 630, 800, 1000, 1250, 1600, 2000,
2500, 3150, 4000, 5000, 6300, 8000, 10000, 12500, 16000]
```

These frequencies align with commonly adopted standards in underwater acoustics (Bellmann et al., 2020), and follow the international IEC 61260 standard for one-third octave filter bands, which is also referenced in that report.

This frequency-based breakdown is particularly useful when assessing underwater noise impacts, as marine species often exhibit frequency-dependent hearing sensitivity. Moreover, many noise mitigation techniques do not attenuate sound uniformly across all frequencies. Instead, their effectiveness varies across the spectrum, often being most efficient within specific bands. By applying frequency-dependent attenuation profiles, the model accurately reflects this variable performance and enables more realistic estimation of the residual sound levels after mitigation.

The noise modelling approach used in this framework follows the frequency-dependent methodology described by (Bellmann et al., 2020), (S. P. Robinson, Theobald, and Lepper, 2012) and (Danish Energy Agency, 2023), and will be further explained in the next subsection. In consultation with an environmental specialist at Van Oord, this spectral method was chosen because it offers a practical balance between accuracy and computational efficiency. It avoids unnecessary complexity while still capturing the essential spectral characteristics of both the noise source and the applied mitigation measures.

4.6.2. Distributing Total SEL Over Frequency Bands

A Python-based model was developed, comprising multiple functions designed to calculate the underwater noise level after the application of mitigation techniques. This subsection provides a structured explanation of the methodology used in this model, detailing each step of the calculation process and the corresponding formulas.

Based on Table 3.2, the relevant sound exposure levels (SEL) for each installation technique can be identified. SEL is defined as:

$$\text{SEL} = 10 \log_{10} \left(\frac{E}{p_{\text{ref}}^2 t_{\text{ref}}} \right), \tag{4.1}$$

where:

- E is the integrated acoustic energy in $\text{Pa}^2 \cdot \text{s}$,
- $p_{\text{ref}} = 1\,\mu\text{Pa}$,
- $t_{\text{ref}} = 1\,\text{s}$.

Since all SEL values used in this work are expressed in dB re $1\,\mu\text{Pa}^2 \cdot \text{s}$, the term $p_{\text{ref}}^2 t_{\text{ref}}$ equals unity, and the conversion from decibels to linear energy simplifies to:

$$E_{\text{total}} = 10^{\text{SEL}_{\text{total}}/10}. \tag{4.2}$$

This total energy is then distributed over N standard one-third octave bands using a predefined energy share vector s, such that:

$$\sum_{i=1}^{N} s_i = 1 \tag{4.3}$$

The energy in each frequency band is calculated as:

$$E_i = E_{\text{total}} \cdot s_i, \quad \text{for } i = 1, \ldots, N \tag{4.4}$$

These values are then converted back into dB units, yielding the initial spectrum:

$$\text{SEL}_i = 10 \cdot \log_{10}(E_i) \tag{4.5}$$

The energy share vector s is based on an empirical distribution (e.g., 10 bands with 4%, 10 with 3%, 10 with 2%, and 2 with 1%), representing the typical frequency distribution of impact pile driving noise (Bellmann et al., 2020).

4.6.3. Applying Frequency-Specific Mitigation

Each mitigation system m is assumed to be effective only within a specific range of frequencies, as defined in Section 3.6.2. This range is translated into a binary mitigation profile $p_i^{(m)}$, defined over the N standard one-third octave bands:

$$p_i^{(m)} = \begin{cases} 1, & \text{if frequency band } i \text{ lies within the effective range of } m \\ 0, & \text{otherwise} \end{cases} \tag{4.6}$$

For each frequency band i, the applied reduction $r_i^{(m)}$ is calculated using a linear interpolation between an assumed minimum and maximum reduction value:

$$r_i^{(m)} = r_{\text{min}}^{(m)} + \left(r_{\text{max}}^{(m)} - r_{\text{min}}^{(m)} \right) \cdot p_i^{(m)} \tag{4.7}$$

In this formulation, all frequency bands receive at least the minimum reduction $r_{\text{min}}^{(m)}$, and bands within the effective range (where $p_i^{(m)} = 1$) receive the full reduction $r_{\text{max}}^{(m)}$. Bands outside the range (where $p_i^{(m)} = 0$) only receive the base reduction $r_{\text{min}}^{(m)}$. Both $r_{\text{min}}^{(m)}$ and $r_{\text{max}}^{(m)}$ are defined per mitigation technique in the project input file as can be seen in Table 4.6.

4.6.4. Combining Multiple Mitigation Measures

If multiple mitigation systems are used, it is assumed that their effects act independently and do not interfere with each other's performance. Under this assumption, the reductions can be summed in the decibel domain as an approximation:

$$R_i = \sum_m r_i^{(m)} \tag{4.8}$$

However, since decibels represent logarithmic energy units, this decibel summation corresponds to multiplication of reduction factors in the linear energy domain. The mitigated energy level per frequency band E_i^{mit} is then calculated as:

$$E_i^{\text{mit}} = E_i^{\text{orig}} \cdot \prod_m 10^{-r_i^{(m)}/10} \tag{4.9}$$

This formulation ensures that mitigation effects are correctly combined according to acoustic principles. It is consistent with the implementation in the Python-based framework.

4.6.5. Computing the Mitigated Spectrum and Total SEL

Once the cumulative frequency-dependent mitigation reduction R_i has been computed for all N third-octave bands, it is subtracted from the original band-specific spectrum to obtain the mitigated sound exposure level per band:

$$SEL_i^{\text{mit}} = SEL_i - R_i \tag{4.10}$$

This step results in a new spectrum that represents the expected sound levels after applying all selected mitigation techniques, accounting for their frequency-specific effectiveness.

To assess whether this mitigated noise profile complies with regulatory thresholds, it is necessary to convert the mitigated band spectrum back into a single total SEL value. This is done by first converting each band to linear energy units and summing them:

$$E_{\text{total}}^{\text{mit}} = \sum_{i=1}^{N} 10^{SEL_i^{\text{mit}}/10} \tag{4.11}$$

The total mitigated energy is then converted back to decibels to yield the overall mitigated source level:

$$SEL_{\text{total}}^{\text{mit}} = 10 \cdot \log_{10}(E_{\text{total}}^{\text{mit}}) \tag{4.12}$$

This final value, $SEL_{\text{total}}^{\text{mit}}$, represents the predicted source sound level at 750 m distance (or another reference range depending on model assumptions), after all mitigation systems have been applied. It provides a single metric that can be directly compared against the user-defined *Project Noise Limit*.
If the calculated $SEL_{\text{total}}^{\text{mit}}$ remains below the limit, the selected combination of installation and mitigation techniques is considered compliant. If the value exceeds the limit, the user is advised to adjust the configuration, for example by adding more effective mitigation or selecting alternative technologies.

4.6.6. Dual Installation Techniques

In cases where two installation techniques are used (for example, *impactIQ6 & vibro*), the compliance is assessed independently for each technique using the same methodology. Final results are printed per technique to assess their individual contributions to underwater noise.

4.7. Computation of Overall Project Costs

The final sheet in the Excel model is the *Costs* sheet, as shown in Table 4.7. Although the confidential values have again been omitted, the figure still provides a clear overview of the various components that make up the total installation costs.

As outlined in Section 3.7.1, the cost structure is divided into three main categories: mobilisation costs, demobilisation costs, and operational costs. The *Costs* sheet presents these categories for the key cost drivers identified as most relevant to offshore monopile installation. Each cost component is directly linked to the project-specific inputs entered in the *General Input* sheet, particularly the selected installation and mitigation techniques.

This sheet also highlights the importance of the parameters calculated in the previous sheets. While mobilisation and demobilisation costs are treated as fixed values, the operational costs are directly linked to the vessel's operation time, after applying weather workability corrections. These time-dependent costs include vessel usage, fuel consumption, noise monitoring equipment, the installation technique applied, and any noise mitigation techniques used.

By adjusting the combination of installation and mitigation techniques, the user can explore different trade-offs between underwater noise emissions and overall project costs. This can be particularly useful in early project phases, such as during tendering, where such trade-offs often need to be made. The framework allows the user to assess whether opting for lower noise emissions justifies higher costs, or whether cost efficiency takes precedence despite higher noise levels. It may also provide insight that, in some cases, the same cost level could lead to significantly different noise outcomes depending on the selected approach, or conversely, that similar noise levels may come at very different costs. Examples of such cases will be presented in Chapter 5.

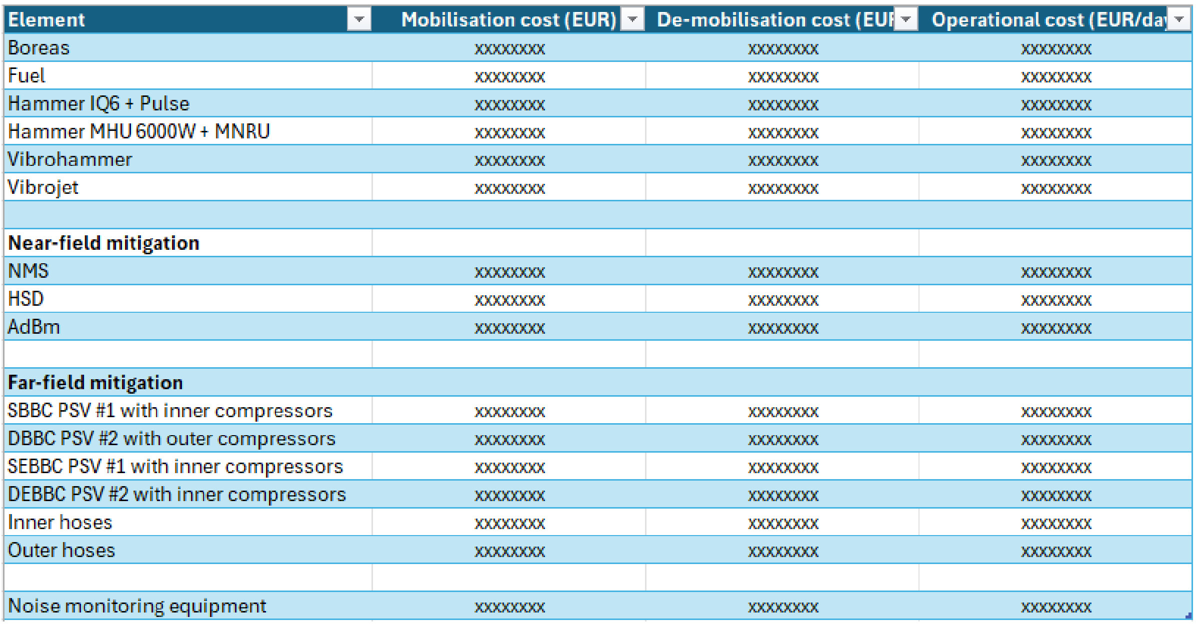

Element	Mobilisation cost (EUR)	De-mobilisation cost (EU	Operational cost (EUR/da
Boreas	xxxxxxxx	xxxxxxxx	xxxxxxxx
Fuel	xxxxxxxx	xxxxxxxx	xxxxxxxx
Hammer IQ6 + Pulse	xxxxxxxx	xxxxxxxx	xxxxxxxx
Hammer MHU 6000W + MNRU	xxxxxxxx	xxxxxxxx	xxxxxxxx
Vibrohammer	xxxxxxxx	xxxxxxxx	xxxxxxxx
Vibrojet	xxxxxxxx	xxxxxxxx	xxxxxxxx
Near-field mitigation			
NMS	xxxxxxxx	xxxxxxxx	xxxxxxxx
HSD	xxxxxxxx	xxxxxxxx	xxxxxxxx
AdBm	xxxxxxxx	xxxxxxxx	xxxxxxxx
Far-field mitigation			
SBBC PSV #1 with inner compressors	xxxxxxxx	xxxxxxxx	xxxxxxxx
DBBC PSV #2 with outer compressors	xxxxxxxx	xxxxxxxx	xxxxxxxx
SEBBC PSV #1 with inner compressors	xxxxxxxx	xxxxxxxx	xxxxxxxx
DEBBC PSV #2 with inner compressors	xxxxxxxx	xxxxxxxx	xxxxxxxx
Inner hoses	xxxxxxxx	xxxxxxxx	xxxxxxxx
Outer hoses	xxxxxxxx	xxxxxxxx	xxxxxxxx
Noise monitoring equipment	xxxxxxxx	xxxxxxxx	xxxxxxxx

Table 4.7: Cost Overview per Component, Categorised into Mobilisation, Demobilisation, and Operational Costs (Confidential Values Not Displayed)

4.8. Final Output Parameters of the Model

Throughout this chapter, references have been made to the general input parameters used within the model. Equally important, however, are the output results generated by the framework. The model calculates the total deck load, the operational time per trip, and the total project duration, both including and excluding the impact of weather workability. It also determines the reduced underwater noise level and verifies whether it complies with applicable noise regulations. In addition, it provides the total project costs as well as the cost per installed monopile.

By adjusting the project-specific parameters in the *General Input* sheet, results can be produced for various scenarios. This enables a structured comparison of different installation and mitigation strategies. The results of these scenarios will be discussed in more detail in Chapter 5.

Finally, a simplified overview of all internal relationships defined within the model is presented in Figure 4.1. This figure provides a clear visualisation of the dependencies between the various components of the framework, supporting both the interpretation of results and potential sensitivity analyses. On the left, the model's general input parameters are listed, with arrows indicating the parameters they influence. Red values represent input parameters from the *General Input* sheet, purple values refer to assumed fixed *Operation Times*, blue values are outputs computed by the model based on these inputs and assumptions, and the black boxes denote the main components that constitute the framework.

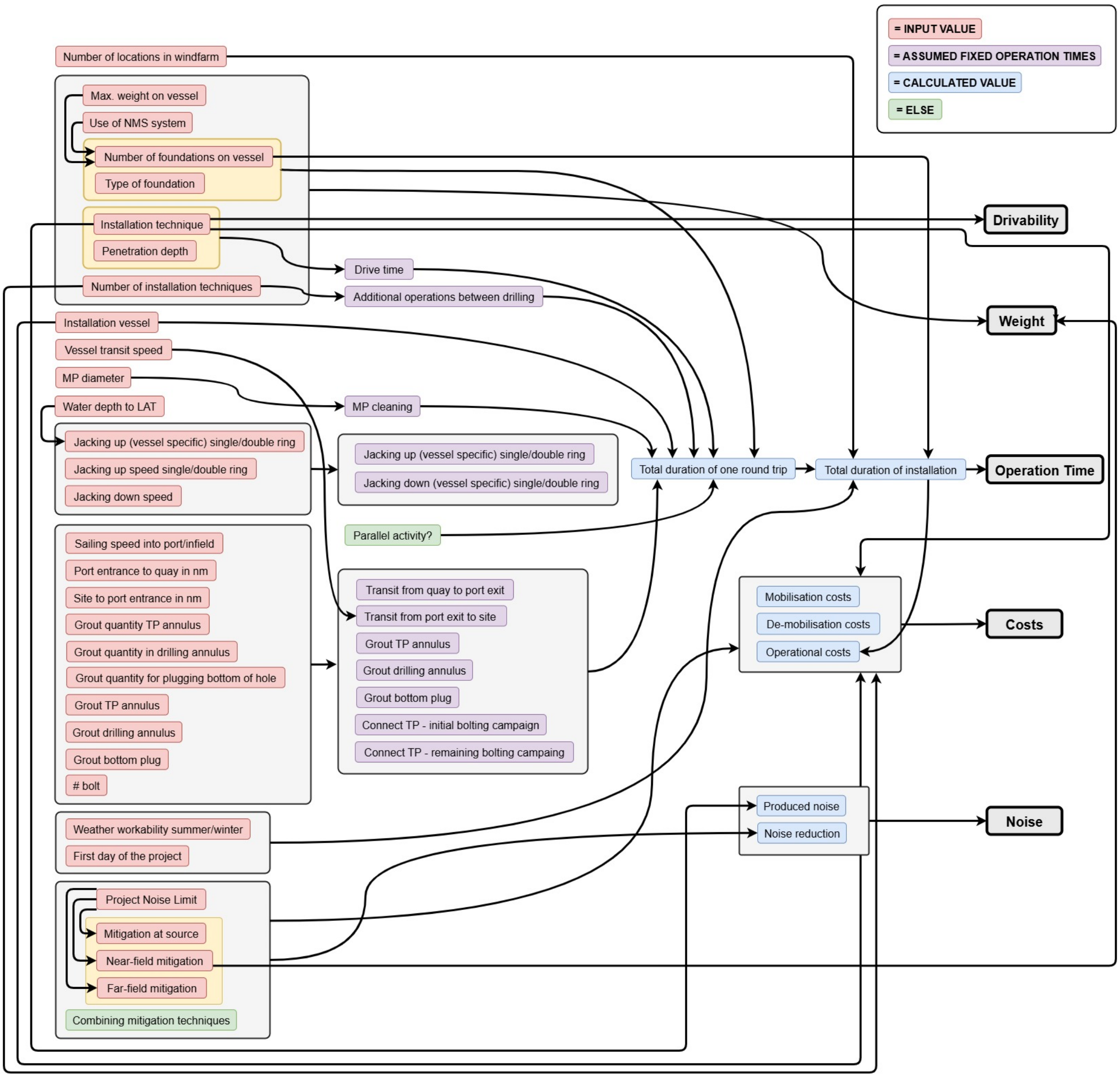

Figure 4.1: Overview of the internal relationships in the model. Arrows indicate dependencies between components: red values are input parameters from the *General Input* sheet, purple values are assumed fixed *Operation Times*, blue values are model outputs based on inputs and assumptions, and black boxes denote the main framework components.

4.9. Verification of Model Functionality

As described in this chapter, the model consists of several interconnected components: general input values, weight, operation times, costs, and noise, all of which interact with one another. To ensure that the model is correctly implemented and functions as intended from both a technical and logical perspective, various checks were performed during its development. This section presents several examples of how the model was verified, demonstrating its reliability for use in further analyses.

4.9.1. General Verification of Individual Functions in the Model

These individual components, which interact with one another, have been translated into separate functions within the model. Before integrating these functions into a complete framework, each function was tested to confirm that it performed as intended. This was achieved by printing a DataFrame for each function that displayed not only the output but also the intermediate values used to generate it. This approach provided clear insight into how the results were constructed.

4.9.2. Verification of Weight Calculation

As previously described, all fixed parameter values for the different installation and mitigation techniques are stored in separate sheets within an Excel file. For example, in the *Weight* sheet (see Section 4.3), equipment is grouped by installation technique. By default, all entries are set to `False` and are therefore excluded from the calculation. When a specific technique is selected in the General Input Parameters, such as `impactMHU`, the corresponding entries within that section are set to `True` and included in the total. Equipment that is used universally across all techniques is always set to `True` by default.

By checking the DataFrame output and confirming that values correctly switched between `True` and `False` when different techniques were selected, the correct behavior of the function was verified across a range of input cases.

4.9.3. Verification of Operation Time Calculation

Operational times are calculated based on individual activities, which, similar to the weight calculations, are toggled between `True` and `False` depending on the selected input parameters. These activities can also be repeated depending on the installation setup. For example, when two installation techniques are combined, all pile driving activities must be performed twice. Similarly, operations directly related to monopile installation need to be repeated for each foundation transported per trip. The number of foundations per trip depends on the *Maximum Deck Load* and whether the `IQIP-NMS` system is used as near-field mitigation, as this system takes up additional deck space.

To verify that these dependencies were correctly implemented, several targeted tests were carried out. The *Maximum Deck Load* was varied to check its influence on the calculated *Number of Foundations on Vessel*. In addition, the `IQIP-NMS` setting was manually switched on and off to assess whether the resulting reduction in transport capacity was accurately reflected in the operational planning. In each case, the relevant DataFrame outputs were reviewed to confirm that the number of repeated operations matched expectations.

4.9.4. Verification of Cost Calculation

To verify the correct implementation of the cost model, several internal consistency checks were performed. A key validation method involved setting the operational duration to zero. In this case, all variable operational costs should drop out of the calculation, and the total cost should equal the sum of the fixed mobilisation and demobilisation costs. This allowed for a straightforward test to confirm whether the separation between fixed and variable components was correctly implemented.

In addition, unit costs and cost rates were manually verified for selected installation steps, by isolating individual activities and checking whether the computed costs matched expectations based on the input data. One important verification focused on the effect of project scale: when increasing the number of monopiles to be installed, the cost per monopile is expected to decrease due to the mobilisation and demobilisation costs being distributed over a larger number of units. This effect was explicitly tested and found to behave as expected within the model as can be seen in Figure 4.2.

Furthermore, scenarios involving the use of two combined installation techniques were assessed. In such cases, the model is expected to output significantly higher total costs due to the fact that certain operations must be performed twice and that duplicate installation equipment is required. These combined cases were tested and confirmed to yield substantially higher costs compared to single-technique installations, in line with expectations.

These verification steps confirm that the cost model produces consistent and realistic outputs across a range of operational scenarios, and that it adequately captures both fixed and variable cost dynamics as well as scaling effects.

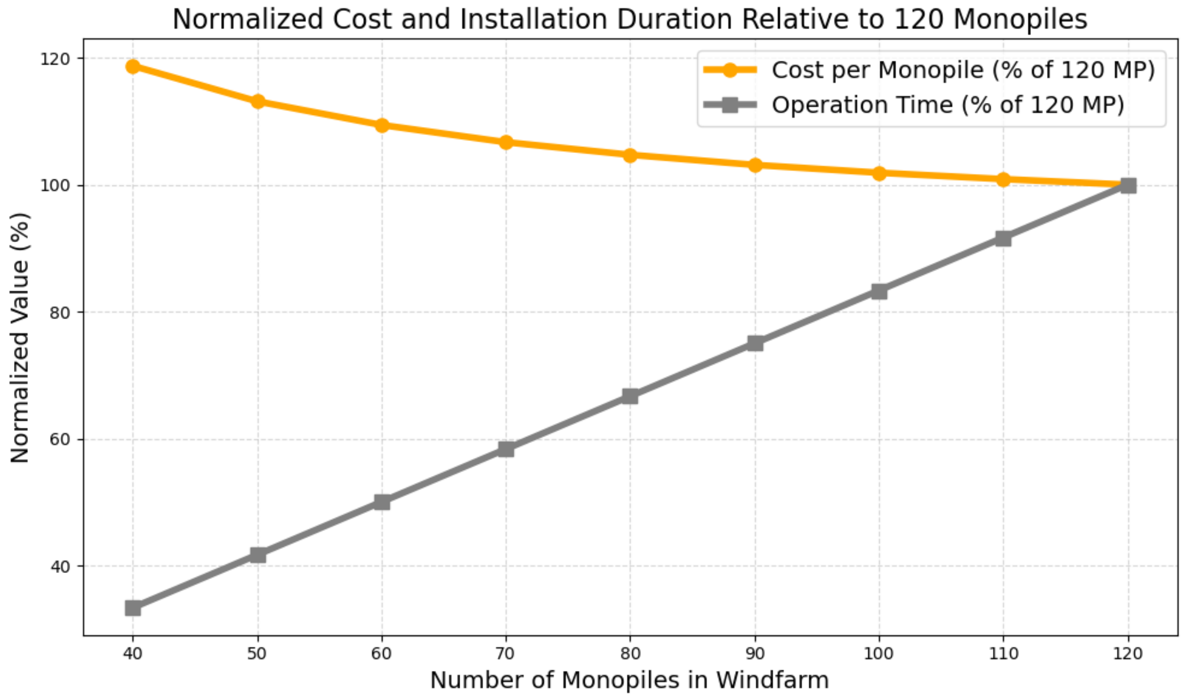

Figure 4.2: Effect of increasing the number of monopiles on cost per monopile and total installation duration. Values are normalised to the same baseline (120 monopiles) for consistent comparison.

4.9.5. Verification of Weather Workability

The function for *Weather Workability* was tested separately to verify its correct implementation. This was done by running a series of targeted test cases, covering both simple and more complex scenarios.

For example, a short installation duration of 60 hours was tested starting in `June`, where only the summer weather factor applied. The expected result of `60 / 0.75 = 80` hours (after weather adjustment) matched the function output exactly.

A longer duration of 40 days starting in *September* was also tested to verify that transitions between months were handled correctly and that the appropriate weather factors were applied to each month.

Finally, an extreme case with a total duration of 360 days starting in `January` was used to ensure that the month logic remained robust across a full year.

These verification steps confirm that the weather workability logic is technically sound and functions reliably under a wide range of input conditions.

4.9.6. Verification of Noise Model

To verify the correct functioning of the noise model, all steps in its computational process were systematically tested. The validation focused on both the frequency-dependent mitigation behaviour and the overall consistency of the total Sound Exposure Level (SEL) reduction.

First, the distribution of a total SEL value across third-octave bands was verified by using a constant input, such as 165 dB, and checking whether the band energies and resulting total SEL remained consistent after recombination. Manual recalculation confirmed that no energy was lost or added during the band distribution and recombination steps.

Second, frequency-selective mitigation was tested using predefined binary effectiveness profiles. For each mitigation technique (such as `AdBm`, `DBBC`, `HSD`), the expected frequency range of effectiveness was translated into a binary profile. The profile-based band reductions were then verified by comparing the adjusted band spectra with the original spectra. For instance, applying a 10-20 dB reduction in the range 250-1000 Hz showed expected reductions only in the affected bands, with unaffected bands remaining stable.

Next, the cumulative SEL reduction for each mitigation layer (*At Source*, *Near Field*, *Far Field*) was evaluated. The total SEL per layer before and after mitigation was recalculated and compared to verify that each mitigation step contributed as expected. This was repeated for various combinations of techniques and installation types, including single and combined methods.

Finally, several full end-to-end simulations were executed using known combinations of installation and mitigation techniques. In each case, the final SEL output was compared to the noise limit defined in the input. For configurations where mitigation was expected to be sufficient (such as *impactIQ6* + *Pulse* + *AdBm* + *DBBC*), the function correctly identified compliance. For unmitigated or partially mitigated cases, the output correctly flagged exceedance of the noise limit.

These verification steps confirm that the model reliably calculates frequency-specific mitigation effects and correctly aggregates them to determine final SEL values relative to the project-specific noise threshold.

4.9.7. Conclusion

The verification steps presented in this section confirm that all core components of the model function correctly across a wide range of input conditions.

In addition to verifying individual functions, interactions between components were tested to ensure that the model captures logical dependencies. For example, it was confirmed that increasing monopile weight reduces the number of foundations per trip, leading to more trips, longer durations, and higher costs. These linked effects were tested step by step to confirm consistency.

Altogether, the verified behaviour of individual modules and their interrelations provides confidence in the model's reliability and supports the analyses presented in the following chapters.

4.10. Limitations Regarding Model Validation

While the model has been verified to ensure that all components function correctly and produce internally consistent results, validation would offer an additional level of confidence by comparing the model outputs to real-world data. However, such validation is currently not possible due to the lack of project-specific or empirical data related to the novel alternative installation technologies.

As a result, the validation process cannot yet be carried out. This step can be performed by Van Oord at a later stage, once more project-specific data becomes available and validation becomes feasible.

In the meantime, the verified model is assumed to function as intended. The following chapter presents several case studies and uncertainty analyses that showcase the model's capabilities and demonstrate its applicability across a variety of input scenarios. The resulting outputs also serve as an implicit validation step, as they confirm that the model behaves logically and produces outcomes that align with expected trends.

5

Case Studies and Sensitivity Analysis

The main objective of this project was to develop a framework that enables comparison of silent installation and mitigation technologies in the early phase of a project. In the preceding chapters, the development process of this framework has been described, and Chapter 4 outlines its technical implementation. Based on a defined set of input parameters, the model generates estimates for expected underwater noise levels, deck load, operational duration, and project costs. By systematically varying these parameters, multiple scenarios can be constructed, each yielding distinct outcomes. These results can then be compared to evaluate the relative performance of different installation and mitigation strategies.

The framework can support Van Oord in identifying, at an early project stage, which installation approach offers the most favourable balance between cost and compliance with underwater noise regulations.

In Section 4.9, a verification procedure was carried out to evaluate whether the model produces realistic and internally consistent outputs. As this has been confirmed, the potential of the framework can now be demonstrated. Several example cases were executed by looping through various combinations of input parameters using the base model developed in Python for the framework. In Section 5.1, a selection of these scenarios is presented to illustrate the types of analyses the framework supports and the insights that can be derived from them.

Because the framework relies on several assumptions due to limited data or necessary simplifications, an uncertainty analysis was performed (see Section 5.3) to evaluate the robustness of the results. In addition, sensitivity analyses were conducted to assess how variations in individual input parameters affect the model outcomes, specifically whether such changes influence the relative ranking of installation techniques in terms of cost-efficiency and compliance with the noise limit. If the ranking remains stable despite these variations, the conclusions can be considered more robust and less sensitive to the underlying assumptions.

5.1. Case Study Results for Different Installation and Mitigation Techniques

The initial step in the analysis involves comparing the different installation techniques without applying any mitigation measures. This comparison provides a baseline understanding of how the eight installation cases introduced in Section 3.2.1 perform in terms of underwater noise generation, operational duration, and associated costs. These baseline results are essential to later assess the added value of mitigation strategies.

It is important to note that in the calculation of both installation duration and costs, as previously stated in Section 3.2.1, all installation cases are assumed to proceed without refusal or interruptions during the pile driving process. In other words, monopile installation is assumed to be completed smoothly, without the need for pauses or delays.

To account for the fact that this assumption does not fully reflect reality for techniques such as vibro piling and vibrojetting, a drivability factor was introduced in Section 3.5. This factor is also applied later in the results. However, the assumption of uninterrupted installation with regard to both duration and cost calculations applies to all results presented in this chapter.

For the results presented in this section, the input parameters for the *Installation technique*, *Near-field mitigation*, and *Far-field mitigation* were systematically varied. All other input parameters were kept constant, using the values shown in Table 4.1.

5.1.1. Comparison of Installation Techniques Without Mitigation

By using the model described in Chapter 4, a loop was executed in Python over all eight installation cases, automatically calculating and plotting the results for each scenario. The outcome of this process is shown in Figure 5.1. The *x*-axis lists the eight installation cases; the left *y*-axis reports the normalised values (%) for total project operation time and cost per monopile, while the right *y*-axis shows the produced noise as sound-exposure level (SEL, dB) at 750 m from the source. Additionally, the regulated *Project Noise Limit* is visualised with a red dashed line, and the produced noise for each installation case is marked with blue dots. For combined installation techniques, two dots are shown, one for each of the applied methods.

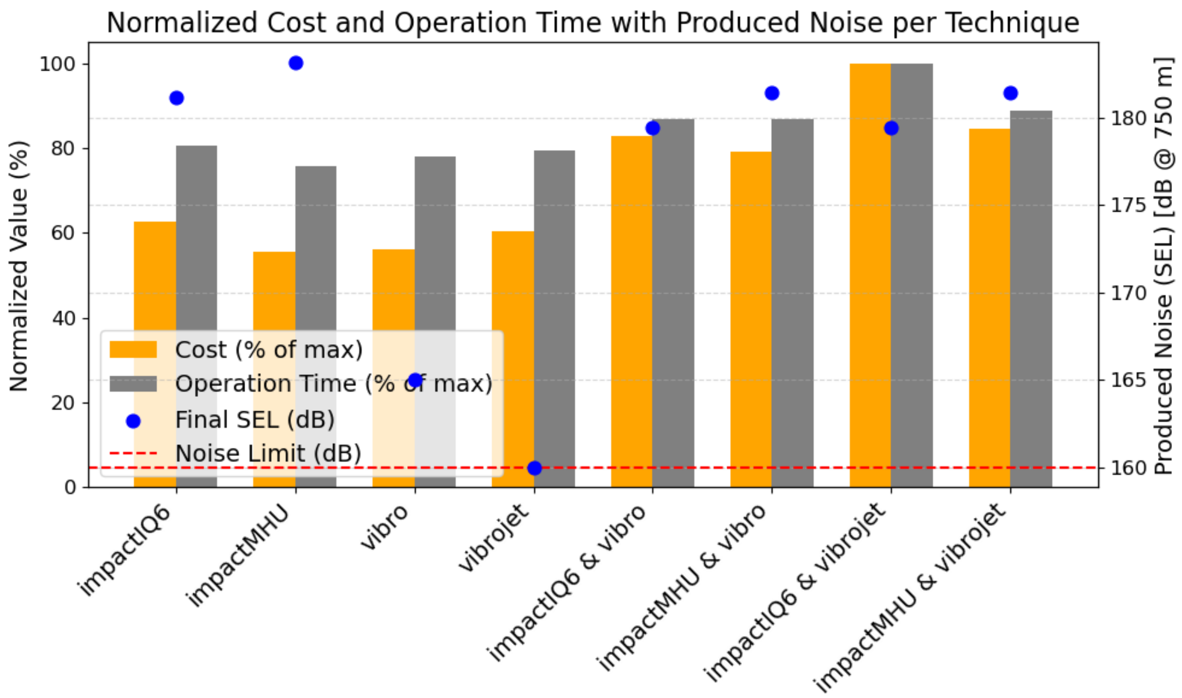

Figure 5.1: Comparison of normalized operation time, cost, and produced underwater noise for eight different installation cases without noise mitigation.

During wind farm construction, it is essential to comply with the imposed maximum noise limits. Exceeding these limits may result in immediate operational delays, regulatory penalties, or suspension of activities. As shown in Figure 5.1, nearly all installation techniques exceed this noise threshold when no mitigation is applied. Vibrojetting is the only case that exactly meets the limit. However, since the data represents average values, it is likely that individual outliers in the vibrojetting case still exceed the permitted level. This already leads to the conclusion that noise mitigation will be necessary in all cases.

Regardless of compliance with the noise limit, the figure also provides valuable insights into the relative operational durations and costs per monopile for each installation technique. The MHU 6000W hammer, for example, results in both the shortest operation time and the lowest cost. This can be attributed to its relatively low weight and favourable day rate in comparison to the other techniques.

In Figure 5.2, the deck loads for all eight cases are shown in light blue, normalised to each other. These deck loads have been compared against the *Max. Deck Load Limit*, which in this case is assumed to be 15,000 mT. This *Max. Deck Load Limit* is indicated by a dark blue dashed line in the figure. As shown, the total deck loads of all cases exceed this limit, except for the *impactMHU* hammer. When the limit is exceeded, the load is corrected by reducing the number of monopiles transported per trip by one. In this analysis, four monopiles are originally carried per trip, but after adjustment only three monopiles per trip are transported for all cases exceeding the limit. The adjusted deck loads with three monopiles instead of four are shown as the dark blue bars in the figure. Since the *impactMHU* hammer does not exceed the *Max. Deck Load Limit*, one additional monopile can be carried per trip. Consequently, fewer transport cycles are required, reducing the total project duration and ultimately lowering overall costs.

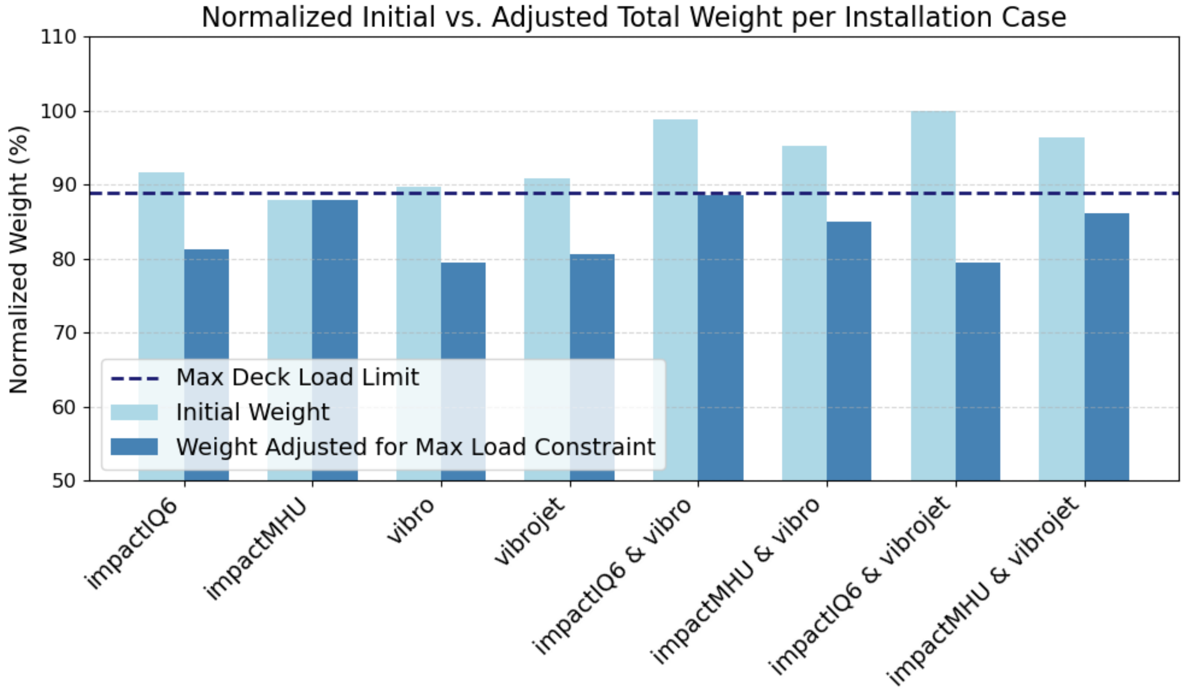

Figure 5.2: Comparison of normalized initial weights and adjusted weights after maximum deck load verification for eight different installation cases without noise mitigation.

However, while the MHU 6000W hammer shows favourable results in terms of operation time and cost, it also generates the highest levels of underwater noise, as shown in Figure 5.1. As a result, it is expected to require the most extensive mitigation measures, which in turn would increase the total project costs.

5.1.2. Comparison of Installation Techniques With Mitigation

Figure 5.3 presents the same comparison as shown in Figure 5.1, but now with noise mitigation applied. The selected mitigation strategies, HSD in the near field and EDBBC in the far field, were chosen to ensure that the produced noise levels for all installation techniques remain below the regulated noise limit. While the vibrojet technique achieves a relatively low SEL of 131.5 dB, the MHU hammer operates much closer to the threshold at 154.55 dB.

It is also noteworthy that, in this figure, the noise levels of the combination cases, where an impact hammer is combined with vibro or vibrojetting, are not significantly lower than those of the cases using only an impact hammer. This can be explained by the fact that in these combination cases, two-thirds of the pile penetration is still performed using impact piling, with only one-third installed using vibro or vibrojetting. Consequently, the impact hammer continues to have a dominant influence on the total SEL. It should be noted, however, that these values may not be fully accurate for actual combination cases in practice, as they are based on the assumptions adopted in this framework. Once projects such as HKW, which will employ combined installation techniques, have been executed, more measurement data are expected to become available to refine these estimates.

Notably, in this scenario (5.3) the installation duration for the MHU hammer is nearly equal to that of the ImpactIQ6 case, whereas it was shorter in the previous comparison without mitigation. This increase is not driven by the far-field system (EDBBC), which is deployed independently of the main vessel and does not affect deck layout or logistics. Instead, it stems from the additional weight introduced by the HSD system. In the MHU case, this extra weight pushes the total deck load just over the vessel's capacity, reducing the number of monopiles that can be transported per trip. As a result, logistical efficiency declines and the total installation duration converges with the other strategies. Although the added weight from HSD is relatively small, it is important to recognise that it can tip the total deck load over the maximum limit, indirectly making the installation method substantially more expensive.

Additionally, Figures 5.1 and 5.3 show that scenarios employing two installation techniques are substantially more expensive than those using a single method. The main reason is the additional handling inherent to dual-technique execution. For example, in the *impactIQ6 & vibro* case, the vibro hammer must first be rigged to the main crane hook to install the pile; it is then de-rigged, the impact hammer is rigged to the main crane to complete installation, and finally de-rigged again, before repeating the sequence for the next pile. Although these combined cases also exhibit longer operational durations, the increase in time alone does not fully explain the higher total cost. This is evident in the plots: for combined cases the gap between normalised operation time and cost is noticeably smaller than for single-technique cases, indicating that costs rise disproportionately relative to time. The primary cost driver is the requirement to carry two complete installation spreads on board the *Boreas*, which significantly increases equipment-related expenses. The extended operation time further adds to total cost, but to a lesser extent.

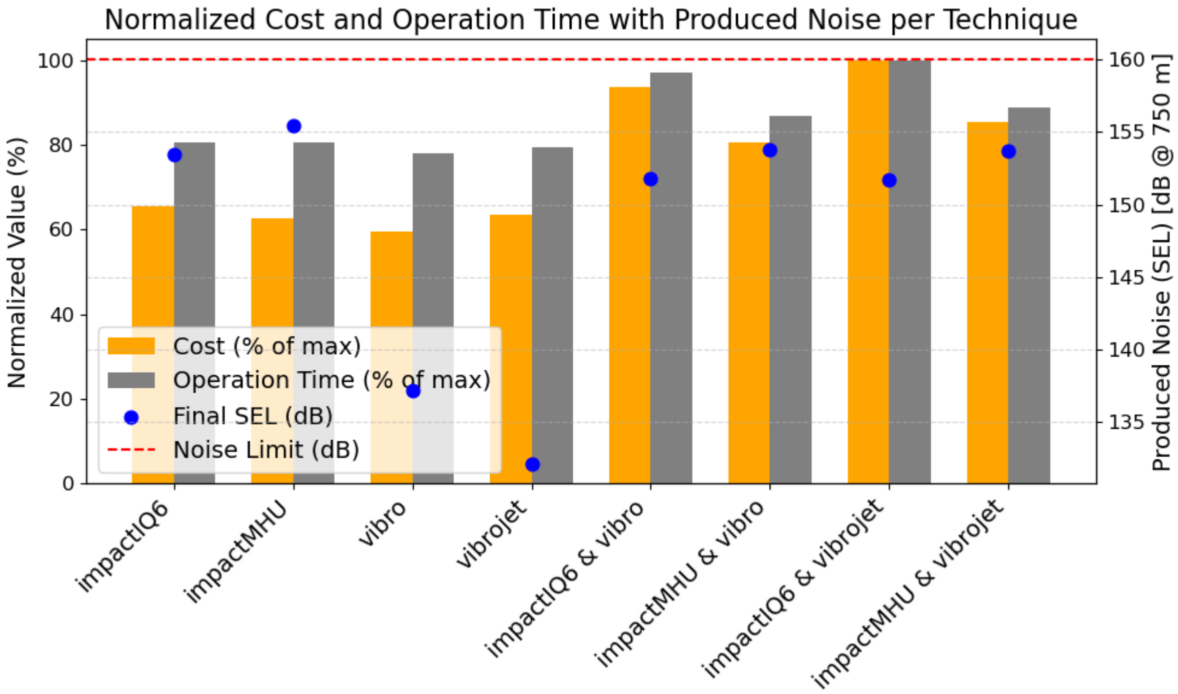

Figure 5.3: Comparison of normalized operation time, cost, and produced underwater noise for eight different installation cases using HSD and EDBBC as mitigation techniques.

A notable observation from the cost comparison is that vibro piling appears to be the most cost-effective installation technique, more attractive than impact piling. This likely reflects two main factors: pile driving with a vibro hammer is expected to be faster than with an impact hammer, and the mobilisation, demobilisation, and operating costs are lower for the vibro hammer. By contrast, vibro-jetting introduces additional jetting steps and associated equipment, which makes it inherently more expensive than vibro piling alone. Nevertheless, vibro-jetting can be advantageous for improving drivability; this is discussed further in Section 5.2.

The plot also shows that the vibro hammer's noise performance is more than 20 dB below the *Project Noise Limit*. While lower noise levels are, of course, preferable, this margin also creates an opportunity to reduce costs by reconsidering the use and combination of mitigation systems. Accordingly, the next section compares several mitigation combinations for a single installation technique to assess their impact on both noise performance and cost.

5.1.3. Comparison of Mitigation Strategies for Selected Installation Techniques

Figures 5.4 and 5.5 compare mitigation combinations for two installation methods, the *impactMHU* hammer and the *vibro* hammer, assessing underwater noise reduction and cost per monopile. As in the previous figures, the left *y*-axis shows the normalised cost per monopile (%), the right *y*-axis shows the produced noise as sound-exposure level (SEL, dB) at 750 m from the source, and the *x*-axis lists the different cases. To improve readability, the three near-field mitigation options are colour-coded, HSD (blue), AdBm (green), and IQIP NMS (pink), each combined in turn with the far-field mitigation systems considered in this framework. Noise levels are indicated by blue dots, and the *Project Noise Limit* is shown as a red dashed line. The aim is to assess whether, and how, both noise and cost can be optimised by varying the combinations of installation and mitigation techniques. Several notable patterns emerge from these plots.

Firstly, all configurations that include the IQIP NMS system lead to substantially higher costs than the alternative mitigation strategies. Although NMS also delivers the strongest noise reduction, the improvement does not appear to justify the disproportionately large increase in cost. This reinforces the earlier conclusion that, under the present assumptions, the cost-effectiveness of IQIP NMS is questionable. It should be emphasised, however, that these findings are based on Van Oord project models (including specific vessel selection and monopile dimensions). Other stakeholders, such as IQIP, may apply different assumptions or operational configurations that yield a more favourable cost-benefit profile; such alternatives were not assessed in this study.

Furthermore, the analysis reveals that the configuration of the bubble curtain has a significant influence on noise reduction, while the associated cost implications remain limited. Specifically, employing a double bubble curtain yields a marked improvement in noise attenuation relative to a single bubble curtain, with only a modest increase in cost. A similar observation holds for enhanced bubble curtains, which outperform standard variants with minimal additional expense.

This relatively modest cost increase can be explained by the fact that the additional expenses for a double bubble curtain primarily consist of extra compressors and hoses. These are minor compared to the fixed costs associated with vessel day rates and crew deployment, which remain largely unchanged. Moreover, bubble curtain systems are typically deployed from a separate support vessel rather than from the main installation vessel. As a result, they do not interfere with critical path operations and have limited impact on overall installation efficiency. This makes the ecological benefits of DBBCs achievable at relatively low additional cost.

As illustrated in Figure 5.4, the *impactMHU* hammer requires the combined use of near-field and far-field mitigation to comply with the regulated *Project Noise Limit*. By contrast, vibro installation can achieve compliance with either near-field or far-field mitigation alone, and, in fact, all tested vibro combinations meet the limit. For example, Figure 5.5 shows that near-field mitigation with the AdBm system is the most cost-effective option. Even so, adding a bubble curtain increases cost only marginally while substantially improving noise reduction, offering clear ecological benefits. This option may therefore still be selected on environmental grounds, with the final trade-off made at the time of decision.

These trade-offs, now made quantitatively transparent through the framework, support more informed decision-making. By clearly visualising the balance between cost and environmental benefit, the results enable project developers to make deliberate and well-substantiated choices. A relatively modest increase in expenditure can, in turn, result in a substantial reduction in underwater noise impact, thereby contributing to the protection of marine ecosystems.

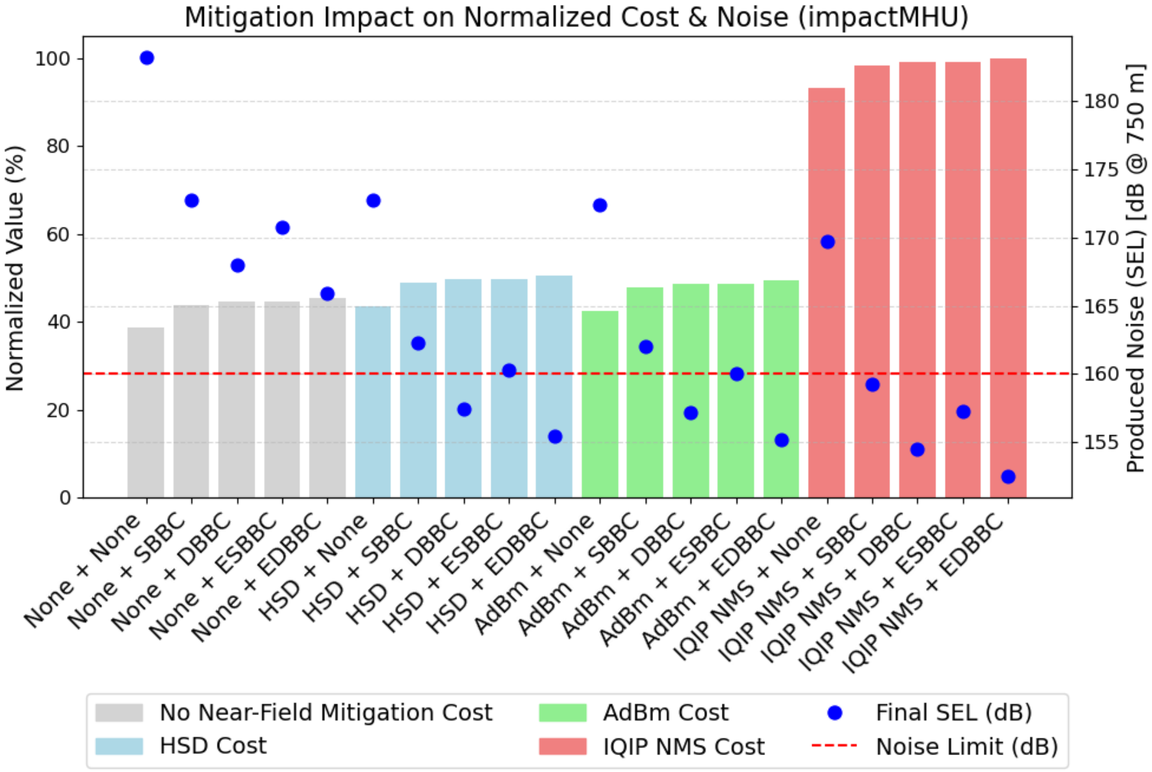

Figure 5.4: Comparison of Normalized Cost and Produced Underwater Noise for ImpactMHU with Different Mitigation Combinations

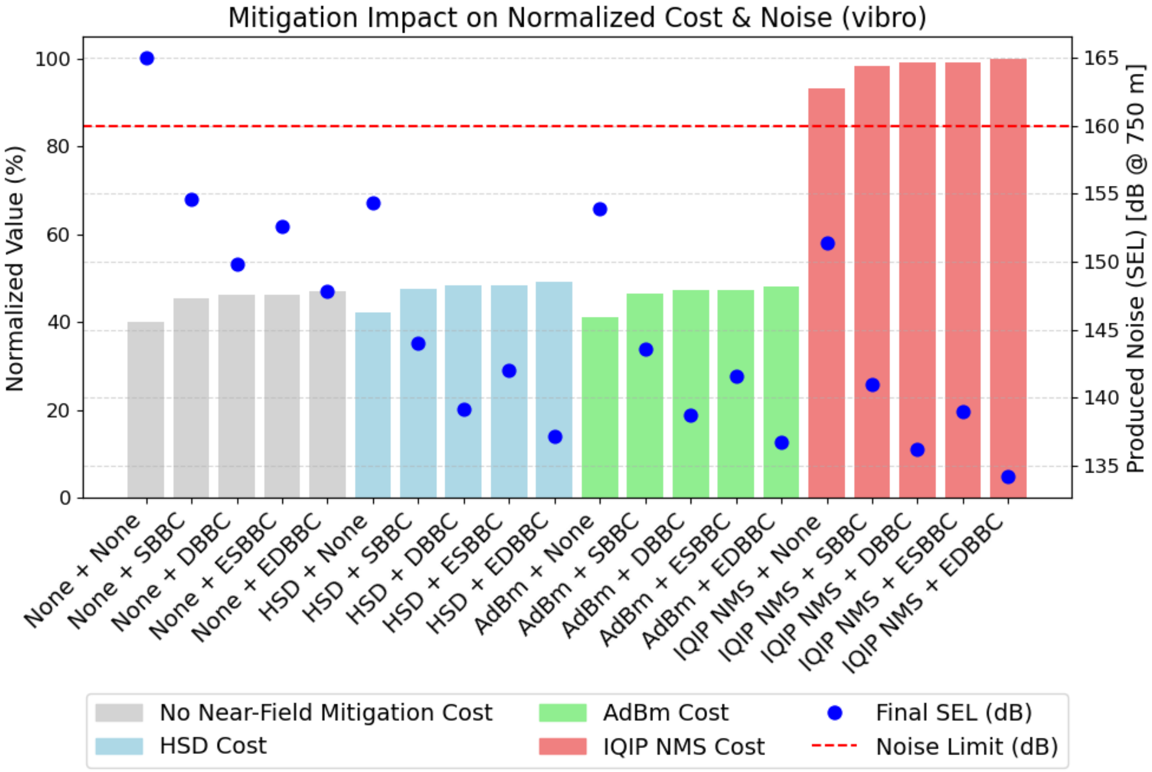

Figure 5.5: Comparison of Normalized Cost and Produced Underwater Noise for Vibro piling with Different Mitigation Combinations

5.1.4. Performance Optimization of Cost and Noise

As illustrated in the figures above, the framework can generate results for a wide range of input combinations. This enables an optimisation over up to $8 \times 4 \times 5 = 160$ configurations, based on eight installation cases, three near-field mitigation options plus a "none" option, and four far-field mitigation options plus a "none" option. In the optimisation considered here, we assume that at-source mitigation is always applied for impact-hammer cases and never for vibro-driven cases. The goal of this optimization is to identify the most cost-effective combination that still complies with the *Project Noise Limit*.

A Python script was developed to perform this optimization, which outputs results such as the following:

```
>>> Optimal combination (lowest total cost):
  - Installation Case: vibro
  - Near-Field Mitigation: AdBm
  - Far-Field Mitigation: None
  - Cost per Monopile: €XXXXXX
  - Total Cost: €XXXXXX
  - Max SEL after mitigation: 152.55 dB
```

As shown above, the most cost-efficient solution that still satisfies the noise constraint is the use of vibro piling in combination with AdBm as near-field mitigation, and no far-field mitigation. It should be noted, however, that this outcome assumes the monopile can be successfully driven to target depth using vibro piling without refusal.

Beyond identifying the single most cost-efficient option, it is also valuable to explore whether there are other combinations that come close in terms of total cost, but offer improved noise performance. To gain insight into this trade-off, Figure 5.6 presents the 20 most cost-effective combinations that comply with the *Project Noise Limit*, plotting both the normalized cost and the resulting noise levels. As in the previous figures, noise performance is indicated by blue dots and the *Project Noise Limit* by a red dashed line. The left *y*-axis shows the normalised cost per monopile (%), while the right *y*-axis reports the sound-exposure level (SEL, dB) at 750 m from the source. The *x*-axis lists the different case combinations. The leftmost case on the *x*-axis represents the most cost-optimal option, with the ranking progressing from left to right in order of increasing cost.

This figure shows, for instance, that the fourth-ranked combination (vibrojet + AdBm + None) results in only a 6.5% increase in total cost, while reducing the produced noise by an average of 5.0 dB. In more extreme cases, such as the 14th-ranked combination, the average noise level is reduced by as much as 17.3 dB, with a cost increase of only 17.2%.

Such trade-offs could be of strategic interest to Van Oord, particularly in tender procedures where additional points may be awarded for staying well below the specified *Project Noise Limit*, thereby increasing the likelihood of winning the contract.

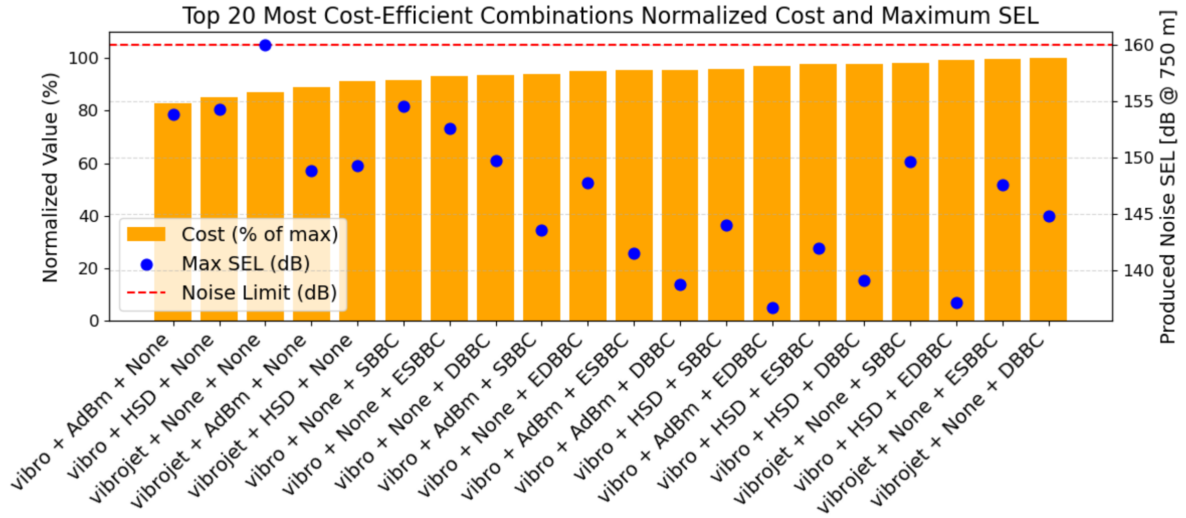

Figure 5.6: Top 20 Most Cost-Efficient Installation and Mitigation Combinations Based on Normalized Cost and Produced Underwater Noise

In addition to the normalized cost and noise levels, a cost breakdown has been provided for the same 20 most cost-efficient combinations. This plot illustrates how the total project cost is distributed across different cost categories.

Interestingly, the distribution is relatively consistent across all installation techniques. It clearly shows that the largest portion of the total cost is associated with operational expenses, which are strongly driven by the total operation time.

This provides an important insight for Van Oord: if cost reductions are desired, the greatest potential for savings lies in optimising the duration of operations. Efficiency improvements in this area could significantly reduce overall project costs.

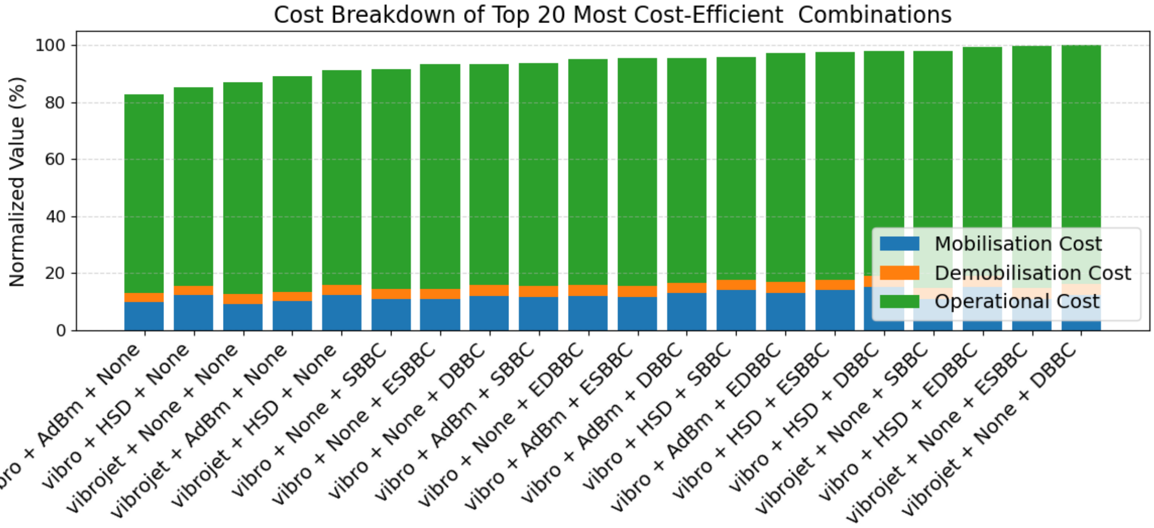

Figure 5.7: Cost Breakdown of Top 20 Most Cost-Efficient Installation and Mitigation Combinations Based on Normalized Cost and Produced Underwater Noise

5.1.5. Results of Frequency-Dependent Noise Reduction Calculations

While the previous comparisons focused on total SEL values at 750 m from the source, the model can also provide insight into how each mitigation technique contributes to noise reduction across specific frequency bands. This is particularly relevant when evaluating the compatibility and complementarity of different mitigation systems in a layered setup (at source, near field, and far field).

The figures below visualise the output of the noise model by showing the sound-exposure level (SEL) per third-octave band before and after applying mitigation. Each line represents the cumulative effect of mitigation at the *At Source*, *Near Field*, and *Far Field* layers. Results are presented for two installation methods: the *impactMHU* hammer and *vibrojet*. The *y*-axis reports the SEL (dB) at 750 m from the source, while the *x*-axis shows the third-octave centre frequencies.

The blue dashed line represents the unmitigated noise spectrum of the installation method, while the other coloured lines show, as indicated in the legend, the mitigated spectra for each mitigation technique and thus the achieved reduction. The sharp drops in specific frequency ranges reflect the frequency-dependent effectiveness of individual mitigation techniques. For instance, *MNRU* and *Pulse* are active between 40-250 Hz, while *DBBC* and *SBBC* target 250-1000 Hz. These profiles were implemented using binary effectiveness filters per frequency band.

The final purple line represents the total reduced spectrum after all selected techniques have been applied. These plots illustrate how frequency-specific attenuation is modelled per mitigation layer, and how the cumulative effect is constructed across the full frequency range.

This frequency-specific modelling approach is not only technically relevant, but also reflects the growing importance of frequency weighting in underwater noise regulation. As shown by Tougaard and Dähne (2017), different countries and regulatory bodies apply diverging approaches when setting acoustic exposure limits for marine species. For example, Germany often relies on unweighted Sound Exposure Level (SEL) values, whereas the United States, such as through NOAA, uses frequency-weighted criteria based on the hearing sensitivity of marine mammals. The study highlights that applying an inappropriate weighting function can lead to either excessive restrictions or insufficient protection in relation to offshore activities. This underlines the need for accurate, frequency-dependent modelling to support effective regulation and ensure consistency across national boundaries.

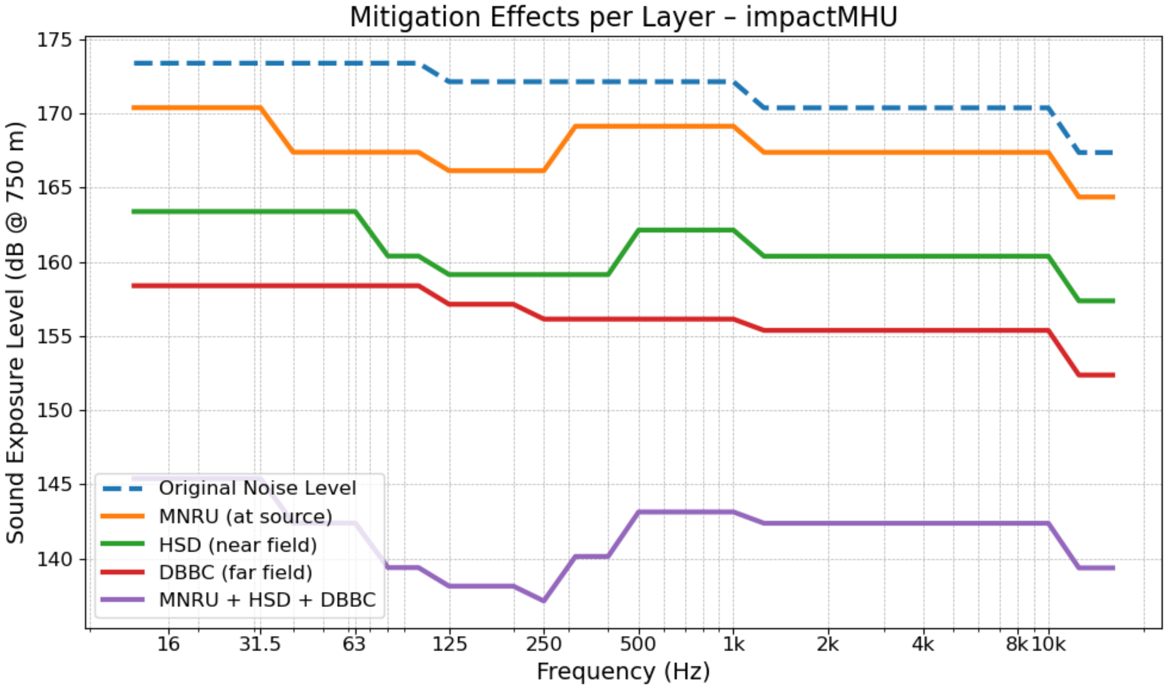

Figure 5.8: Sound exposure level per frequency band for the installation method *impactMHU*, showing the effect of individual mitigation layers including MNRU in the at-source layer, HSD in the near field, and DBBC in the far field, as well as the cumulative effect of all applied techniques.

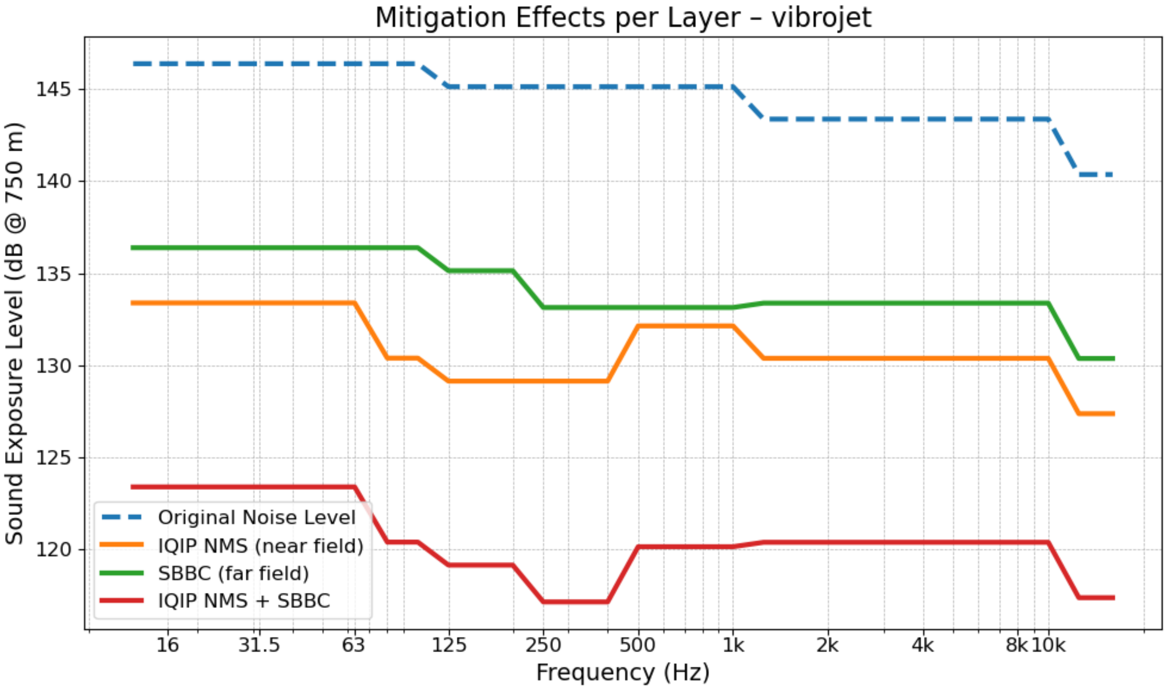

Figure 5.9: Sound exposure level per frequency band for the installation method vibrojet, showing the effect of individual mitigation layers including IQIP NMS in the near field and SBBC in the far field, as well as the cumulative effect of all applied techniques.

5.2. Installation Technique Performance Relative to Base Case and Noise Limit

In coordination with Van Oord, the following Figures (5.10 & 5.11) were developed to provide a clear comparison between various monopile installation techniques. Unlike earlier comparisons, this assessment includes drivability. The evaluation is based on five key factors that influence environmental performance as well as operational and economic performance:

- **Underwater Noise Emission**: indicates the produced noise level relative to the project noise limit, showing whether the limit is exceeded and to what extent.
- **Drivability Risk**: indicates the likelihood that the chosen installation method will achieve the required penetration depth, with 100% representing full certainty. Values above 100% reflect an increased risk of not reaching the target depth.
- **Total Installation Duration**: shows the total time required to install the wind farm relative to the base case, including weather workability effects.
- **Installation Duration per Monopile per Trip**: shows the time required to install a single monopile, excluding weather workability effects.
- **Cost per Monopile**: shows the cost relative to the base case for the different installation strategies.

The figures compare various monopile installation techniques, including cases where two installation methods are combined. Both figures represent a different noise mitigation scenario:

- Figure 5.10: No near-field or far-field mitigation (only Pulse and MNRU are applied by default for impact hammers).
- Figure 5.11: Near-field mitigation using HSD, combined with far-field mitigation using EDBBC.

All values, except for the noise levels, which are shown relative to the project-specific noise limit, are normalised with respect to the following base case:

impactIQ6 + Pulse + AdBm + DBBC.

This configuration has been chosen as the reference case because it is frequently applied in Van Oord's current offshore wind projects and, for now, still complies with the regulated noise limit of 160 dB. Normalizing the data against this reference allows for a direct and transparent comparison with the current practice, highlighting the relative performance of alternative installation methods in terms of environmental impact, technical feasibility, efficiency, and cost-effectiveness.

Each bar group in the figures (5.10 & 5.11) represents a specific installation technique or combination of techniques, shown on the x-axis. Each colour indicates performance on a different factor: noise emission relative to the project limit (blue), drivability risk (green), total installation duration (grey), duration per monopile per trip (light blue), and cost per monopile (orange). All values are shown as a percentage of the base case, with noise expressed as a percentage of the project-specific noise limit.

When examining Figure 5.10, several key insights emerge. First, the cases involving only a single installation method are noticeably more cost-effective than the base case. This cost difference arises because, in this analysis, no mitigation measures are applied, except in the base case. In addition, as already discussed in Section 5.1.2, the combined techniques generally perform the worst in terms of both cost and duration. This is due to the fact that both installation methods must be executed sequentially, which significantly increases the total installation time and, consequently, the cost. The produced noise levels for these cases are also relatively high. On the other hand, these combinations ensure that the pile reliably reaches the required depth, which is reflected in their high drivability scores.

Since it is assumed that mitigation measures are applied in parallel to the installation activities, their presence does not affect the critical pact, and thus the operational duration. This explains why in Figure 5.10 the total duration of single-technique methods (especially impact-based ones) is comparable to that of the base case, in which mitigation is applied.

The effect of mitigation is most clearly visible in the noise emissions. As shown in Figure 5.10, the blue bar, representing underwater noise, exceeds 100% in all cases except the base case, indicating that the noise limit is not met without mitigation. This underlines the importance of sound mitigation systems when environmental compliance is required. Since non-compliance would render installation unfeasible under current regulations, a second analysis was performed in which both near-field (HSD) and far-field (EDBBC) mitigation were applied across all installation cases. As shown in Figure 5.11, this approach ensures compliance with the project noise limit in every scenario.

With regulatory compliance ensured, the focus can shift to evaluating the remaining performance factors for each method. For example, the fourth bar group from the left in Figure 5.11 corresponds to the *vibro* installation technique. While this option meets the noise requirement, the green bar, representing drivability, reaches 130%, indicating reduced confidence in achieving the required penetration depth without refusal. For Van Oord, both noise compliance and drivability are considered critical; if either condition is not met, the method is deemed non-viable, regardless of other advantages.

Nevertheless, the remaining three indicators present a favourable profile: the grey bar shows a total installation duration of approximately 95% compared to the base case, indicating a slightly faster execution; the light blue bar is similar in height, suggesting comparable trip efficiency; and the orange bar drops to around 75%, meaning the cost per monopile is significantly lower. Combined with one of the best-performing noise levels across all cases, this makes vibro piling a particularly attractive option.

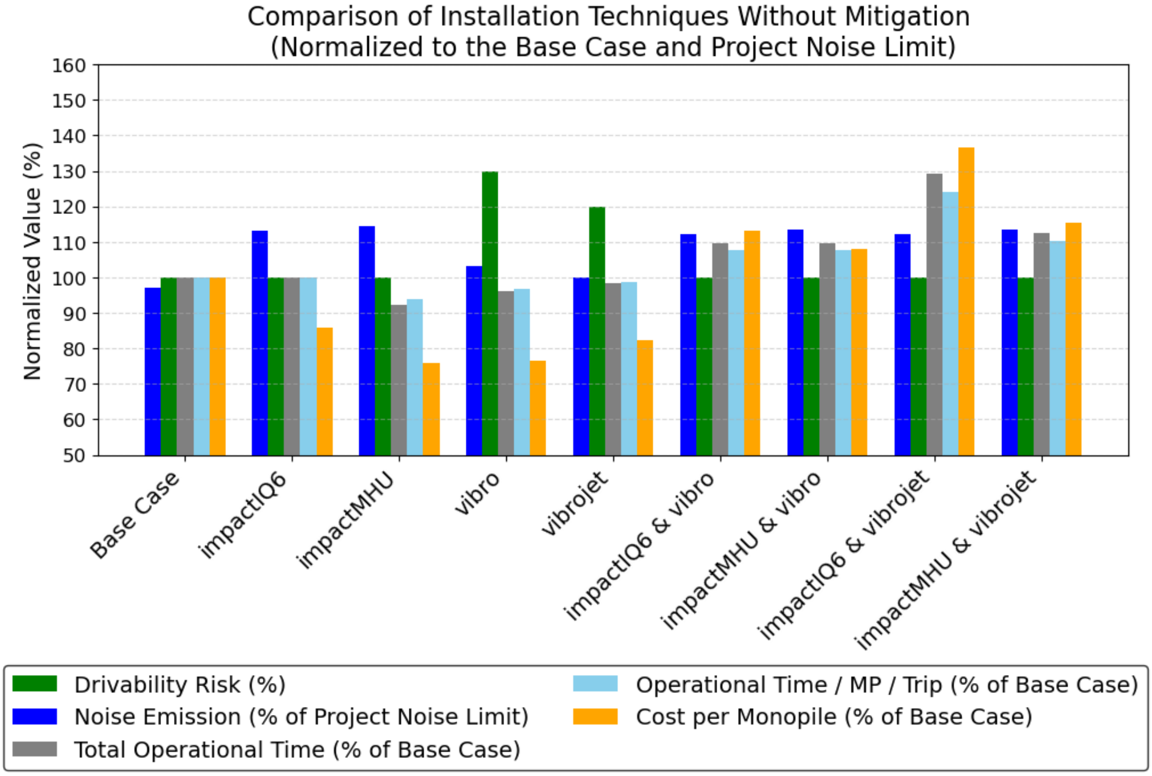

Figure 5.10: Normalized comparison of cost, duration, noise, and drivability across installation techniques without near- or far-field mitigation, relative to the base case and project noise limit.

However, because noise compliance and drivability remain the primary decision criteria, operational and cost benefits are considered secondary. Consequently, if vibro piling is pursued, an impact hammer must still be retained as contingency. This effectively shifts the operation to a combined installation case, such as *impactIQ6 & vibro* or *impactMHU & vibro*, which, as shown in earlier results, performs significantly worse in terms of cost. As a result, the most optimal technique in practice shifts towards the *impactMHU*. This hammer shows low drivability risk and offers a high level of reliability at relatively low cost. However, this comes at the expense of environmental performance, as it generates the highest underwater noise emissions among all evaluated techniques. From an operational and economic perspective, *impactMHU* may therefore be attractive, but from both a regulatory and ecological standpoint it is less favourable, making it unlikely to be a viable option in projects with strict environmental constraints. The *impactIQ6* hammer produces lower noise levels, but at higher cost, which introduces an additional trade-off: whether to prioritise lower environmental impact or lower project costs. Exceeding the noise limit also carries the operational risk of immediate installation shutdowns, further complicating this decision.

Furthermore, when considering the mitigated results in Figure 5.11, it is evident that the impact hammers operate with very little margin below the project noise limit. Since this framework is based on a 15MW turbine and turbine capacities are expected to increase towards 20MW, impact hammers are likely to exceed the noise threshold under future conditions. This underlines the importance of advancing vibro hammers and vibrojetting, particularly by improving their drivability, to ensure they can become viable alternatives. While combined installation cases remain possible, they are neither cost-effective nor sustainable solutions, as two-thirds of the pile penetration still relies on impact piling, generating the same high impulse noise ($\mathrm{SEL}_{\mathrm{ss}}$) that is particularly harmful to marine life. The apparent reduction in total SEL levels arises only from the shorter piling duration, not from a reduction in the severity of the individual blows. If drivability concerns can be resolved, however, vibratory techniques could emerge as highly attractive installation methods, offering not only substantial noise reduction but also potential cost advantages over impact piling, as suggested by Figure 5.11.

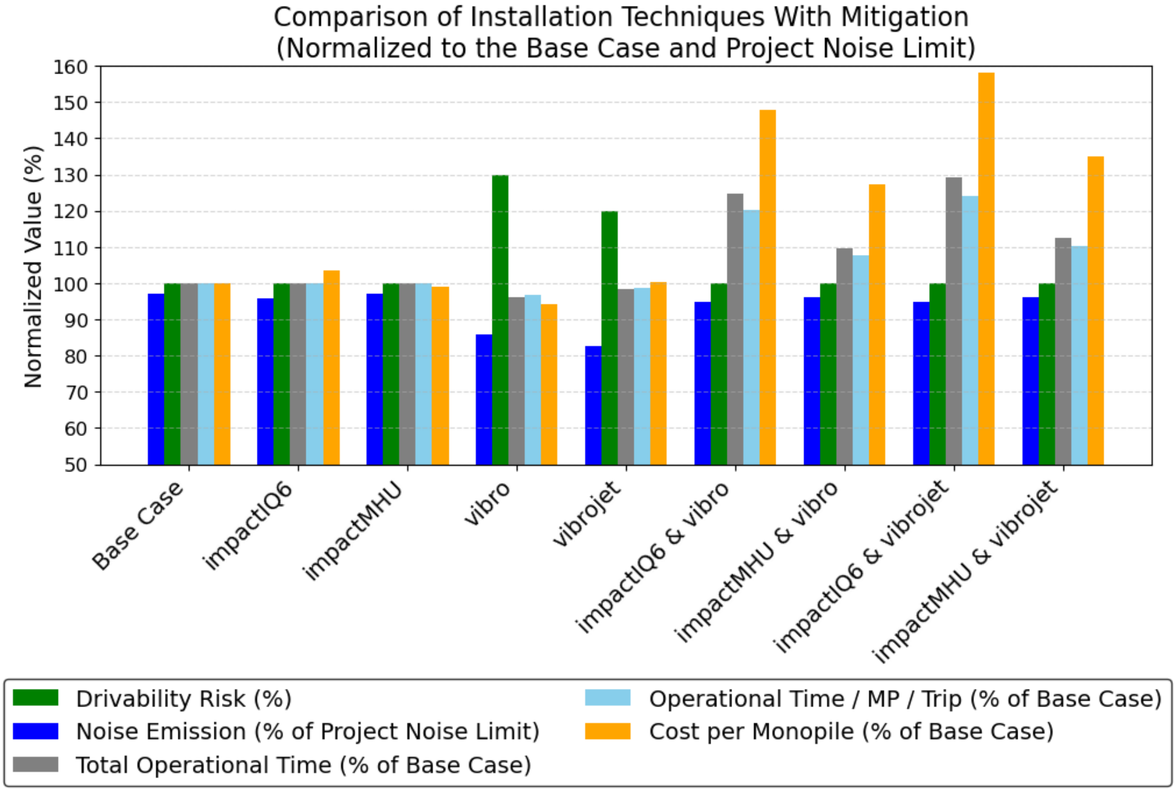

Figure 5.11: Normalized comparison of cost, duration, noise, and drivability across installation techniques with HSD and EDBBC applied, relative to the base case and project noise limit.

5.3. Uncertainty and Sensitivity Analysis of Assumed Input Parameters within the Installation Framework

To support a deeper understanding of the model's behaviour and reliability, an uncertainty analysis was conducted for a number of key assumptions to evaluate the model's robustness. This was done by testing how sensitive the results are to variations in these assumptions. The corresponding analyses and findings are discussed in this section.

Two types of uncertainty analysis were carried out. The first type involved hypothetical variations, for example, in soil conditions, for which no alternative data are available within the framework. In such cases, the expected influence of changing these parameters on the model outcomes is qualitatively assessed. The second type involved varying assumed input values within realistic ranges to quantify their effect on key output parameters.

Together, these analyses provide insight into the model's reliability and clarify the impact of simplifications made during its development.

5.3.1. Uncertainty Analysis of Assumed Soil Type

The current framework assumes sandy soil conditions. However, seabed compositions at offshore wind farm sites can vary significantly, from loose sediments to cohesive clay, silt, gravel, glacial till, or even weathered rock. This variability introduces uncertainty in the applicability and performance of installation techniques, particularly for vibropiling and vibrojetting.

Vibropiling is generally effective in sandy or gravelly soils, particularly when these are water-saturated and of low to medium density. In such conditions, the vibrations from the hammer can reduce soil resistance around the pile, allowing for efficient penetration. However, in stiff or highly plastic clays, vibropiling becomes significantly less reliable. These cohesive soils absorb vibrational energy rather than allowing it to loosen the soil structure. As a result, the pile may encounter strong resistance and reach refusal before the target depth is achieved. In such cases, the use of heavier hammers or a switch to an alternative installation technique may be necessary to reach the required embedment (Pile Buck, 2024). Additionally, the presence of dense or cemented layers, such as glacial till or compacted silts, further reduces the effectiveness of vibropiling and increases the risk of incomplete installation.

Vibrojetting also performs well in loose sandy soils, where the high permeability and low cohesion allow the jetting fluid to effectively displace and fluidise the surrounding sediment. However, in cohesive soils such as clay, the technique encounters considerable limitations. The low permeability and strong inter-particle bonding in clay prevent the water jets from penetrating and loosening the soil effectively. As a result, far more energy and water flow are required to achieve any significant displacement (Sol and Tack, 2022). In practice, this leads to a marked reduction in efficiency and can result in incomplete penetration, prolonged installation durations, or the need to combine jetting with other techniques to achieve the desired depth.

Impact hammering remains the most robust technique across soil types. However, in very soft soils, it introduces a different risk: pile run. This occurs when a monopile rapidly sinks below the target depth due to insufficient ground resistance, particularly in heavy XXL foundations. Such uncontrolled settlement can lead to structural issues or damage (CAPE Holland, 2024). In contrast, in hard or very dense soils, increased driving energy and longer durations may be required to reach the planned penetration depth.

Soil composition remains a key source of uncertainty in monopile installation modelling. While the current framework assumes sandy soil, favourable for most techniques, this simplification limits the model's applicability to real-world conditions where heterogeneous or cohesive seabeds are often encountered. Research initiatives such as those conducted by the Noise Desk in Germany (Bellmann et al., 2020) have shown that soil dependency plays a significant role in both installation efficiency and underwater noise propagation. Due to the complexity and site-specific variability of these geotechnical conditions, this aspect has been consciously excluded from the current model. Nevertheless, expanding the framework to incorporate a broader range of soil types, such as clay, silt, or layered strata, represents an important avenue for future work to enhance the model's robustness and real-world relevance.

5.3.2. Uncertainty in the Assumed Monopile Design

This framework uses the extended monopile (Ext. MP) as the baseline foundation configuration. In this design, the transition piece is integrated into the monopile, eliminating the need for a separate component and simplifying the installation process. However, in current industry practice, monopiles with a separate transition piece (MPTP) are still commonly used. To reflect the uncertainty introduced by this design variation, an uncertainty analysis was conducted to assess the impact of using MPTP on model outcomes.

Although the framework accounts for the additional installation time associated with handling a separate transition piece, other implications of using MPTP, such as altered deck layouts or the presence of additional equipment like grouting or bolting systems, are not explicitly included. The vessel configurations used in this model are based on the NSC and HKW projects, both of which assume the use of Ext. MPs and do not reflect the spatial and logistical constraints introduced by MPTP handling. These constraints could notably reduce the number of monopiles transported per trip due to limited deck space or integration of specialised equipment. Accurately modelling such effects would require a dedicated configuration update, which falls outside the scope of this study. Therefore, MPTP is not fully embedded in the framework and is instead assessed through a targeted sensitivity analysis.

It is also important to note that this framework is not intended to compare different foundation concepts, such as *Ext. MP* versus *MPTP*. Such comparisons may be considered in future extensions of the model.

However, to quantify the potential impact of the additional installation time associated with using *MPTP*, all installation scenarios were re-evaluated with MPTP-specific additional activities included. The results were compared against the *Ext. MP* baseline, focusing on relative differences in total installation time and associated costs, as shown in Figure 5.12. In this figure, all values are normalised with respect to the *impactIQ6* case using *Ext. MP*. The grey bars represent the operation times, while the orange bars indicate the costs. The hatched bars correspond to the *MPTP* values. In all scenarios, it can be seen that using *MPTP* instead of *Ext. MP* results in substantially longer operation times, which subsequently increases the total costs. From this, it could be concluded that switching to a different monopile type already has a considerable negative impact on both operation time and costs. However, this is not a fully comprehensive comparison, as, as previously noted, many factors have been excluded from this analysis that could potentially offset part of this large cost difference.

Among the single-technique cases, vibropiling exhibits the largest relative increase. This is due to its initially short baseline duration, as shown in Figure 5.3. Applying the same absolute additional time across all cases results in a proportionally greater effect on methods with shorter original durations. This also translates into a stronger relative cost increase. As a result, when considering only the additional operational activities introduced by MPTP handling, the differences between installation techniques become less pronounced.

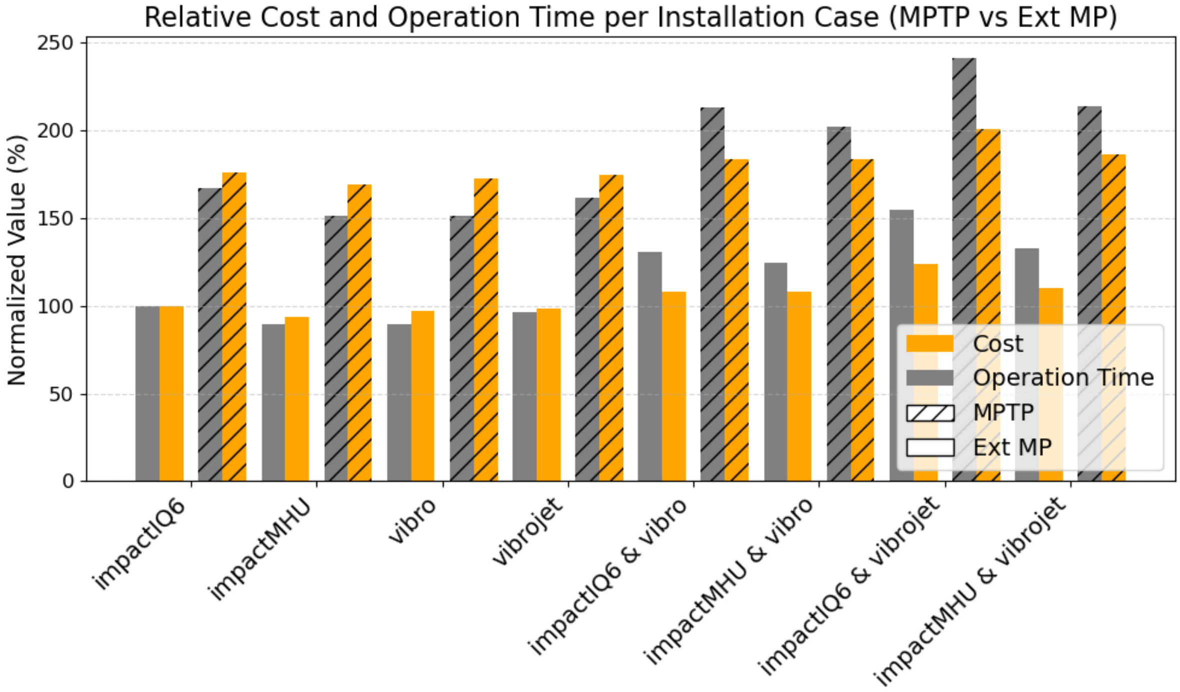

Figure 5.12: Relative installation cost and operation time for different foundation configurations (MPTP vs. External MP). The values reflect the additional time required for separate transition piece installation. No corrections were applied for changes in foundation weight or vessel layout; the cost impact shown is solely attributed to increased operational duration.

5.3.3. Uncertainty in the Assumed Frequency Ranges in the Noise Model

To calculate the reduced noise levels, a noise model was developed based on assumed values for the noise produced by the installation techniques, the frequency ranges in which the mitigation techniques are most effective (based on literature), and the average noise reduction (in dB) per mitigation technique.

Figure 5.13 presents an uncertainty analysis in which different frequency ranges were assumed in which the SBBC mitigation technique performs best. The figure illustrates how the final reduced SEL changes depending on the frequency band in which the technique is assumed to be most effective. The y-axis reports the SEL (dB) at 750 m from the source, while the x-axis shows the third-octave centre frequencies. Each line in the plot represents a different frequency range, namely:

- Original range (orange): 250-1000 Hz
- Wider range (green): 200-1250 Hz

- Narrower range (red): 315-800 Hz
- High frequency range (purple): 500-1000 Hz
- Low frequency range (brown): 250-500 Hz

The original unmitigated SEL used as the starting point for this analysis (indicated by the blue dotted line) is 185 dB. Although the plot initially suggests that the variations in frequency ranges lead to large differences in output, the final reduced noise levels, after conversion back to dB, show relatively minor variation. The specific SEL values for each frequency range are provided in the legend of the figure, where it can be seen that all values are close to that of the original frequency range and are also comparable to one another.

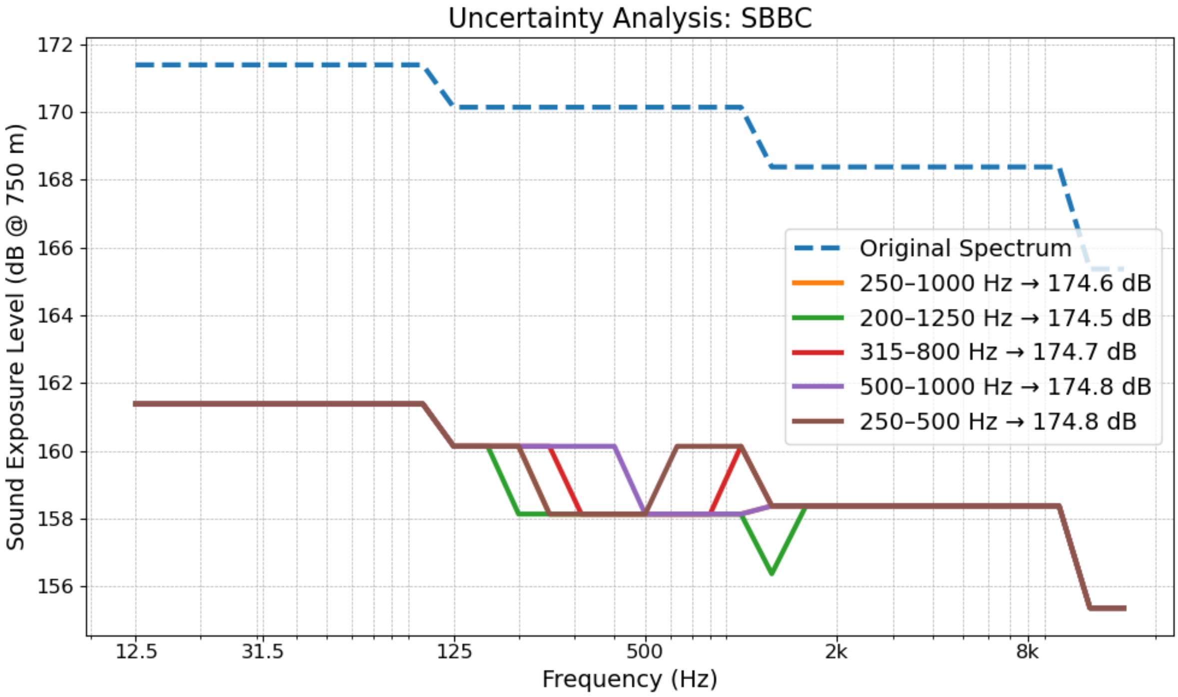

Figure 5.13: Uncertainty analysis showing the effect of varying assumed frequency bands for the SBBC mitigation technique on the resulting noise reduction (SEL).

When multiple mitigation techniques are applied simultaneously, each with its own assumed frequency range of effectiveness, the overall uncertainty naturally increases. Figure 5.14 illustrates this by showing how the resulting noise spectrum changes when three mitigation techniques, Pulse, AdBm, and SBBC, are used in combination.

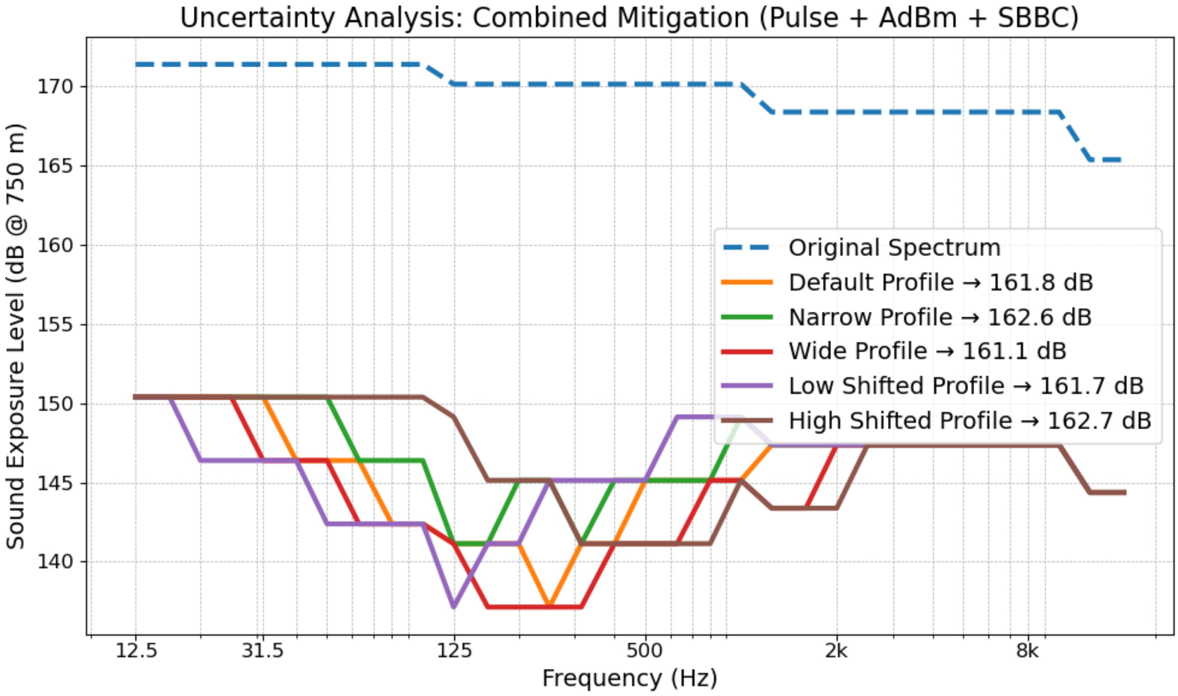

Figure 5.14: Uncertainty analysis showing the effect of varying assumed frequency bands when the Pulse, AdBm, and SBBC mitigation techniques are applied simultaneously, and their combined impact on the resulting noise reduction (SEL).

Five different frequency band combinations were defined for this uncertainty analysis, each representing a different assumption regarding the effective frequency range of the mitigation techniques:

- Original range (orange): Pulse (40-250 Hz), AdBm (80-400 Hz), SBBC (250-1000 Hz)
- Narrower range (green): Pulse (63-160 Hz), AdBm (125-315 Hz), SBBC (315-800 Hz)
- Wider range (red): Pulse (31.5-315 Hz), AdBm (63-630 Hz), SBBC (160-1600 Hz)
- Low frequency range (purple): Pulse (20-125 Hz), AdBm (50-200 Hz), SBBC (125-500 Hz)
- High frequency range (brown): Pulse (160-500 Hz), AdBm (315-800 Hz), SBBC (630-2000 Hz)

These combinations were used to evaluate the sensitivity of the total reduced spectrum to variations in the assumed frequency ranges. As in the previous analysis, the original (unmitigated) SEL used as the starting point is 185 dB. The results, shown in the legend of Figure 5.14, indicate that while spectral shifts occur across the scenarios, the overall variation remains within a reasonable and non-critical range. However, a clear difference can be observed when comparing Figure 5.13 and Figure 5.14: in the latter, the differences between the SEL levels for the various frequency ranges are larger than in the former. This suggests that when using a single mitigation technique, the influence of the assumed frequency range is smaller, whereas when multiple mitigation systems are applied, these effects accumulate.

5.3.4. Sensitivity in Assumed Pile Driving Time for Impact Piling

As outlined in Section 3.4, assumptions were made regarding the duration of various operational activities, including pile driving. For impact piling, the assumed pile drive time is relatively well-founded, as it is based on average durations observed in several completed projects. However, it remains relevant for Van Oord to assess how sensitive the model outcomes are to variations in this parameter. To this end, a sensitivity analysis was conducted for the impactIQ6 installation technique.

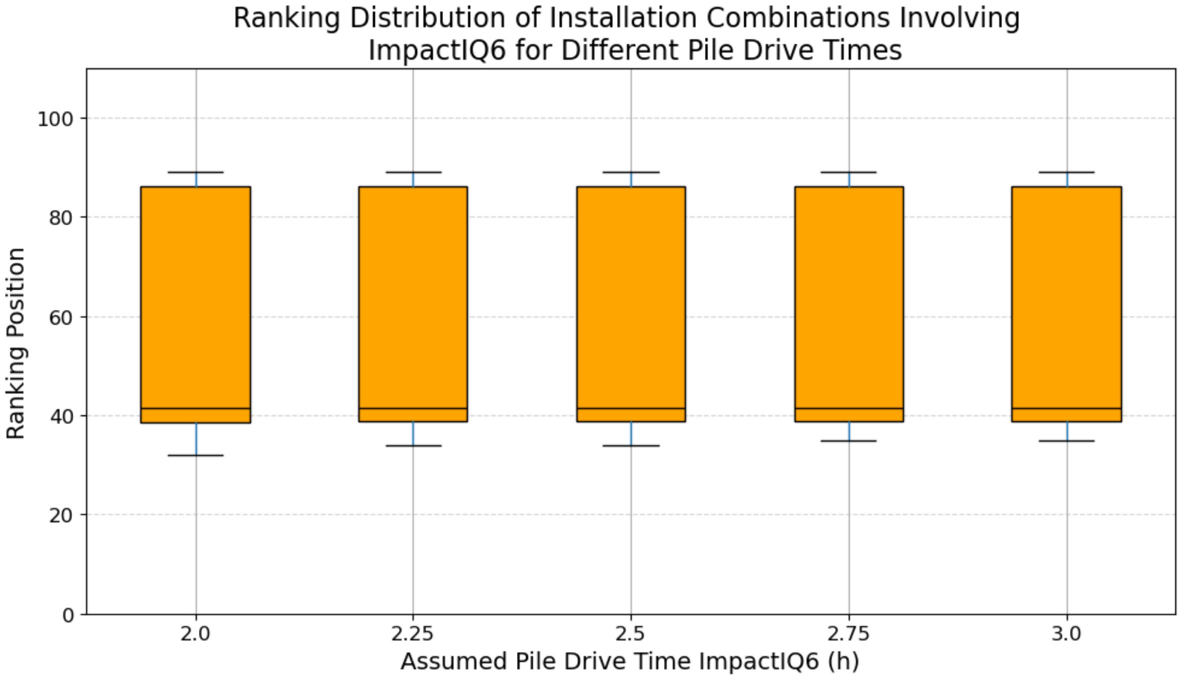

Figure 5.15: Boxplot showing the distribution of cost-efficiency rankings for installation combinations involving impact piling, evaluated across a range of assumed pile drive times. Only combinations that comply with the project noise limit are included. Lower ranking values indicate better performance.

As explained in Section 5.1.4, all 160 combinations of installation and mitigation techniques were assessed for compliance with the project noise limit. Those that met the requirements were ranked based on their cost-efficiency, from most to least favourable.

The boxplots in Figure 5.15 show how the cost-efficiency rankings of combinations involving impactIQ6 change when the assumed pile drive time is varied between 2 and 3 hours per monopile, a realistic range based on available project data. These plots provide insight into the influence of this assumption on the comparative performance of different techniques.

If changes in the assumed pile drive time cause large shifts in the relative ranking of techniques, this would indicate that the model outcomes are sensitive to the assumption. Conversely, if the rankings remain largely unchanged, the assumption can be considered to have limited impact, making the conclusions more robust.

As the figure demonstrates, the rankings of combinations involving impactIQ6 remain highly consistent across the tested range. This suggests that the model's conclusions regarding the performance of impact piling are not significantly affected by the precise value assumed for pile drive time.

5.3.5. Sensitivity in Assumed Pile Driving Times for Vibro Piling and Vibrojetting

For vibro piling and vibrojetting, little to no project data is available. The pile driving durations for these techniques were estimated in consultation with a geotechnical specialist at Van Oord, drawing on earlier test campaigns. Given the higher degree of uncertainty in these assumptions, it is also important to assess their impact on the overall comparison between installation techniques. For this reason, a similar sensitivity analysis was performed for vibro piling and vibrojetting.

While vibrojetting is generally associated with higher costs due to additional time allocation for supporting activities, it typically results in lower underwater noise levels. As a result, less mitigation is required, which can partially offset the added costs. Moreover, it is initially assumed that pile installation using vibrojetting proceeds faster than with vibro piling.

Figures 5.16 and 5.18 present the top 10 most cost-efficient installation and mitigation combinations for varying assumed pile driving times for vibro piling and vibrojetting, respectively. In both cases, the assumed installation duration per monopile was varied from 0.5 to 3.0 hours in six increments. The figures clearly demonstrate that the composition of the top 10 is sensitive to this input parameter.

To further illustrate this sensitivity, Figures 5.17 and 5.19 present boxplots showing the distribution of cost-efficiency rankings for combinations involving vibro piling and vibrojetting, respectively, for the same range of pile driving times. These plots provide insight into the variability of performance rankings and the robustness of each method under uncertain assumptions.

Taken together, these results indicate that the cost-efficiency ranking of installation and mitigation combinations is sensitive to uncertainty in the assumed pile driving time. This underscores the importance of accurately estimating this parameter when comparing alternative installation strategies.

In practice, pile driving times may vary due to factors such as soil conditions, monopile diameter, and required penetration depth. These variations can significantly influence the total installation duration and associated costs. However, such factors are also likely to affect other installation techniques, such as impact piling. Future research should therefore examine whether these uncertainties affect all methods equally or whether certain techniques are more sensitive to specific project conditions.

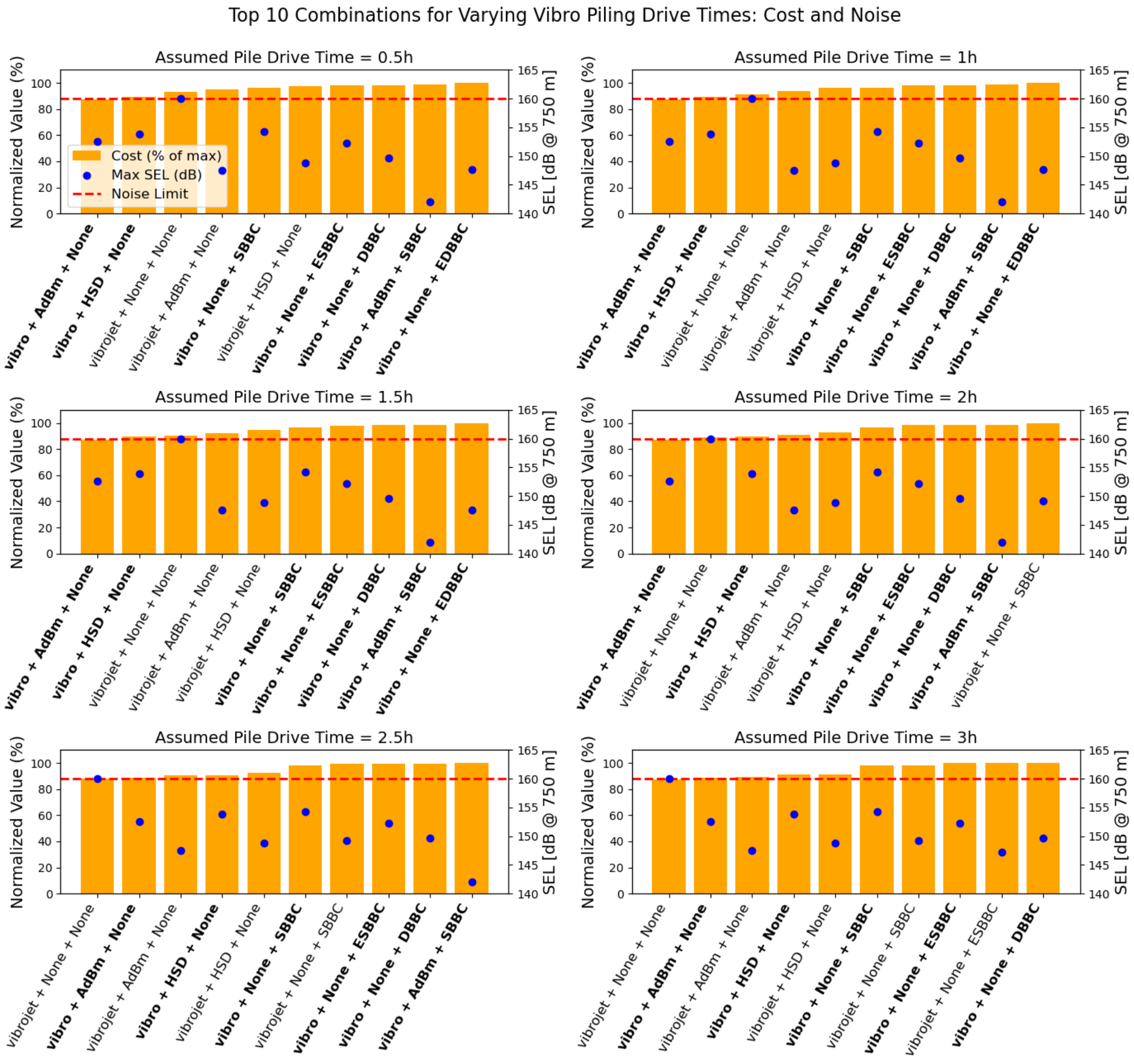

Top 10 Combinations for Varying Vibro Piling Drive Times: Cost and Noise

Assumed Pile Drive Time = 0.5h

Assumed Pile Drive Time = 1h

Assumed Pile Drive Time = 1.5h

Assumed Pile Drive Time = 2h

Assumed Pile Drive Time = 2.5h

Assumed Pile Drive Time = 3h

Figure 5.16: Top 10 most cost-efficient installation and mitigation combinations for six different values of the Pile Drive Time of Vibro Piling.

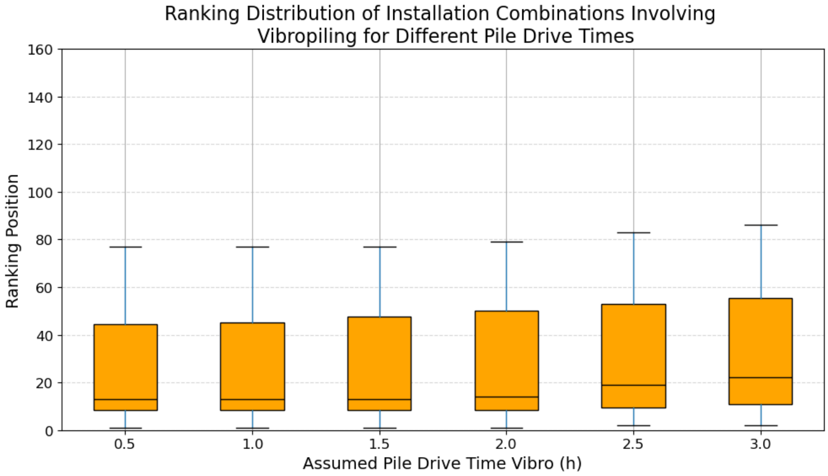

Figure 5.17: Boxplot showing the distribution of cost-efficiency rankings for installation combinations involving vibro piling, evaluated across a range of assumed pile drive times. Only combinations that comply with the project noise limit are included. Lower ranking values indicate better performance.

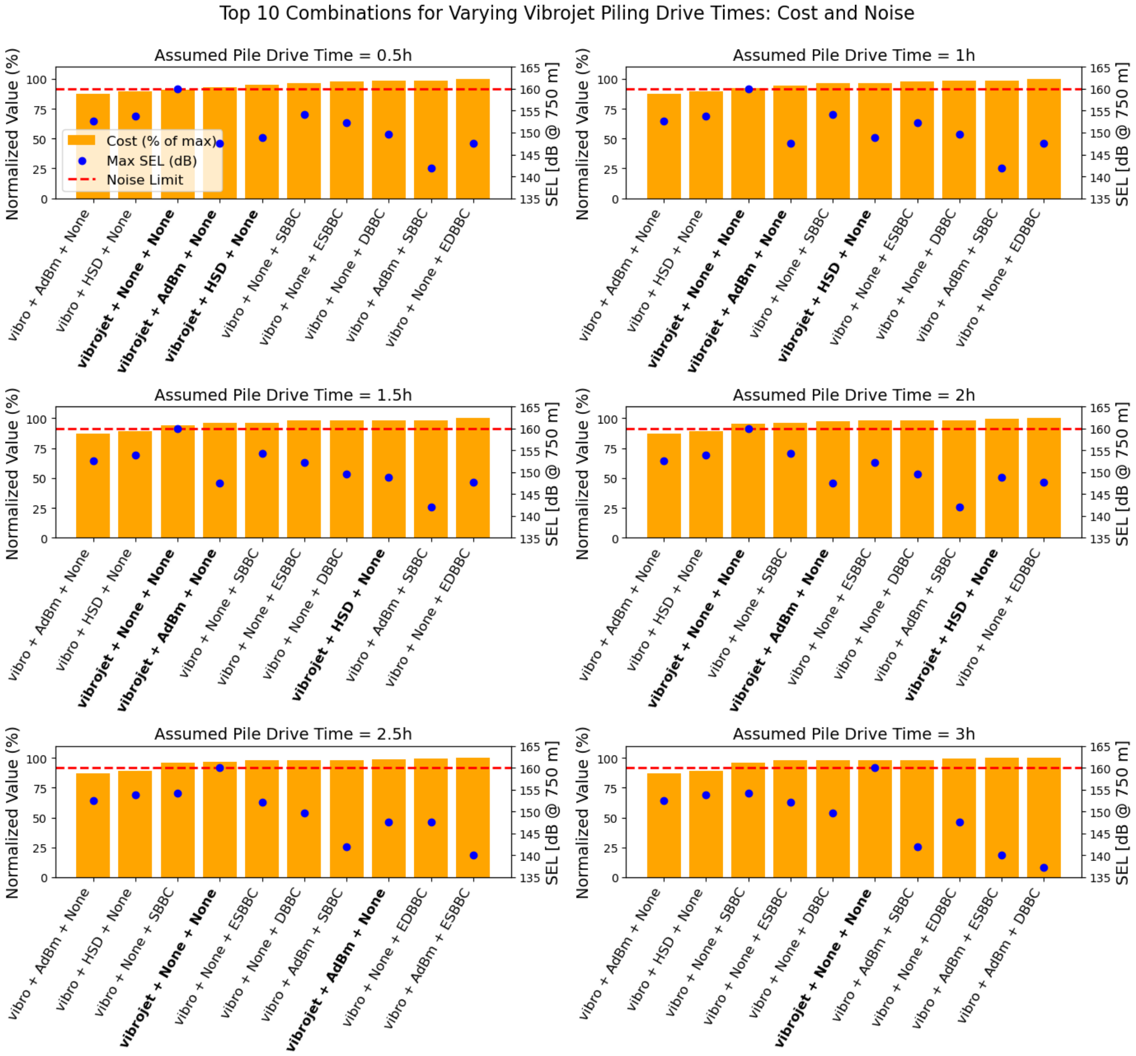

Figure 5.18: Top 10 most cost-efficient installation and mitigation combinations for six different values of the Pile Drive Time of Vibro-Jetting.

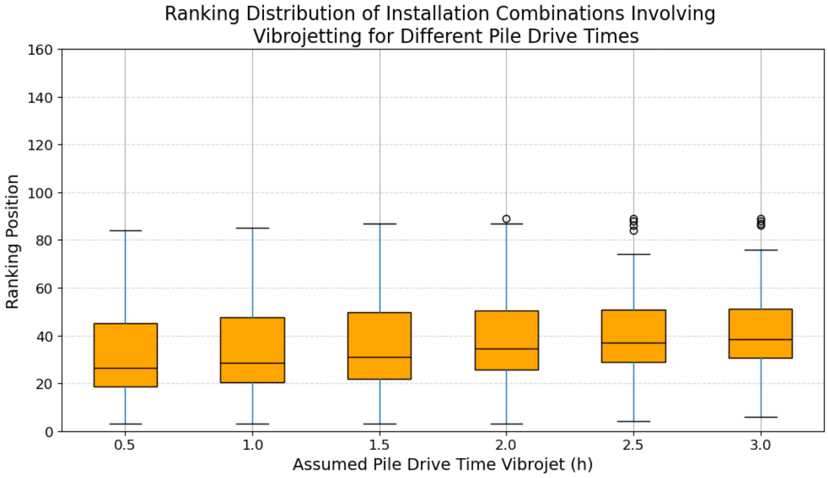

Figure 5.19: Boxplot showing the distribution of cost-efficiency rankings for installation combinations involving vibrojetting, evaluated across a range of assumed pile drive times. Only combinations that comply with the project noise limit are included. Lower ranking values indicate better performance.

5.3.6. Sensitivity Analysis of Vibrojetting Time Allocation for Supporting Activities

As described in Section 3.4, it remains challenging to estimate the additional duration required for the jetting component of the installation process. This includes activities such as connecting the umbilicals and deploying the pump. In the current model, an additional time allocation of 2.5 hours per monopile is assumed for these operations. To assess the influence of this assumption on the model outcomes, particularly on total cost, an sensitivity analysis was performed.

In this analysis, six different values were assigned to represent the additional time required for vibrojetting-related activities. As shown in Figure 5.20, this variation affects only the operational cost component, which is in line with expectations. However, the figure also illustrates the sensitivity of the total project cost to variations in the assumed additional time allocation. Below the figure, the corresponding percentage increases in total cost for each jetting duration are provided. This offers clear insight into how the total cost per monopile responds to variations in the assumed additional jetting time.

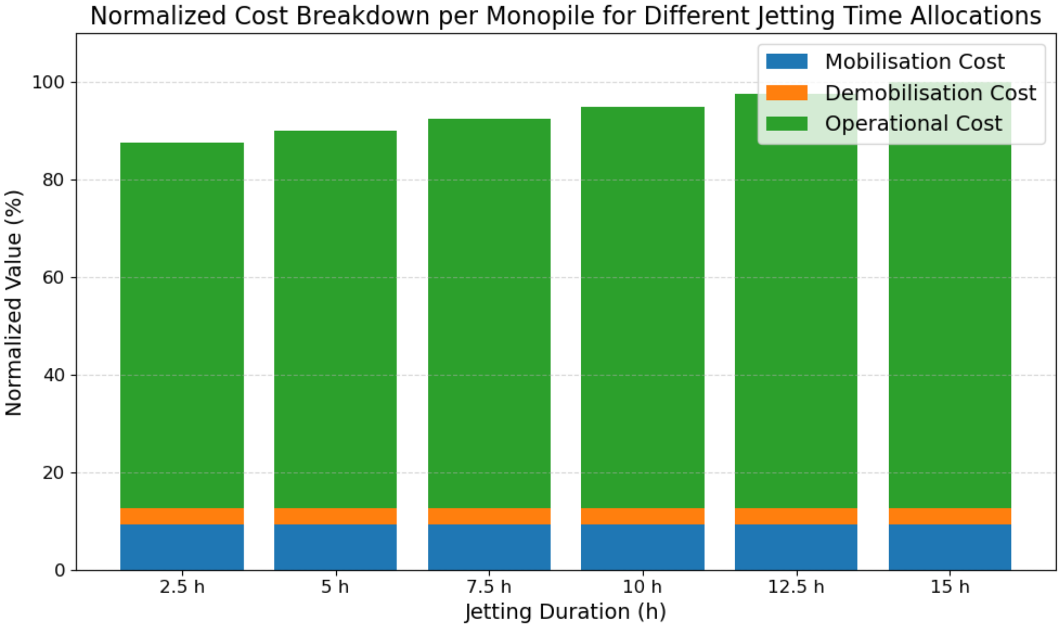

Figure 5.20: Cost breakdown for six different values of the additional time allocation related to vibrojetting activities.

```
>>>
5h time allocation increases cost per monopile by 2.8% (vs 2.5h).
7.5h time allocation increases cost per monopile by 5.6% (vs 2.5h).
10h time allocation increases cost per monopile by 8.3% (vs 2.5h).
12.5h time allocation increases cost per monopile by 11.1% (vs 2.5h).
15h time allocation increases cost per monopile by 13.9% (vs 2.5h).
```

Additionally, Figure 5.21 Presents the top 10 most cost-efficient combinations for each of the six time allocation values. For every case, an optimization was performed to determine which combinations result in the lowest total cost while still meeting the noise requirements. The plot shows a clear trend: increasing the time allocation reduces the number of cost-optimal solutions involving vibrojetting. This confirms that higher operational penalties reduce the cost-competitiveness of this installation method.

The results indicate that the viability of vibrojetting as an installation technique is highly dependent on the duration of the additional jetting-related activities. However, the impact on overall cost remains limited as long as the additional time stays below approximately 7.5 hours per monopile. It is expected that the actual jetting operations will not exceed this threshold, but this sensitivity remains an important consideration for future project planning and technology selection.

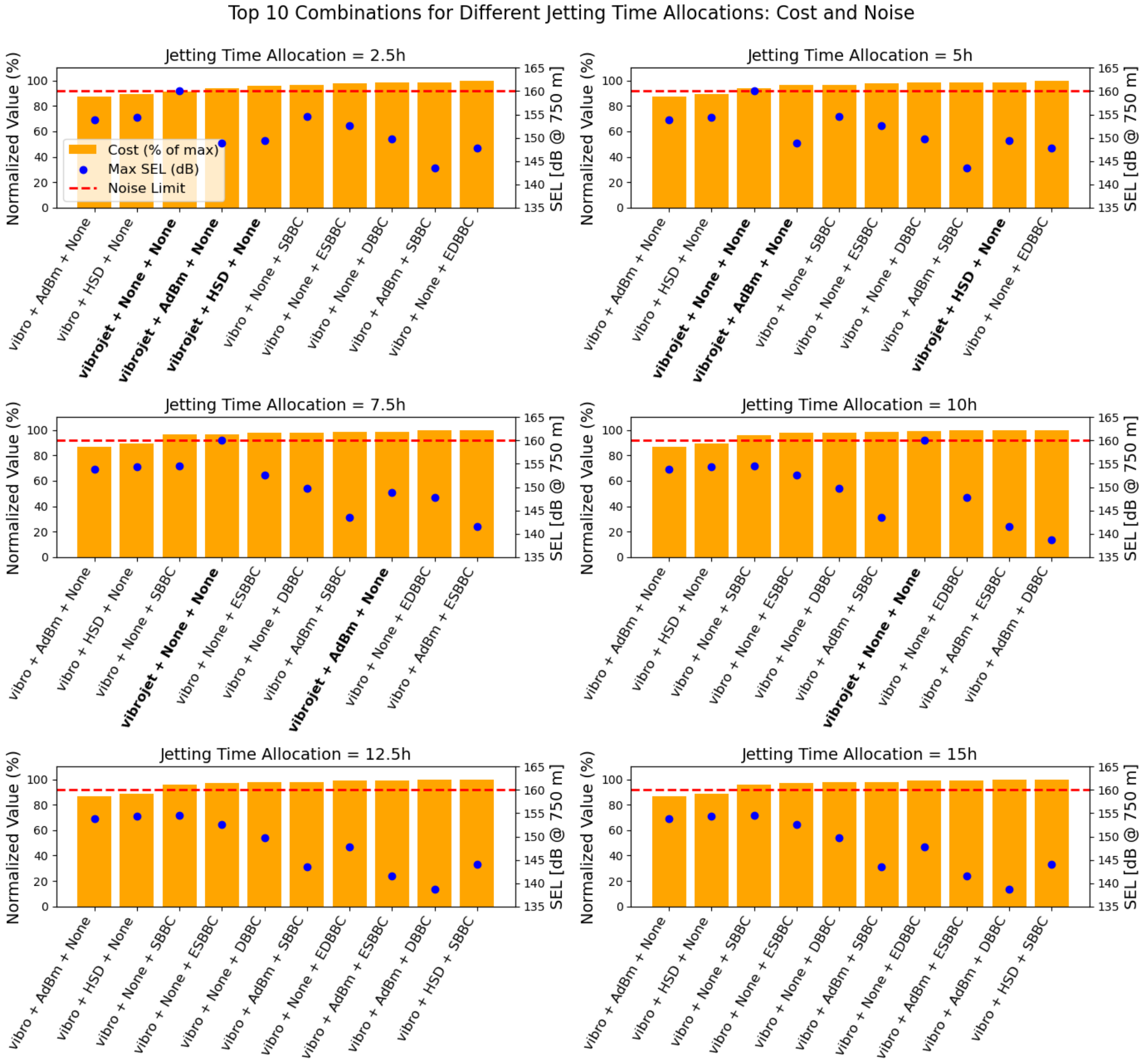

Figure 5.21: Top 10 most cost-efficient installation and mitigation combinations for six vibrojet time allocation values.

6

Conclusion & Recommendations

6.1. Conclusion

The objective of this project was to develop a comparative framework to evaluate monopile installation and noise mitigation strategies in the early design phase. The framework successfully quantifies trade-offs between installation duration, underwater noise generation, and operational cost for a set of predefined installation and mitigation combinations. It enables flexible evaluation of project-specific configurations and is built on a modular structure that combines Python and Excel. The verification steps confirm that the model structure behaves as intended and produces consistent and explainable outputs.

To identify the parameters that should be incorporated into the framework for assessing offshore installation performance and environmental impact, an analysis was conducted using internal project data supplemented by expert input. For Van Oord, it is essential to apply responsible engineering practices that minimise harm to marine life and the natural environment during installation. Another fundamental requirement is ensuring that the monopile can be successfully installed to the required depth. Only once these objectives are met can the focus shift to optimising operations and costs. Taking these priorities into account, drivability, noise compliance, and operational time were identified as the key parameters shaping installation outcomes, and were therefore prioritised in the framework's logic and structure.

Collecting relevant input from the different expertise areas within Van Oord and structuring it within the framework ensures that knowledge is no longer limited to the perspective of individual specialisations. Instead, the framework integrates these contributions into a coherent model. This enables consistent comparison of installation strategies by linking environmental, technical, and operational data. By modelling the interactions between installation methods, mitigation strategies, and project-specific constraints, the framework provides a structured overview that supports well-informed evaluations and highlights trade-offs that would otherwise remain unclear.

Results from the case studies indicate that, under the assumptions applied in this model, impact piling with near-field and far-field mitigation remains the most cost-effective method within the current technical and regulatory landscape. This outcome is primarily driven by the uncertainty surrounding the drivability of vibropiling and vibrojetting, which necessitates the availability of a backup impact hammer. The resulting increase in operational complexity and associated costs makes these alternatives less attractive. In addition, combined cases still generate high SEL levels, since a substantial portion of the pile is ultimately installed using impact piling, which further reduces their overall attractiveness.

It should be noted, however, that while the results of this framework indicate that impact hammers can comply with the noise limit, this does not guarantee that compliance will always be achieved in practice. The results show that impact hammers operate very close to the noise threshold when full mitigation (at source, near-field, and far-field) is applied, leaving only a narrow margin for unforeseen variations in site conditions or modelling assumptions. Moreover, the model has been parameterised for a 15MW turbine. As the industry advances toward 20MW units, monopile dimensions and the required driving energy are expected to increase, which will generally elevate noise emissions. Under such conditions, achieving compliance with the same noise limits through impact piling may no longer be feasible, even with extensive mitigation. This highlights the need for alternative installation methods, as reliance on impact hammers entails increasing uncertainty and the operational risk of exceeding noise limits, which could result in costly installation shutdowns.

An important consideration for future assessments is the impact of reducing or eliminating drivability uncertainty for vibratory methods. In the current model, the requirement for a backup impact hammer is a major cost driver for both vibropiling and vibrojetting, reducing their competitiveness despite their lower noise emissions. If these vibratory installation techniques can be further improved and demonstrated to reliably achieve target depth without refusal, the need for backup equipment could be removed. This would substantially reduce installation costs and logistical complexity, thereby strengthening the position of vibratory methods as a viable low-noise alternative for future monopile installations.

In such a case, vibropiling is likely to be the more favourable option, as it involves a simpler setup and fewer handling steps compared to vibrojetting. Jetting is primarily applied to facilitate penetration depth, but it also introduces additional equipment requirements and operational activities, which increase costs. It would therefore be highly valuable to explore ways of improving vibropiling as a standalone method capable of achieving full penetration depth. If this can be realised, vibropiling has strong potential to become a preferred installation technique, offering both lower costs and reduced noise emissions compared to impact piling.

The choice of mitigation strategy can also substantially influence the overall outcomes. Comparisons of different mitigation combinations within the same installation method show that, for example, using a double instead of a single bubble curtain, or an enhanced instead of a standard bubble curtain, can deliver disproportionately large noise reductions relative to their additional costs. This underscores the importance of explicitly incorporating mitigation strategy selection into the framework, as it can shift the balance between cost and noise compliance and thereby inform more effective decision-making.

Uncertainty analyses further highlight how assumptions in key input parameters affect outcomes. For example, variations in pile drive time for vibropiling and vibrojetting were shown to influence the cost-optimal installation strategy, suggesting that reducing drive time could be an important lever for improving competitiveness. Similarly, the analysis of assumed frequency ranges in the noise model demonstrated that, while the impact on reduced noise levels remains limited when a single mitigation technique is applied, the influence becomes more pronounced when multiple mitigation measures are combined. This finding stresses the need to validate and refine such assumptions to ensure accurate noise predictions.

In addition, several limitations of the current framework have been identified throughout the analysis. These are consolidated in the recommendations, which propose specific improvements to enhance both accuracy and robustness, as well as practical steps for how such improvements could be implemented in subsequent projects.

The framework has been designed to be transferable and easy to use across Van Oord, supported by the Framework Usage Guide in Appendix A. Its modular structure and intuitive Excel-based interface enable application in future projects and tender phases without requiring detailed knowledge of the underlying code. With further development and validation, the framework could be integrated as an internal decision-support tool, providing consistent and data-driven guidance for monopile installation planning throughout the organisation.

Finally, it should be emphasised that the aim of this study was not to identify a single “best” installation method, but to provide a structured way of comparing alternatives based on transparent input, traceable logic, and quantifiable trade-offs. The framework’s adaptable structure ensures it can evolve as new empirical data becomes available, for example from future vibrojetting projects or updated regulatory requirements. By bringing together valuable information from multiple disciplines in an integrated manner, the framework creates a holistic perspective that supports more informed and balanced decision-making. This integrative capability represents its key strength and main contribution.

6.2. Recommendations

Throughout the development of the comparative framework, several assumptions had to be made due to limitations in available data, scope, or time. In some cases, elements were deliberately simplified to maintain model usability and focus on the integrative comparison rather than detailed subsystem accuracy. As a result, certain technical aspects were kept outside the scope of this project.

To enhance the reliability, applicability, and future relevance of the framework, a number of recommendations are presented below. These suggestions aim to strengthen the model's accuracy, expand its coverage of installation and mitigation methods, and improve its alignment with real-world conditions. By implementing these improvements, the framework can evolve into a more robust and widely applicable decision-support tool for offshore monopile installation planning.

Based on the findings and limitations encountered during this project, the following recommendations are proposed to further improve the accuracy, completeness, and usability of the developed framework:

- **Expand validation with real project data:** Once new measurement data becomes available, for example, from upcoming vibrojet or vibropile installation projects, the framework should be validated against real-world records of installation duration and underwater noise levels. This would significantly increase the reliability and credibility of the results.

- **Improve drivability modelling:** The current framework applies a simplified drivability factor to account for installation uncertainty associated with vibratory techniques such as vibropiling and vibrojetting. While this provides a first-order correction, it does not reflect site-specific soil conditions or detailed installation performance. To enable a more technically robust and fair comparison between installation methods, the drivability assessment should be expanded. For example, replace the single factor with a physics-informed, layer-by-layer prediction based on CPT data (qc, fs, soil behavior type), incorporating vibratory settings (frequency, amplitude, crowd force), jetting parameters (flow, pressure), plugging state, and layer transitions to estimate penetration resistance, margin, and penetration rate versus depth. In addition, project data from sites such as Hollandse Kust West (HKW) can be used to quantify how often target depth is achieved for given soil conditions and installation methods, and to calibrate the model accordingly.

- **Improve noise model and include peak sound pressure levels in noise modelling:** It is recommended to refine the noise-reduction model used in the framework. At present, it applies fixed effectiveness profiles for each mitigation system and assumes binary attenuation within predefined frequency bands. This could be improved by incorporating more detailed, frequency-dependent mitigation profiles based on empirical frequency-response data, by making more accurate assumptions about the specific frequency ranges in which mitigation systems perform best, and by accounting for variations in system configuration. As more data becomes available, these profiles should be updated with more precise estimates of actual noise reduction. In addition, more sophisticated modelling approaches could be adopted to better capture frequency-dependent effects and site-specific propagation conditions.

  As mentioned earlier in this report, for all four installation techniques the assumed SEL levels were derived from a combination of experience, available data, and logical reasoning. However, a more reliable approach would be to derive these values directly from actual measurement data. For impact piling, this would involve converting measured $\mathrm{SEL}_{\mathrm{ss}}$ values into total SEL, while for vibro (and vibrojetting) it would be preferable to convert measured SPL data into SEL values. This would allow the assumed SEL levels to be more accurately matched to the actual duration of the activity, resulting in significantly improved accuracy. Furthermore, such an approach would also make the calculation of the produced noise for combined installation methods more precise, as the contributions from each method could then be scaled according to their respective operating durations based on real measurements.

Furthermore, the framework currently evaluates noise solely in terms of Sound Exposure Level (SEL), which measures the total acoustic energy over a given period. While effective for assessing cumulative exposure, this can underestimate risks when high-intensity noise occurs over short durations. For example, if installation is carried out predominantly with vibro piling but completed with impact hammering to reach the final penetration depth, the brief but intense impulses from impact driving may contribute little to the SEL yet still reach peak levels harmful to marine life. Extending the model to also assess Peak Sound Pressure Level (L_{peak}) metrics would capture these instantaneous peaks alongside integrated energy, enabling a more complete evaluation of potential environmental impacts, particularly in situations where peak noise is the primary risk.

- **Incorporate additional cost components:** The current cost calculations in the framework primarily consider vessel day rates, equipment rental, and operational time. While this offers a consistent foundation for comparison, it excludes several important method-specific cost drivers that can substantially affect the overall project budget. For instance, vibrojetting requires monopiles to be equipped with integrated jetting channels or external nozzles, leading to notable additional fabrication and material costs per unit. Other techniques may similarly involve design modifications or specialised handling requirements. Incorporating such secondary cost elements would enhance the accuracy and realism of the framework's economic assessment, enabling more representative and decision-relevant cost comparisons across installation strategies.

- **Re-evaluate vibrojet noise assumptions:** As mentioned in Section 3.6, the current framework assumes that vibrojetting produces, unmitigated, 5 dB less underwater noise than vibro piling when measured at 750 m from the source. This assumption is based on the rationale that jetting reduces soil resistance, thereby lowering the required vibratory energy. However, recent internal feedback, communicated by a Van Oord noise specialist and supported by theoretical considerations from Delft Cymatics, indicates that jetting may also reduce the lateral confinement of the embedded monopile. This could increase vibratory amplitudes and associated noise levels, suggesting that vibrojetting might produce noise levels comparable to vibro piling. On the other hand, vibrojetting is expected to allow for faster installation, which would reduce SEL values given their time dependency. Overall, these uncertainties highlight the need for more empirical data to validate the assumptions. Where possible, measurements from future vibrojetting projects should be incorporated to refine the noise estimates and ensure a more accurate comparison with other installation methods.

- **Confirm bearing capacity after vibro-jetting:** As noted in Section 3.8, jetting may loosen soils around the monopile and reduce lateral resistance, creating uncertainty in the achieved axial and lateral capacities post-installation. For future applications, it is recommended to include: (i) a site-specific geotechnical check that accounts for installation-induced disturbance; (ii) limited verification on the first pile(s), for example: pre-/post-installation CPTs or a simple lateral response check; and (iii) predefined contingency measures (backup impact driving) if acceptance criteria are not met. The framework can reflect this via a capacity-uncertainty factor and a decision rule to trigger the contingency.

- **Account for fatigue and structural effects:** In future iterations of the framework, it can be valuable to incorporate considerations related to fatigue and structural response resulting from different installation techniques. Vibratory methods such as vibropiling and vibrojetting introduce continuous dynamic loading to both vessel equipment (such as cranes and lifting tools) and the monopile structure itself. Over time, these vibrations may contribute to cumulative fatigue damage or require additional maintenance. Including a basic fatigue assessment, such as indicative load cycles or simplified fatigue life estimations, would enhance the understanding of long-term mechanical implications, particularly if vibratory techniques become more widely adopted in offshore practice.

- **Sustainability measures in installation planning:** Van Oord can further improve its environmental performance by embedding explicit sustainability measures in work methods and contracts. Prioritise certified low-CO_2 marine fuels (for example, HVO/bio-MGO and, where feasible, methanol or other drop-in blends) over conventional MGO, and reduce reliance on diesel-powered compressors for bubble curtains by switching to electric or battery-hybrid units.

- **Assess impact on other marine species:** The current framework assesses underwater noise impact based solely on the hearing thresholds and behavioural sensitivity of harbour porpoises, as these are currently the most stringently regulated. However, other marine species, including seals, fish, and invertebrates, may also be affected by construction noise, each with different sensitivities across the frequency spectrum. To improve ecological relevance and comprehensiveness, future studies should evaluate how noise levels predicted by the model align with known disturbance thresholds for a wider range of marine organisms. This would enable more inclusive environmental assessments and help support compliance with broader ecological standards beyond the current regulatory focus.

- **Extend the model to include additional installation methods:** As discussed in Chapter 2, several alternative installation technologies are currently under development. Including these in the framework would provide a more complete overview of future installation strategies and improve the tool's long-term relevance.

- **Deepen component-level modelling:** As outlined in Chapter 3, the integrated nature of this framework required several simplifications to ensure usability and maintain an overview across components. While this is appropriate for high-level comparisons, technical accuracy can be improved by deepening the modelling of individual components. In particular, the noise calculations and drivability risk can be incorporated more accurately, as discussed earlier. In addition, the weather-workability module could be extended with probabilistic downtime modelling based on seasonal metocean statistics and threshold exceedances, and the durations of operational activities could be parameterised in greater detail, for example, to capture vessel- and site-specific effects, learning effects, and standby/contingency logic. Enhancing these subcomponents will make the framework more adaptable to site-specific conditions and enable more accurate project-specific assessments.

By addressing these points, the framework can be further developed into a more robust and flexible decision-support tool. It will be able to adapt to new technologies and environmental regulations, while continuing to support data-informed decision-making in future offshore wind projects.

References

Achmus, Martin et al. (2020). “Lateral bearing behaviour of vibro- and impact-driven large-diameter piles in dense sand”. In: *Geotechnik*. First published: 10 June 2020. DOI: `10.1002/gete.202000006`.

Acteon (2024). *Underwater Noise Environmental Impact Assessment*. Accessed: 2025-06-29. Acteon Group Ltd. URL: `https://acteon.com/products-services/underwater-noise-environmental-impact-assessment/`.

AdBm Technologies (2024). *The AdBm Noise Abatement System Technology*. Accessed: 2025-06-29. AdBm Technologies. URL: `https://adbmtech.com/technology/`.

Ainslie, M.A. (Sept. 2011). *Standard for measurement and monitoring of underwater noise, Part I: physical quantities and their units*. Tech. rep. TNO-DV 2011 C235. The Hague, The Netherlands: TNO, p. 67.

Atlas Copco Specialty Rental (2025). *The right bubble curtain for the right job*. Accessed: 2025-06-29. URL: `https://www.atlascopco.com/en-uk/rental/resources/blog/the-right-bubble-curtain-for-the-right-job`.

Bellmann, Michael A. et al. (2020). *Underwater noise during percussive pile driving: Influencing factors on pile-driving noise and technical possibilities to comply with noise mitigation values*. Tech. rep. Translation of the German version from May 2020. Supported by the German Federal Ministry for the Environment, Nature Conservation and Nuclear Safety (BMU). Commissioned and managed by the Federal Maritime and Hydrographic Agency (BSH). Oldenburg, Germany: itap GmbH. URL: `https://www.bsh.de/EN/TOPICS/Offshore/Noise-protection/Reports/_Anlagen/Downloads/era-report.pdf`.

Buitendijk, Mariska (Dec. 20, 2023). *Heerema installs top section of new Noise Mitigation System*. Accessed: 2025-06-06. SWZ Maritime. URL: `https://swzmaritime.nl/news/2023/12/20/heerema-installs-top-section-of-new-noise-mitigation-system/?utm_source=chatgpt.com`.

CAPE Holland (2024). *Pile Driving Challenge: Pile Run*. Accessed: 2025-07-08. URL: `https://www.cape-holland.com/pile-driving-challenge-pile-run/`.

Cefas Noise and Bioacoustics Team (2020). *Evidence on the Efficacy of Underwater Noise Abatement*. Tech. rep. Accessed: July 2025. Centre for Environment, Fisheries and Aquaculture Science (Cefas). URL: `https://data.jncc.gov.uk/data/e1d38ce8-9bc6-4fb5-b867-f7f595caa25a/cefas-noise-abatement-evidence-review.pdf`.

Danish Energy Agency (Mar. 2023). *Guideline for Underwater Noise: Installation of Impact or Vibratory Driven Piles*. Published with photo credit to Van Oord. Danish Energy Agency. Copenhagen, Denmark.

DredgeWire (2025). *Celebrate Boreas’ christening with us at Global Offshore Wind*. Accessed: 20 June 2025. URL: `https://dredgewire.com/van-oord-celebrate-boreas-christening-with-us-at-global-offshore-wind/`.

Elmer, K.H. (2018). “HSD: Effective Offshore Piling Noise Mitigation with Big Monopiles”. In: *Noise Mitigation for the Construction of Increasingly Large Offshore Wind Turbines*. Berlin.

Fabo, Chen et al. (2021). “Effect of Installation Platform on Bearing Capacity of an Offshore Monopile Foundation”. In: *Frontiers in Physics* 9. DOI: `10.3389/fphy.2021.809581`. URL: `https://doi.org/10.3389/fphy.2021.809581`.

Group, Acteon (2025). *Installing the Future: Meet the MHU Hydraulic Hammer Family*. URL: `https://www.acteon.com/blog/installing-the-future-meet-the-mhu-hydraulic-hammer-family/` (visited on 06/30/2025).

Hydrotechnik Lübeck GmbH (2024). *Hydrotechnik Lübeck GmbH Image*. Accessed: 2024-10-16. URL: `https://www.hydrotechnik-luebeck.de/`.

IQIP (Dec. 1, 2020). *Pulse – a smarter way to mitigate noise*. Accessed: 2025-06-29. IQIP. URL: `https://www.iqip.com/news/pulse-a-smarter-way-to-mitigate-noise/`.

— (2023). *IQIP’s Largest Noise Mitigation Innovation Progresses*. Accessed: 2025-06-29. IQIP. URL: `https://iqip.com/iqips-latest-and-largest-innovation-in-noise-mitigation-well-on-its-way/`.

IQIP (2024). *Noise Mitigation Systems – IQIP*. Accessed: 2025-06-29. IQIP. URL: `https://iqip.com/expertise/noise-mitigation/`.

Jongbloed, R.H. et al. (Jan. 2021). *Bubbles JIP project: Efficient and effective use of bubble curtains for noise mitigation in offshore installation projects – WP1: Defining the starting conditions*. In collaboration with Boskalis, Van Oord, Seaway7, TNO, MARIN, TU Delft, Wageningen Marine Research, and others. Bubbles JIP / TKI Wind op Zee.

Koschinski, Sven and Karin Lüdemann (2020). "Noise mitigation for the construction of increasingly large offshore wind turbines: Technical options for complying with noise limits". In: The IHC Noise Mitigation Screen (NMS) has achieved a noise reduction of approximately 13 to 16 dB SEL in various projects, with even higher reductions of 40 dB or more at specific frequencies. URL: `https://www.bfn.de/en/publications/noise-mitigation-offshore-wind-turbines`.

Lamiman, Ethan C. and Brent Robinson (2022). "Bearing Capacity Reduction of Vibratory Installed Large Diameter Pipe Piles". In: *Proceedings of the International Foundations Congress and Equipment Expo (IFCEE)*. Chesapeake, Virginia: ASCE. URL: `https://www.grlengineers.com`.

Lewis, Michelle (May 2023). *This US offshore wind farm is piloting a bubble curtain – what it is and why it's cool*. Accessed: 2024-10-16. URL: `https://electrek.co/2023/05/12/us-offshore-wind-farm-piloting-bubble-curtain`.

Maquil, Thierry, Andreas Müller, and Matthias Wildemann (Mar. 2024). *Prognose der zu erwartenden Hydroschallimmissionen während der Rammarbeiten – Vorhaben Offshore-Windpark Gennaker*. Tech. rep. Bericht Nr. M177781/01. Commissioned by OWP Gennaker GmbH. Hamburg, Germany: Müller-BBM Industry Solutions GmbH.

OffNoise-Solutions (n.d.). *The Hydro-Sound-Damper-System (HSD-System)*. Accessed: 2024-10-16. URL: `https://www.offnoise-solutions.com/the-hydro-sound-damper-system-hsd-system/`.

Oord, Van (2025). *Noise and Mitigation Technologies*. Accessed: 2025-07-10.

Pile Buck (Feb. 7, 2024). *Mastering Pile Driving and Foundation Drilling Across Diverse Soil Types*. Accessed: 2025-07-08. URL: `https://www.pilebuck.com/mastering-pile-driving-and-foundation-drilling-across-diverse-soil-types/`.

Robinson, Stephen P., Pete D. Theobald, and Paul A. Lepper (2012). "Underwater noise generated from marine piling". In: *Meetings on Acoustics*.

Secretariat, ACCOBAMS Permanent (2019). *Methodological Guide: Guidance on Underwater Noise Mitigation Measures*. Available in electronic format during the Meeting. Seventh Meeting of the Parties to ACCOBAMS, Istanbul, Republic of Turkey, 5 - 8 November 2019. Agreement on the Conservation of Cetaceans of the Black Sea, Mediterranean Sea and contiguous Atlantic area. URL: `path/to/MOP7.Doc31Rev1_Methodological-Guide-Noise.pdf`.

Sol, Johan and Bruno Tack (2022). *Introducing Pre-Cutting & Clearance Technology: The Future of Cable Burial*. Whitepaper. Seatools B.V. URL: `https://www.seatools.com/`.

Tougaard, Jakob and Michael Dähne (Oct. 2017). "Why is auditory frequency weighting so important in regulation of underwater noise?" In: *The Journal of the Acoustical Society of America* 142.5, El409. DOI: `10.1121/1.5011331`. URL: `https://www.researchgate.net/publication/320643213`.

Wentink, Eva (Dec. 2024). *Noise Reduction in Offshore Wind Turbine Installations*. TBM 4501 - Civil and Environmental Engineering, Specialization Project. Supervisors: Prof. Dr. Gudmund Reidar Eiksund (NTNU), Ir. J.S. Jeroen Hoving (TU Delft), Ferdy Hengeveld (Van Oord).

WindpowerNL (2023). *IQIP's IQ6 hydraulic hammer for offshore wind foundations ready to use*. URL: `https://windpowernl.com/2023/04/14/iqips-iq6-hydraulic-hammer-for-offshore-wind-foundations-ready-to-use/` (visited on 06/30/2025).

A

Framework Usage Guide

This appendix provides a practical guide for using the framework developed in this project to evaluate offshore monopile installation and noise mitigation strategies. The tool is designed to support early-phase decision-making by allowing users to systematically compare technology combinations based on installation duration, underwater noise levels, and total cost.

The framework is structured around a Python model that reads input from a linked Excel file. It is built to be transparent, adaptable, and suitable for use by other users within Van Oord. This guide explains how to prepare inputs, run the model, and interpret the results.

A.1. Structure of the Framework

The framework consists of two components:

- A central Python script: `Framework.py`, which performs all calculations.
- An Excel input file: `Fixed Values Framework.xlsx`, which defines all fixed input values such as operational durations, deck load limits, and cost parameters.

Users only need to modify the Excel file. No changes to the Python script are required. After updating the Excel file, remember to:

- Save the file before running the model.
- Remove existing variables in your Python environment to avoid outdated values.

The Excel file contains the following seven sheets:

- **General Input:** Main user interface for defining a case
- **Weight:** Weight parameters for each component, which are used to estimate the total deck load imposed by the installation equipment on the vessel.
- **Operation Times:** Time assumptions for each individual activity involved in the monopile installation process.
- **Drivability:** Parameters related to soil resistance during monopile installation.
- **Noise Inst Tech:** Estimated average noise levels generated by each installation method.
- **Noise Mit Tech:** Estimated average reduction in underwater noise levels for each mitigation technique.
- **Cost:** Cost parameters including mobilization, demobilization, and operational costs per component.

A.2. How to Use the Framework

1. Enter Project Parameters

Navigate to the **General Input** sheet. This is where the user defines the specific case. For each parameter:

- The first column describes the parameter.
- The third column indicates the type of input expected (e.g. integer, float).
- The fourth column is where the user enters the input value.

Some cells are coloured red, these values are currently fixed and cannot be changed in this version. Green cells are adjustable. Ensure all required input fields are filled in.

2. Check Mitigation Activation

Go to the *Noise Inst Tech* sheet and verify that the correct mitigation options are activated (indicated by *yes* or *no*) based on your selection in the *General Input* sheet.

3. Save and Run

Save the Excel file and open `Framework.py` in Python. Make sure to:

- Clear previously loaded variables.
- Run the script from start to finish.

The script will automatically process the input, perform the calculations, and output results.

A.3. Output Interpretation

Once executed, the model returns the following outputs:

- Total weight of deck layout
- Installation duration (with and without weather-related delays)
- Total cost per monopile
- Underwater noise level at the source (with and without mitigation)
- Compliance check against the project noise limit

The main output tables are printed in the console and can be saved or used for further analysis.

Batch Analysis (Optional)

`Framework.py` can also be imported into other Python scripts to perform batch analyses. For example:

- Vary installation techniques
- Loop over different mitigation combinations
- Perform sensitivity analyses

A.4. Customization and Extension

The framework is designed to be adaptable and expandable. As new data becomes available, users can update the corresponding Excel sheets to reflect improved insights. Examples include:

- Updating weights and deck loads
- Refining activity durations and operational costs
- Modifying produced noise levels per installation technique
- Adjusting mitigation effectiveness
- Improving drivability assumptions

For advanced users, the Python code can also be modified to incorporate more complex or project-specific requirements, such as:

- Adding new installation or mitigation techniques
- Including additional input parameters (e.g., soil types, vessel configurations, foundation types)
- Improving the accuracy of the noise propagation model
- Enhancing the weather workability calculations
- Integrating a more advanced approach for modelling [drivability]

Closing Note

The framework is designed to provide insight into the trade-offs between cost, time, and environmental performance during the early planning stages of a offshore wind project. With further development and integration, it can serve as a valuable internal decision-support tool within Van Oord.

B

Underlying Python Code of the Framework Model

```
import pandas as pd
import numpy as np
import math
import matplotlib.pyplot as plt

#%% Loading excel file

excel_file = r"C:\PYTHON\Fixed Values Framework.xlsx"

#%% Reading the relevant sheets

gen_input_df = pd.read_excel(excel_file, sheet_name="General Input").fillna(0)
weight_df = pd.read_excel(excel_file, sheet_name="Weight").fillna(0)
operation_times_df = pd.read_excel(excel_file, sheet_name="Operation Times").fillna(0)
noise_inst_tech_df = pd.read_excel(excel_file, sheet_name="Noise Inst Tech").fillna(0)
noise_mit_tech_df = pd.read_excel(excel_file, sheet_name="Noise Mit Tech").fillna(0)
cost_df = pd.read_excel(excel_file, sheet_name="Cost").fillna(0)

#%% Extracting input values from Excel sheets

gen_input_parameter = gen_input_df["General specifications"].tolist()
gen_input_values = gen_input_df["Input Case"].tolist()

weight_parameter = weight_df["Deck Component"].tolist()
weight_quantity = weight_df["Quantity"].tolist()
weight_value = weight_df["Weight"].tolist()

operation_times_parameter = operation_times_df["Standard operation times"].tolist()
operation_times_value = operation_times_df["General Values"].tolist()
operation_times_paral_act = operation_times_df["Parallel Activity"].tolist()

noise_inst_tech_parameter = noise_inst_tech_df["Installation Technique"].tolist()
noise_inst_tech_value = noise_inst_tech_df["Assumed SEL at 750 m distance"].tolist()

noise_mit_tech = noise_mit_tech_df["Mitigation Technique"].tolist()
noise_mit_tech_min_value = noise_mit_tech_df["Assumed min. Noise Reduction"].tolist()
noise_mit_tech_max_value = noise_mit_tech_df["Assumed max. Noise Reduction"].tolist()

cost_parameter = cost_df["Element"].tolist()
cost_mob_value = cost_df["Mobilisation cost (EUR)"].tolist()
cost_demob_value = cost_df["De-mobilisation cost (EUR)"].tolist()
cost_op_value = cost_df["Operational cost (EUR/day)"].tolist()


#%% Weight

def create_weight_dataframe(gen_input_values, weight_parameter, weight_value, weight_quantity, ge
    def calculate_total_weight(weight_quantity_adjusted):
        include_flags_weight = [False] * len(weight_parameter)

        for i in list(range(0, 27)) + list(range(70, 90)):
            include_flags_weight[i] = True

        install_techs = [t.strip() for t in gen_input_values[0].split('&')]
```

```
        if 'impactIQ6' in install_techs:
            for i in range(27, 36):
                include_flags_weight[i] = True
        if 'impactMHU' in install_techs:
            for i in range(37, 46):
                include_flags_weight[i] = True
        if 'vibro' in install_techs:
            for i in range(47, 56):
                include_flags_weight[i] = True
        if 'vibrojet' in install_techs:
            for i in range(47, 69):
                include_flags_weight[i] = True

        if gen_input_values[34] == 'IQIP NMS':
            include_flags_weight[91] = True
            include_flags_weight[92] = True
            include_flags_weight[12] = False
        elif gen_input_values[34] in ['AdBm', 'HSD']:
            include_flags_weight[93] = True


        multiplied_values = np.array(weight_value) * np.array(weight_quantity_adjusted)
        df_weight = pd.DataFrame({
            "Component": weight_parameter,
            "Weight [tons]": multiplied_values,
            "Included": include_flags_weight
        })

        df_weight["Weight [tons]"] = df_weight["Weight [tons]"].round(2)

        total_weight = df_weight[df_weight["Included"] == True]["Weight [tons]"].sum()
        df_weight.loc[len(df_weight)] = ["Total Weight [tons]", total_weight, ""]

        return df_weight, total_weight, weight_quantity_adjusted

    df_weight, total_weight, current_quantity = calculate_total_weight(weight_quantity.copy())

    print(f">>> Initial total weight before max weight check: {round(total_weight, 1)} tons")

    max_weight = gen_input_values[37]
    while total_weight > max_weight:
        for i in [0, 1, 4, 7]:
            current_quantity[i] = max(0, current_quantity[i] - 1)
        df_weight, total_weight, current_quantity = calculate_total_weight(current_quantity)

    pd.set_option('display.max_rows', None)
    pd.set_option('display.max_columns', None)
    pd.set_option('display.precision', 2)

    print(df_weight)
    return df_weight, total_weight, current_quantity


df_weight, total_weight, current_quantity = create_weight_dataframe(gen_input_values, weight_para
                                                  weight_quantity, gen_input_parameter)
```

```
#%% Operation Times

def create_operation_dataframe(gen_input_values, operation_times_parameter, operation_times_value
    operation_times_value = operation_times_value.copy()
    include_flags_operation = [True] * len(operation_times_parameter)

    dep_on_fou_on_ves = [3] + list(range(5, 14)) + list(range(22, 84))
    for i in dep_on_fou_on_ves:
        operation_times_value[i] *= current_quantity[0]

    for i, act in enumerate(operation_times_paral_act):
        if str(act).strip().lower() == 'x':
            include_flags_operation[i] = False

    if gen_input_values[10] == 'Ext MP':
        for i in range(4, 9):
            include_flags_operation[i] = False
        for i in range(63, 80):
            include_flags_operation[i] = False
            include_flags_operation[67] = True
    elif gen_input_values[10] == 'MPTP':
        for i in range(4, 9):
            include_flags_operation[i] = True
        for i in range(63, 80):
            include_flags_operation[i] = True

    if gen_input_values[4] == 'boreas':
        include_flags_operation[23] = True
        include_flags_operation[24] = False
    elif gen_input_values[4] == 'aeolus':
        include_flags_operation[23] = False
        include_flags_operation[24] = True

    include_flags_operation[26] = False

    for i in range(28, 31):
        include_flags_operation[i] = False

    for i in range(53, 58):
        include_flags_operation[i] = False


    install_techs = [t.strip() for t in gen_input_values[0].split('&')]

    for i in [44, 45, 46]:
        include_flags_operation[i] = False

    if len(install_techs) == 1:
        tech = install_techs[0]

        for i in range(47, 49):
            include_flags_operation[i] = False
```

```
    if tech in ['impactIQ6', 'impactMHU']:
        include_flags_operation[44] = True
    elif tech == 'vibro':
        include_flags_operation[45] = True
    elif tech == 'vibrojet':
        include_flags_operation[46] = True

elif len(install_techs) == 2:
    first_tech = install_techs[0]
    second_tech = install_techs[1]

    for i in range(41, 44):
        include_flags_operation[i] = True

    if first_tech in ['impactIQ6', 'impactMHU']:
        include_flags_operation[44] = True
    elif first_tech == 'vibro':
        include_flags_operation[45] = True
    elif first_tech == 'vibrojet':
        include_flags_operation[46] = True

    for i in range(47, 49):
        include_flags_operation[i] = True

    for i in range(41, 44):
        include_flags_operation[i] = True

    if second_tech in ['impactIQ6', 'impactMHU']:
        include_flags_operation[44] = True
    elif second_tech == 'vibro':
        include_flags_operation[45] = True
    elif second_tech == 'vibrojet':
        include_flags_operation[46] = True

    if ('impactIQ6' in install_techs or 'impactMHU' in install_techs) and ('vibro' in install
        operation_times_value[44] *= 2/3
        if 'vibro' in install_techs:
            operation_times_value[45] *= 1/3
        elif 'vibrojet' in install_techs:
            operation_times_value[46] *= 1/3
        operation_times_value[42] *= 2
        operation_times_value[43] *= 2

if 'vibrojet' in install_techs:
     include_flags_operation[89] = True
else:
     include_flags_operation[89] = False
     operation_times_value[89] = 0

df_operation = pd.DataFrame({
    "Operation": operation_times_parameter,
    "Duration": operation_times_value,
    "Included": include_flags_operation})

df_operation["Duration"] = df_operation["Duration"].round(2)
```

```
    total_round_trip = round(df_operation[df_operation["Included"] == True]["Duration"].sum(), 2)
    total_duration = total_round_trip * (gen_input_values[5] / current_quantity[0])
    df_operation.loc[len(df_operation)] = ["Total Round Trip [hours]", total_round_trip, ""]
    df_operation.loc[len(df_operation)] = ["Total Duration [hours]", total_duration, ""]
    df_operation.loc[len(df_operation)] = ["Total Duration [days]", total_duration/24, ""]

    pd.set_option('display.max_rows', None)
    pd.set_option('display.max_columns', None)
    pd.set_option('display.precision', 2)

    print(df_operation)
    return df_operation, total_round_trip, total_duration


df_operation, total_round_trip, total_duration = create_operation_dataframe(gen_input_values, ope


#%% Weather Workability

def apply_weather_workability_improved(total_duration_hours, gen_input_values):
    import calendar

    summer_months = ['May', 'June', 'July', 'August', 'September']
    winter_months = ['October', 'November', 'December', 'January', 'February', 'March', 'April']
    all_months = summer_months + [m for m in winter_months if m not in summer_months]

    # Ophalen input
    start_month = gen_input_values[39].strip()
    summer_factor = float(gen_input_values[30])
    winter_factor = float(gen_input_values[31])

    # Controle of maand geldig is
    if start_month not in all_months:
        raise ValueError(f"Invalid month: {start_month}")

    # Bereken totaal in dagen
    total_duration_days = total_duration_hours / 24
    remaining_days = total_duration_days

    # Begin bij startmaand
    month_index = all_months.index(start_month)
    month_adjusted_durations = []

    # Ga door totdat alle dagen zijn verdeeld
    while remaining_days > 0:
        current_month = all_months[month_index % 12]
        days_this_month = min(30, remaining_days)

        if current_month in summer_months:
            factor = summer_factor
        else:
            factor = winter_factor

        adjusted = days_this_month / factor
        month_adjusted_durations.append({
```

```
            "month": current_month,
            "days": round(days_this_month, 1),
            "factor": factor,
            "adjusted_days": round(adjusted, 1)
        })

        remaining_days -= days_this_month
        month_index += 1

    # Sommeer aangepaste dagen naar aangepaste uren
    total_duration_with_weather_workability_days = sum(item["adjusted_days"] for item in month_ad
    total_duration_with_weather_workability = total_duration_with_weather_workability_days * 24

    # Print overzicht
    df_weather = pd.DataFrame(month_adjusted_durations)
    print("\nWeather Workability Breakdown:")
    print(f"\nTotal Duration with Weather Workability [hours]: {round(total_duration_with_weather
    print(f"Total Duration with Weather Workability [days]: {round(total_duration_with_weather_wo
    print(df_weather)

    return total_duration_with_weather_workability, total_duration_with_weather_workability_days

total_duration_with_weather_workability, total_duration_with_weather_workability_days = apply_wea

#%% Mitigation Dictionairy

def build_mitigation_dict(noise_inst_tech_df):
    noise_inst_tech_df.columns = [col.strip() for col in noise_inst_tech_df.columns]
    mitigation_dict = {}
    for _, row in noise_inst_tech_df.iterrows():
        tech = str(row['Installation Technique']).strip()
        mitigation_dict[tech] = {
            "base_noise": float(row['Assumed SEL at 750 m distance']),
            "use_at_source": str(row.get("At source", "no")).strip().lower() == "yes",
            "use_near": str(row.get("Near-Field", "no")).strip().lower() == "yes",
            "use_far": str(row.get("Far-Field", "no")).strip().lower() == "yes"
        }
    return mitigation_dict

mitigation_assign_dict = build_mitigation_dict(noise_inst_tech_df)


#%% Costs

def create_costs_dataframe(gen_input_values, gen_input_parameter, total_duration_with_weather_wor
                           cost_parameter, cost_mob_value, cost_demob_value, cost_op_value,
                           mitigation_assign_dict):

    def activate_cost(i):
        include_flags_costs[i] = True
        mob_costs[i] = cost_mob_value[i]
        demob_costs[i] = cost_demob_value[i]
        op_costs[i] = cost_op_value[i] * (total_duration_with_weather_workability/24)

    include_flags_costs = [False] * len(cost_parameter)
```

```
mob_costs = [0] * len(cost_parameter)
demob_costs = [0] * len(cost_parameter)
op_costs = [0] * len(cost_parameter)

if gen_input_values[4] == 'boreas':
    for i in [0, 1]:
        activate_cost(i)

install_techs = [t.strip() for t in gen_input_values[0].split('&')]
tech_to_index = {'impactIQ6': 2, 'impactMHU': 3, 'vibro': 4, 'vibrojet': 5}
near_field_map = {'HSD': 9, 'IQIP NMS': 8, 'AdBm': 10}
far_field_map = {
    'SBBC': [13, 17], 'DBBC': [14, 17, 18],
    'ESBBC': [15, 17], 'EDBBC': [16, 17, 18]
}

near_field = gen_input_values[34]
far_field = gen_input_values[35]

for tech in install_techs:
    if tech in tech_to_index:
        activate_cost(tech_to_index[tech])

    mit_data = mitigation_assign_dict.get(tech, {})

    if mit_data.get("use_near") and near_field in near_field_map:
        activate_cost(near_field_map[near_field])

    if mit_data.get("use_far") and far_field in far_field_map:
        for idx in far_field_map[far_field]:
            activate_cost(idx)

activate_cost(20)

df_costs = pd.DataFrame({
    "Parameter": cost_parameter,
    "Mob Cost": mob_costs,
    "Demob Cost": demob_costs,
    "Op Cost": op_costs,
    "Included": include_flags_costs
})

df_costs["Total"] = df_costs["Mob Cost"] + df_costs["Demob Cost"] + df_costs["Op Cost"]
total_costs = df_costs[df_costs["Included"]]["Total"].sum()

df_costs.loc[len(df_costs)] = {
    "Parameter": "Total Costs",
    "Mob Cost": df_costs.loc[df_costs["Included"], "Mob Cost"].sum(),
    "Demob Cost": df_costs.loc[df_costs["Included"], "Demob Cost"].sum(),
    "Op Cost": df_costs.loc[df_costs["Included"], "Op Cost"].sum(),
    "Included": "",
    "Total": total_costs
}

print(df_costs)
```

```
    return df_costs, total_costs, mob_costs, demob_costs, op_costs


df_costs, total_costs, mob_costs, demob_costs, op_costs = create_costs_dataframe(
    gen_input_values, gen_input_parameter, total_duration_with_weather_workability,
    cost_parameter, cost_mob_value, cost_demob_value, cost_op_value, mitigation_assign_dict
)


cost_per_monopile = total_costs / gen_input_values[5]

#%% Noise

# Step 1: Standard third-octave band center frequencies (in Hz)
tert_bands = [12.5, 16, 20, 25, 31.5, 40, 50, 63, 80, 100, 125, 160, 200,
              250, 315, 400, 500, 630, 800, 1000, 1250, 1600, 2000, 2500,
              3150, 4000, 5000, 6300, 8000, 10000, 12500, 16000]

# Step 2: Distribute total SEL across third-octave bands
def distribute_total_SEL(total_sel, share_pattern=None):
    if share_pattern is None:
        share_pattern = np.array([0.04]*10 + [0.03]*10 + [0.02]*10 + [0.01]*2)
    share_pattern = share_pattern / share_pattern.sum()
    E_total = 10 ** (total_sel / 10)
    E_bands = E_total * share_pattern
    return 10 * np.log10(E_bands)

# Step 3: Apply profile-based reduction per band
def apply_profiled_band_reduction(spectrum_db, reduction_min, reduction_max, profile):
    profile = np.array(profile)
    profile = profile / profile.max()
    reduction = reduction_min + (reduction_max - reduction_min) * profile
    reduced_spectrum = spectrum_db - reduction
    return reduced_spectrum, reduction

# Step 4: Recalculate total SEL from spectrum
def recalculate_total_SEL(spectrum_db):
    energies = 10 ** (spectrum_db / 10)
    return 10 * np.log10(np.sum(energies))

# Step 5: Frequency-dependent effectiveness profiles
def binary_profile(freq_ranges):
    profile = np.zeros(len(tert_bands))
    for i, f in enumerate(tert_bands):
        for (fmin, fmax) in freq_ranges:
            if fmin <= f <= fmax:
                profile[i] = 1
    return profile

mitigation_profiles = {
    'pulse': binary_profile([(40, 250)]),
    'MNRU': binary_profile([(40, 250)]),
    'HSD': binary_profile([(80, 400)]),
    'AdBm': binary_profile([(80, 400)]),
    'IQIP NMS': binary_profile([(80, 400)]),
```

```
    'SBBC': binary_profile([(250, 1000)]),
    'DBBC': binary_profile([(250, 1000)]),
    'ESBBC': binary_profile([(250, 1000)]),
    'EDBBC': binary_profile([(250, 1000)]),
}

# === Nieuw: helpers voor combinaties ===

BASE_DURATIONS_H = {
    'impactIQ6': operation_times_value[44],
    'impactMHU': operation_times_value[44],
    'vibro': operation_times_value[45],
    'vibrojet': operation_times_value[46],
}

def scale_sel_by_fraction(sel_db, fraction):
    """Schaal SEL op basis van tijdsfractie van de referentieduur."""
    if fraction <= 0:
        raise ValueError("Fractie moet > 0 zijn.")
    return float(sel_db + 10.0 * np.log10(fraction))

def energetic_sum_sels(sel_list):
    """Energetisch optellen van SEL-waarden (dB)."""
    if len(sel_list) == 0:
        return None
    return float(10.0 * np.log10(np.sum(10.0 ** (np.array(sel_list) / 10.0))))

def run_mitigation_for_tech(
    tech, starting_total_sel_db, at_source, near_field, far_field,
    mit_min_map, mit_max_map
):
    """Voer bestaande mitigatielogica uit voor één techniek, vanaf een (al tijd-geschaalde) SEL."
    original_spectrum = distribute_total_SEL(starting_total_sel_db)
    current_spectrum = original_spectrum.copy()

    layer_reduction_spectra = {
        "At Source": np.zeros_like(current_spectrum),
        "Near Field": np.zeros_like(current_spectrum),
        "Far Field": np.zeros_like(current_spectrum)
    }

    mitigation_layers = [
        ("At Source", at_source),
        ("Near Field", near_field),
        ("Far Field", far_field)
    ]

    for layer_name, layer_keys in mitigation_layers:
        # At Source niet toepassen voor vibro/vibrojet
        if tech in ['vibro', 'vibrojet'] and layer_name == "At Source":
            continue

        spectrum_before_layer = current_spectrum.copy()

        if isinstance(layer_keys, str):
```

```
            for subkey in [k.strip() for k in layer_keys.split(',') if k.strip()]:
                if subkey in mit_min_map and subkey in mit_max_map:
                    rmin = mit_min_map[subkey]
                    rmax = mit_max_map[subkey]
                    profile = mitigation_profiles.get(subkey, np.ones_like(current_spectrum))
                    current_spectrum, _ = apply_profiled_band_reduction(
                        current_spectrum, rmin, rmax, profile
                    )

        layer_reduction_spectra[layer_name] = spectrum_before_layer - current_spectrum

    final_spectrum = current_spectrum
    final_sel_db = recalculate_total_SEL(final_spectrum)

    return {
        "original_spectrum": original_spectrum,
        "final_spectrum": final_spectrum,
        "final_sel_db": float(final_sel_db),
        "layer_reduction_spectra": layer_reduction_spectra,
    }

# === Drop-in vervanging ===
def simulate_from_input(gen_input_values, inst_sel_values, mit_min_values, mit_max_values):
    inst_tech_names = ['impactIQ6', 'impactMHU', 'vibro', 'vibrojet']
    inst_sel_map = dict(zip(inst_tech_names, inst_sel_values))

    noise_limit = float(gen_input_values[32])
    at_source = gen_input_values[33]
    near_field = gen_input_values[34]
    far_field = gen_input_values[35]

    mit_min_map = dict(zip(noise_mit_tech, mit_min_values))
    mit_max_map = dict(zip(noise_mit_tech, mit_max_values))

    # Parse installatietechnieken uit input, bv. "impactIQ6 & vibro"
    techs = [t.strip() for t in str(gen_input_values[0]).split('&') if t.strip()]
    if not techs:
        print("⚠️ Geen installatietechniek opgegeven in gen_input_values[0].")
        return {}

    # Default fracties bij twee technieken: 2/3 en 1/3 (volgorde zoals opgegeven)
    fractions = None
    if len(techs) == 2:
        fractions = {techs[0]: 2.0/3.0, techs[1]: 1.0/3.0}
    elif len(techs) == 1:
        fractions = {techs[0]: 1.0}
    else:
        # Als je ooit 3+ technieken wil ondersteunen, kun je dit uitbreiden.
        # Voor nu normaliseren we gelijke fracties.
        equal = 1.0 / len(techs)
        fractions = {t: equal for t in techs}
        print(f"ℹ️ {len(techs)} technieken gedetecteerd; gebruik gelijke fracties van {equal:.3f}

    # 1) Unmitigated: tijd schalen en energetisch optellen
    per_tech_unmit_sels = {}
```

```
for tech in techs:
    base_sel = inst_sel_map.get(tech, 165.0)
    if tech not in inst_sel_map:
        print(f"⚠️  Waarschuwing: Geen SEL-waarde gevonden voor '{tech}', gebruik 165 dB als c
    frac = fractions[tech]
    # tijds-schaal: SEL_new = SEL_base + 10*log10(frac)
    scaled_sel = scale_sel_by_fraction(base_sel, frac)
    per_tech_unmit_sels[tech] = float(scaled_sel)

unmitigated_total_sel = energetic_sum_sels(list(per_tech_unmit_sels.values()))
combo_label = " + ".join([f"{t}({fractions[t]:.2f})" for t in techs])

print("\n🔧  Ongecorrigeerde (unmitigated) SEL — na tijdsschaal per techniek")
for tech in techs:
    print(f"  - {tech}: base SEL = {inst_sel_map.get(tech, 165.0):.2f} dB,"
          f" fractie = {fractions[tech]:.3f} → geschaald = {per_tech_unmit_sels[tech]:.2f} dB
print(f"➡ Energetisch totaal ({combo_label}) = {unmitigated_total_sel:.2f} dB")

# 2) Mitigatie: per techniek vanaf de tijd-geschaalde SEL, dan energetisch combineren
per_tech_mitig = {}
for tech in techs:
    result = run_mitigation_for_tech(
        tech,
        starting_total_sel_db=per_tech_unmit_sels[tech],
        at_source=at_source,
        near_field=near_field,
        far_field=far_field,
        mit_min_map=mit_min_map,
        mit_max_map=mit_max_map
    )
    per_tech_mitig[tech] = result

    # Optioneel: korte samenvatting per laag (zoals je eerdere print)
    print(f"\n📘  Reductie per mitigatielaag voor installatie: {tech}")
    layer_df = pd.DataFrame(columns=['Layer', 'Total Reduction (dB)'])
    original_spectrum = result["original_spectrum"]
    for layer_name, reduction_spectrum in result["layer_reduction_spectra"].items():
        # NB: we hergebruiken je bestaande manier om 'Total Reduction' te tonen
        total_reduction_db = recalculate_total_SEL(original_spectrum) - recalculate_total_SEL
        layer_df.loc[len(layer_df)] = [layer_name, round(total_reduction_db, 2)]
    print(layer_df.to_string(index=False))
    print(f"🎯  Final SEL after mitigation ({tech}): {result['final_sel_db']:.2f} dB")

mitigated_total_sel = energetic_sum_sels([per_tech_mitig[t]["final_sel_db"] for t in techs])

print("\n🔗  Energetische combinatie na mitigatie:")
for tech in techs:
    print(f"  - {tech}: gemitigeerde SEL = {per_tech_mitig[tech]['final_sel_db']:.2f} dB")
print(f"✅  Totaal gemitigeerde SEL ({combo_label}) = {mitigated_total_sel:.2f} dB")
if mitigated_total_sel <= noise_limit:
    print(f"✅  COMPLIANT met limiet {noise_limit:.2f} dB")
else:
    print(f"❌  NIET COMPLIANT met limiet {noise_limit:.2f} dB")
```

```
    # Voor compatibiliteit: geef ook per techniek het (gemitigeerde) resultaat plus 'combined'
    results = {tech: per_tech_mitig[tech]['final_sel_db'] for tech in techs}
    if len(techs) > 1:
        results['combined_unmitigated'] = unmitigated_total_sel
        results['combined_mitigated'] = mitigated_total_sel

    print("----------------------------------------------------------")
    return results

final_sel_dict = simulate_from_input(gen_input_values, noise_inst_tech_value, noise_mit_tech_min_


#%%

print('Total Weight:', total_weight)
print('Total Installation Duration PO:', total_duration, 'hours')
print('Total Installation Duration With Weather Workability:', total_duration_with_weather_workab
print('Total Costs:', total_costs)
print('Total Costs Per Monopile:', cost_per_monopile)
print("\n=== Summary of Final SEL Values ===")
for tech, sel in final_sel_dict.items():
    print(f"{tech}: {round(sel, 2)} dB")
```